



Arianna Sinibaldi – Tackling challenges in asymmetric aminocatalysis for better sustainability



UNIVERSITÀ DEGLI STUDI DELL'AQUILA
DIPARTIMENTO DI SCIENZE FISICHE E CHIMICHE

Dottorato di Ricerca in Scienze Chimiche
XXXIV ciclo

***Tackling challenges in asymmetric
aminocatalysis for better sustainability***

SSD CHIM/06

Dottoranda
Arianna Sinibaldi

Coordinatore del corso
Prof. Massimiliano Aschi

Tutor
Prof. Armando Carlone

a.a. 2020/2021



**UNIVERSITÀ DEGLI STUDI
DELL'AQUILA
DIPARTIMENTO DI SCIENZE FISICHE E CHIMICHE**

Dottorato di Ricerca in Scienze Chimiche

XXXIV ciclo

*Tackling challenges in asymmetric aminocatalysis for
better sustainability*

SSD CHIM/06

Dottoranda

Arianna Sinibaldi

Arianna Sinibaldi

Coordinatore del corso

Prof. Massimiliano Aschi

MAschi

Tutor

Prof. Armando Carlone

Armando Carlone

a.a. 2020/2021

Abstract

The concept of chirality is a recurrent fundament at the base of all animate and inanimate matter in the universe. We find chirality in everything around us, and that constitutes us. Reproducing reactions that introduce elements of asymmetry inside increasingly complex molecules is a concept that has been extensively explored in research in the past, present, and certainly will be in the future.

The various synthetic strategies for carrying out an asymmetric synthesis of optically active compounds have, over the years, led to a change in these approaches towards the development of increasingly sustainable and green methodologies. The most outstanding contribution comes from pressure from global governments and the fact that it is ethically correct towards ourselves, our offspring, and our surroundings. According to the G20 report (Italy - August 2021),¹ all member countries are committed to strengthening "the many synergies in financial flows for climate, biodiversity, and ecosystems" by alining the "investments towards sustainable development and growth" and "to build the necessary skills, innovations, and infrastructure". In this, asymmetric organocatalysis offered a good starting point. Since the catalysts used are often derived from natural sources, are non-toxic, stable to air and moisture, they do not need special requirements in the reaction set-up.

During these three years of my PhD, I have tried to overcome, in my small way, those critical issues frequently found in the use of organocatalysis, and, in particular, focusing on aminocatalysis, always looking at the green aspect. To do this, I focused on a type of carbonyl compounds activation to perform catalysis via enamine mediated by the recurrent presence of an α -amino acid, Proline and its derivatives.

The first project concerned the use of short heterochiral peptide sequences as catalysts to activate carbonyl compounds. In this work, we

1

https://www.mite.gov.it/sites/default/files/archivio_immagini/G20_Napoli_2021/2021_07_22_ITG20_ENV_Final.pdf

have demonstrated that it is possible to increase the catalytic efficiency of reactions carried out in aqueous media by exploiting a peptide sequence capable of pre-organising itself supramolecularly.

The second work concerned the optimisation of a synthetic protocol using prolinol derivatives with alkyl chains in an aqueous solvent. In addition to optimising the synthesis of an important pharmacological precursor in a green solvent, the second strength of this work was the methodology used to find the optimal reaction condition, the DoE.

The latest work reported is a study that attempts to clarify the phenomena that could hamper the success of a reaction mediated by a supported catalyst. Despite heterogenisation of catalyst for future recovery and reuse being an extremely attractive concept for industry, there are still some critical issues related to the imperfect inertia of the support itself. With this aim, we have studied the relationship between activity and affinity for the matrix of substituted series of benzaldehydes that could lead to substrate inhibition in an aldol reaction with hydroxyacetone.

List of Publications

Insights into substituent effects of benzaldehyde derivatives in an organocatalyzed aldol reaction via NMR relaxation techniques – G. Di Carmine, F. Pesciaoli, S. Wang, **A. Sinibaldi**, G. Giorgianni, C. M. A. Parlett, A. Carlone, C. D'Agostino – *ChemCatChem*, **2022**. DOI: 10.1002/cctc.202200405.

F. Pesciaoli, V. Nori, **A. Sinibaldi**, A. Carlone, *Synergistic organo-organocatalysis*. In "Asymmetric Organocatalysis: New Strategies, Catalysts, and Opportunities"; Dell'Amico, L.; Albrecht, Ł.; Albrecht, A. Eds.; Wiley-VCH: Weinheim, **2022**. (In press)

DoE-driven development of an organocatalytic protocol for the enantioselective preparation of γ -aminoacids precursors in water – V. Nori, **A. Sinibaldi**, G. Giorgianni, F. Pesciaoli, E. Di Cocco, F. Di Donato, A. Biancolillo, A. Landa, A. Carlone – *Chem. Eur. J.*, **2022**, e202104524

Impact of Design of Experiments in the optimisation of catalytic reactions in academia – V. Nori, F. Pesciaoli, **A. Sinibaldi**, G. Giorgianni, A. Carlone – *Synthesis*, **2022**. DOI: 10.1055/a-1736-6703

Boron-based Lewis acid catalysis: challenges and perspectives – V. Nori, F. Pesciaoli, **A. Sinibaldi**, G. Giorgianni, A. Carlone – *Catalyst* **2022**, *12*, 1, 5.

Asymmetric Organocatalysis Accelerated via Self-Assembled Minimal Structures – **A. Sinibaldi**, F. Della Penna, M. Ponzetti, F. Fini, S. Marchesan, A. Baschieri, F. Pesciaoli, A. Carlone – *Eur. J. Org. Chem.* **2021**, *39*, 5403.

Organocatalysis and Beyond: Activating Reactions with Two Catalytic Species – **A. Sinibaldi**, V. Nori, A. Baschieri, F. Fini, A. Arcadi, A. Carlone – *Catalysts* **2019**, *9*, 11, 928.

A Technology Platform to Chiral Amines: selected examples in asymmetric organocatalysis – A. Carlone, F. Fini, V. Nori, **A. Sinibaldi** – *Chemistry Today* **2019**, *37*, 18.

Table of contents:

<i>Chapter 1: Asymmetric Organocatalysis</i>	2
1.1 <i>Asymmetric synthesis: four methods and diastereomorphic TS</i> ...	8
1.2 <i>Asymmetric organocatalysis: types of activations</i>	15
1.2.1 <i>Non-covalent catalysis</i>	16
1.2.2 <i>Covalent catalysis</i>	19
1.3 <i>Amino-organocatalysis: proline and its derivatives</i>	21
1.4 <i>Organocatalysis drawbacks: how to overcome it and aim of the thesis</i>	28
<i>Chapter 2: Asymmetric Organocatalysis Accelerated via Self-Assembled Minimal Structures</i>	33
2.1 <i>Peptidic sequences in organocatalysis</i>	34
2.2 <i>Self-assembly and supramolecular structures</i>	42
2.2.1 <i>Selected examples</i>	45
2.3 <i>Target of the project</i>	53
2.4 <i>Results and discussion</i>	57
2.4.1 <i>Materials and methods</i>	69
2.4.2 <i>Synthesis of the catalysts</i>	71
2.4.3 <i>Characterisation data for compounds 3aa-ci</i>	87
<i>Chapter 3: DoE-driven development of an organocatalytic protocol for the enantioselective preparation of γ-aminoacids precursors in water</i>	99
3.1 <i>Dialkylprolinol ethers: water-compatible catalysts</i>	100
3.2 <i>DoE: a rational approach to improve the experimental responses</i>	102

3.2.1 Chemometrics	103
3.2.2 Mathematical information: from chemist to chemometrician	103
3.2.3 The selection of the correct DoE: how to proceed.....	106
3.2.4 Example of DoE in organic synthesis	108
3.3 Target of the project.....	115
3.4 Results and discussion	118
3.4.1 Experimental section.....	129
3.4.2 Characterisations.....	146
Chapter 4: Investigation of the effect of reagents in an aldol reaction catalysed by an immobilised organocatalyst.....	149
4.1 Heterogeneous catalysis.....	150
4.1.1 Supported catalyst	151
4.1.2 Matrix: types and structural characteristics	154
4.1.3 Selected examples	160
4.2 T_1/T_2 parameter as indicator of surface affinity with the molecules	164
4.3 Target of the project.....	167
4.4 Result and discussion	169
4.4.1 Experimental section (performed in L'Aquila University)...	175
4.4.2 Characterisations.....	177
Chapter 5: Conclusion	180

*“Look wide,
and even when you think you are looking wide,
look wider still.”*

B.P.

Chapter 1: Asymmetric Organocatalysis

Asymmetric synthesis is an important branch of organic synthesis that aims to obtain enantiomerically enriched or pure compounds starting from a precursor that may be chiral or achiral.

The importance of controlling the introduction of an element of asymmetry derives from the necessity to obtain an optically pure compound. This is because enantiomers have the same chemical-physical properties except for their rotation in polarised plane light and how they react in chiral environments. The development of this branch has not only facilitated the development of this synthetic strategy in the purely academic field but has also allowed to obtain optically active compounds useful in several industrial applications. Chiral compounds are frequently used in the agrochemical industry¹ (e.g. for the synthesis of fungicides, fertilisers, and pesticides), in the production of fragrance and flavouring,² and, in particular, in the pharmaceutical industry, since two enantiomers react differently in chiral environments, such as in biological systems (Figure 1.1).³ In the best-case scenario, if the “undesirable” enantiomer of an active substance does not have a biologically harmful function, for instance, the enantiomer (R) of the ibuprofen drug, it can be commercialised as a racemic mixture.

In other cases, the unwanted enantiomer could lead to serious side effects, such as arrhythmias, or even cause anomalies and malformations during embryonic growth (teratogenic effects). In light of this, in the late 1980s, the FDA regulated the production of drugs in racemic form, forcing pharmaceutical companies to investigate the possible side effects of both enantiomeric forms separately. Moreover, the production of an active

¹ P. Jeschke, *Pest Manag Sci*, **2018**, 74, 2389. b) S. K. Sharma, A. S. R. Paniraj, Y. B. Tambe; *J. Agric. Food Chem* **2021**, 69, 14761.

² U. Schäfer, J. Kiefl, W. Zhu, M. Kempf, M. Eggers, M. Backes, T. Geissler, R. Wittlake, K. V. Reichelt, J. P. Ley, G. Krammer, *Authenticity Control of Food Flavorings - Merits and Limitations of Chiral Analysis*, *ACS Symposium Series*, **2015**, 1212, 1, 3.

³ B. Han, X. H. He, Y. Q. Liu, G. He, C. Peng, J. L. Li, *Chem. Soc. Rev.* **2021**, 50, 1522.

pharmaceutical ingredient (API) as a racemic mixture represents for the pharmaceutical industry a considerable waisting in terms of purification and disposal cost of 50% of unwanted enantiomer.⁴

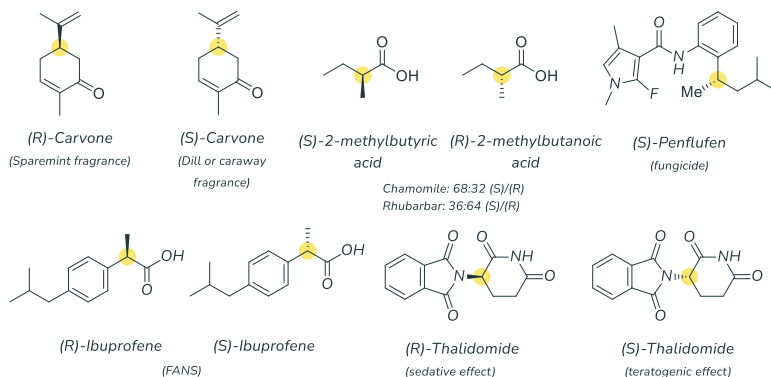


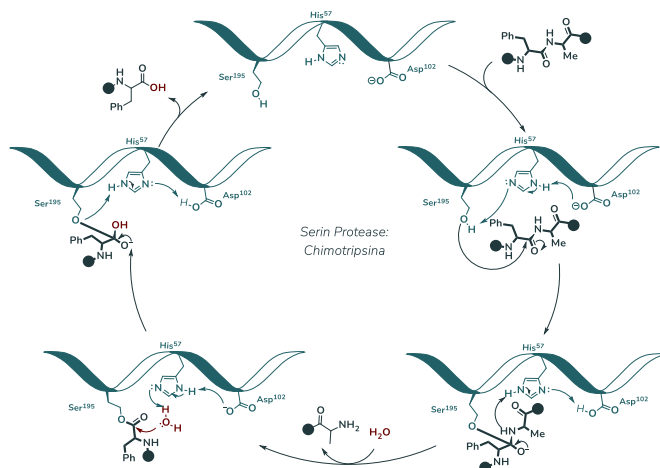
Figure 1. 1 Some examples of enantiopure compounds with different activities

Historically, until the late 1990s, asymmetric synthesis was based on two pillars, biocatalysis and transition metal catalysis. These approaches ensure the formation of enantio-enriched compounds by using a catalytic amount of enantiomerically pure catalyst, enzyme, or soluble metal complex.⁵

In more detail, biocatalysis involves biological molecules to catalyse chemical reactions. The biological reactions leading to the formation of optically pure compounds is performed in nature by the enzymes. The perfect performance of enzymes is the outcome of millennia of evolution that has led them to synthesise increasingly complex compounds in an enantiospecific fashion (Scheme 1. 1).

⁴ Stinson, S. C. *Chem. Eng. News* **1992**, 39, 46-79.

⁵a) D. Seebach *Angew. Chem. Int. Ed. Engl.*, **1990**, 29, 1320; b) K.C. Nicolaou, E.J. Sorensen, *Classics in total synthesis I: Targets, strategies, methods*, Weinheim VCH, **1996**.



Scheme 1. 1 Example of biocatalytic reaction performed with Chymotripsin.

An initial critical aspect of the use of enzyme systems was correlated with their low bioavailability. Enzymes were initially isolated from natural sources such as fungi, microorganisms, or plant and animal species. Only after the second half of the 1970s, following the discovery of the recombinant DNA technique, it was possible to synthesise artificial enzymes in large quantities.⁶

Although the use of enzyme catalysts guarantees perfect stereospecificity of the desired product, even with a high turnover, its use is often limited to specific substrates.⁷ Indeed, each enzyme is able to perform its specific catalytic function only on reagents that have a

⁶ a) L. Pasteur, *C. R. Seances Acad. Sci.* **1858**, 46, 615; (b) J. Gal, *J. Chirality* **2008**, 20, 5. b) *Enzyme Catalysis in Organic Synthesis*, 3rd ed.; K. Drauz, H. Gröger, O. May, O., Eds.; Wiley-VCH: Weinheim, **2012**; c) K. Faber, *K. Biotransformations in Organic Chemistry*, 6th ed.; Springer: Heidelberg, **2011**.

⁷ a) E. Buchner, *Ber. Dtsch. Chem. Ges.*, **1897**, 36, 117; b) J. Gal, *Chirality*, **2008**, 20, 5; c) K. Drauz, H. Gröger, O. May, *Enzyme Catalysis in Organic Synthesis*, 3rd Ed. Eds., Wiley-VCH, Weinheim, **2012**; d) K. Faber, *Biotransformations in Organic Chemistry*, 6th Ed. Springer, Heidelberg, **2011**; e) E., Fischer, *Ber. Dtsch. Chem. Ges.*, **1894**, 27, 2985; f) E. Buchner, *Ber. Dtsch. Chem. Ges.*, **1897**, 36, 117.

geometric complementary to the cavity and the binding site.⁸ Another critical issue to be faced in bio-catalysis arises from the instability of the enzyme itself under classical experimental conditions in organic chemistry (solvent, pH, temperature, etc.).⁹

Biomimetic strategies provide a good starting point for asymmetric synthesis because it is possible to carry out appropriate syntheses of specific peptide sequences, as in the case of enzyme mimesis, in an attempt to limit the drawbacks of using them.

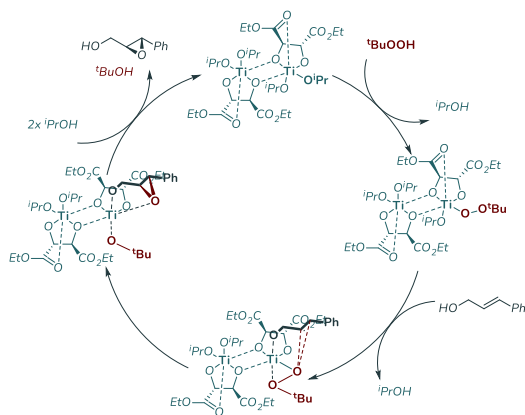
In parallel, asymmetric transition metals catalysis received considerable attention from the scientific community during the second half of the 20th century. Indeed, by using transition metals with chiral ligands, a large number of asymmetric reactions of extreme synthetic importance were identified, culminating in the award of Nobel Prizes to Sharpless, Noyori, and Knowles in 2001 (Scheme 1. 2).¹⁰

The use of transition metals as catalysts also requires some precautions; metal catalysts are very often used under inert conditions because they are unstable to air and moisture and can also be toxic and difficult to dispose.

⁸ M. T. Reetz, *J. Am. Chem. Soc.* **2013**, *135*, 12480.

⁹ S. Hammes-Shiffler, *Biochemistry* **2013**, *52*, 2012.

¹⁰ a) E. N. Jacobsen, A. Pfaltz, H. Yamamoto, *Comprehensive Asymmetric Catalysis*, Eds. Springer, Heidelberg **1999**; (b) R. Noyori, *Asymmetric Catalysis in Organic Synthesis* Ed. Wiley, New York **1994**; c) I. Ojima, *Asymmetric Synthesis*, Ed. VCH, New York **1993**.



Scheme 1. 2 Sharpless epoxidation performed with chiral ligand.

Until the advent of modern organocatalysis in the early 2000s, a versatile approach such as organocatalysis was not mentioned at all. Although the first enantioselective synthesis, using purely organic catalysts, was discovered in 1912 by Bredig and Fiske.¹¹ This branch did not initially attract much interest in the scientific community and only a very limited number of research groups persevered with these primordial studies.¹² As Benjamin List wrote in 2007, "it is quite remarkable that organic chemists had long ignored the fact that the very first catalysts they used in ancient times were purely organic molecules [...] As organic molecules readily react with each other, why did we disregard these compounds as

¹¹ G. Bredig, P. S. Fiske, *Biochem. Z.*, **1912**, 46, 7.

¹² a) C. Agami, F. Meyneir, C. Puchot, *Tetrahedron* **1984**, 40, 1031. For phase-transfer catalysis: b) M. J. O'Donnell, W. D. Bennett, S.Wu, *J. Am. Chem. Soc.* **1989**, 111, 2353; c) E. J. Corey, F.-Y. Zhang, *Org. Lett.* **1999**, 1, 1287; d) E. J. Corey, Y. Bo, J. Busch-Petersen, *J. Am. Chem. Soc.* **1999**, 120, 13000. e) E. J. Corey, F. Xu, M. C. Noe, *J. Am. Chem. Soc.* **1997**, 119, 12414. For Epoxidation: f) D. Yang, Y.-C. Yip, M.-W. Tang, M.-K. Wong, J.-H. Zheng, K.-K. Cheung, *J. Am. Chem. Soc.* **1996**, 118, 491; g) D. Yang, M.-K. Wong, Y.-C. Yip, X.-C. Wnag, M.-W. Tang, J.-H. Zheng, K.-K. Cheung, *J. Am. Chem. Soc.* **1998**, 120, 5943; h) Y. Tu, Z.-X. Wang, Y. Shi, *J. Am. Chem. Soc.* **1996**, 118, 9806; i) S. E. Denmark, Z. Wu, *Synlett* **1999**, 847. For Bayliss-Hillman reaction: j) Y. Iwabuchi, M. Nakatani, N. Yokoyama, S. Hatakeyama, *J. Am. Chem. Soc.* **1999**, 120, 10219.

catalysts and rather relied on the assistance of biologists and inorganic chemists to provide enzymes or explain the foreign world of d-orbitals to us? Why did we not expect catalytic competence from organic molecules - exactly those compounds we can truly design, make, and know most about?"¹³

The use of purely organic catalysts has laid the groundwork for a large number of researchers in the field of asymmetric catalysis, triggering a properly "gold rush".¹⁴ This is because the organocatalysts used in asymmetric reactions are readily available from nature's building blocks, often available in both enantiopure form, inexpensive, and easy to handle and prepare. In particular, their use does not require any special precautions for the storage or in the reaction set-up (the use of gloveboxes, anhydrous solvents, or inert gases), since they well tolerate moisture and oxygen in the air. Organocatalysts also have a low toxicity level and can be recovered at the end of the reaction without undergoing structural modifications, which makes them more environmentally sustainable than organometallic catalysts.¹⁵

Finally, in 2021, organocatalysis was recognised for its unique qualities, with a Nobel Prize awarded to two pioneers of the modern asymmetric organocatalysis, Benjamin List and David W. C. MacMillan.

¹³ B. List, *Chem. Rev.* **2007**, 107, 5413.

¹⁴ P. Melchiorre, M. Marigo, A. Carlone, G. Bartoli *Angew. Chem. Int. Ed.* **2008**, 47, 6138.

¹⁵ D.W.C. MacMillan *Nature* **2008**, 455, 304.

1.1 Asymmetric synthesis: four methods and diastereomeric TS

Asymmetric synthesis refers to the synthetic strategy that offers the possibility of introducing a new element of asymmetry into a starting compound, whether it is an achiral compound or one that already has such an element. According to the nature of the asymmetry element (point, plane, or axis), there are different types of chirality (Figure 1. 2).

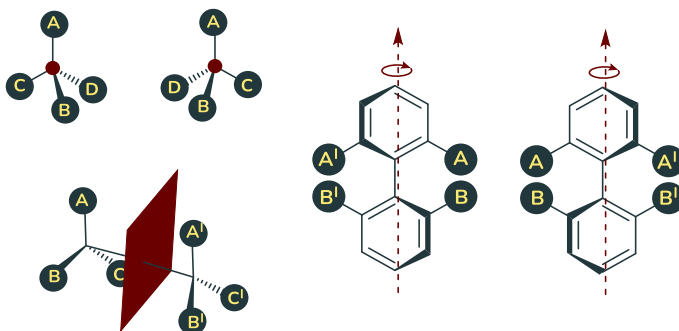


Figure 1. 2 Different chirality elements: point, plane, and axis.

The asymmetric synthesis of the enantio-enriched compound could be performed using four different approaches.

All these methods require the use of chiral molecules that can be used as starting materials or reagents, as auxiliaries, or as catalysts.

Chiral Substrate (Scheme 1. 3): By reacting a chiral compound with a second achiral reagent, it is possible to induce asymmetry in the resulting product. For example, nucleophilic addition with a Grignard reagent (achiral) to an electrophilic prochiral centre of the carbonyl compound **1** leads to the formation of two diastereoisomers. The resulting predominate diastereoisomer will be **2a** because the presence of the substituent in position 2, relative to the reactive centre in 1 position, will confer a steric hindrance that will favour the approach of the nucleophilic reagent from the less congested face. It is interesting to remark that the induction of asymmetry occurs when the substrate

interacts with the second reagent at the transition state level, therefore, without considering the steric hindrance and the relative stability of the final product.

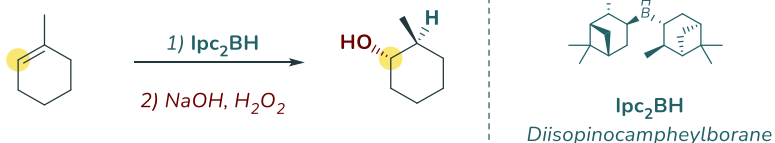
This type of asymmetric induction is called 1,2 precisely to emphasise the position in which the substituent is present, which provides the steric hindrance necessary to induce asymmetry in the prochiral centre 1.



Scheme 1.3 First generation method for asymmetric synthesis: Chiral substrate.

By moving the asymmetric element away, in position 3, for example, we would have asymmetric induction 1,3 or remote. Obviously, the nature of the bulk of the substituent and the position, more or less close to the reactive centre, will be factors affecting the diastereomeric ratio of the product.

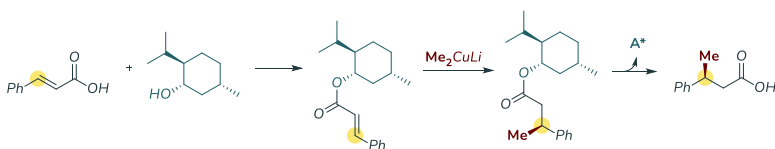
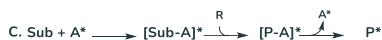
Chiral reagent (Scheme 1. 4): As in the first case, the use of a chiral reagent to induce asymmetry can be considered a good synthetic strategy. In the example shown, the hydride that will be reacting with the reactive partner is part of an extremely cluttered molecule. The chiral information, transferred during the formation of the transition state, will block the approach of one of the two stereogenic faces of the prochiral substrate.



Scheme 1. 4 Second generation method for asymmetric synthesis: Chiral reagent.

Chiral auxiliaries (Scheme 1. 5): is a method involving the prior functionalization of an achiral reagent, on which the asymmetry element is to be induced, with a chiral reagent. This functionalization results in the formation of a diastereoisomeric product. In this way, it is more probable that a second achiral reagent, as the cuprate organometallic reagent reported in the example, will approach the less hindered face of the activated substrate. As shown in the example, (+)-menthol provides a good steric clutter such that the alkylation reaction mediated by the cuprate organic reagent is enantioselective.

At the end of the reaction, the chiral auxiliary is removed from the compound as if it were a protecting group. It must therefore be simultaneously stable under the reaction conditions and easily removable at the end of the reaction.



Scheme 1. 5 Third generation method for asymmetric synthesis: Chiral Auxiliaries.

In the first three cases, a stoichiometrical amount of chiral reagents is required, with relative increases in synthetic costs, and without considering that not all the products are available in both enantiopure forms. Furthermore, by using chiral reagents or auxiliaries, another critical issue relating to the atomic economy arises. This is due to the fact that

the enantiopure molecule required to introduce the asymmetry element is removed at the end of the reaction itself.

For this reason, the **catalytic approach** (Scheme 1. 6) is the most exploited method because the chiral catalyst is employed in a sub-stoichiometric amount and is frequently recycled.



Scheme 1. 6 Fourth generation method for asymmetric synthesis: Chiral catalyst.

As defined from IUPAC, “A catalyst is a compound that can increase the speed at which reactions occur, and lower the energy required for the reaction to take place. One of the key features of a catalyst is that it is not consumed by the chemical reaction and can be re-used in subsequent reactions”. (**Figure 1. 3**)

The probability of forming a generic chemical bond between a nucleophile and an electrophile depends essentially on the difference in the electron density of the two reactants considered separately. Examining the frontier orbitals, we can see how the energy gap between the energy of the highest occupied molecular orbital (HOMO) of the electron donor and the energy of the lowest unoccupied molecular orbital (LUMO) of the acceptor can be decreased in the presence of a catalyst that activates either or both of the two reactants. If

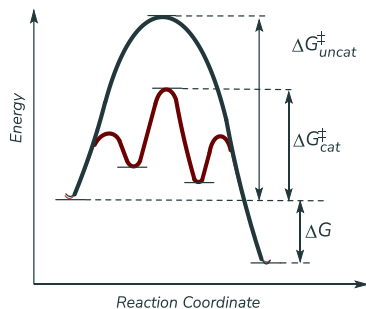


Figure 1. 3 Reaction performed without catalyst (blue) and with catalyst (red)

the energy gap decreases, the orbital overlap and the probability of the reactants forming a chemical bond will increase.

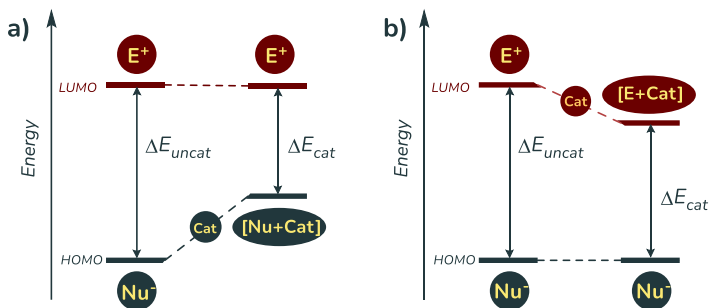


Figure 1. 4 a) Mono-catalytic HOMO raising activation b) Mono-catalytic LUMO lowering activation.

Considering the frontier orbitals, we will see how a catalyst interferes with the electronic distribution of the two reactants and, in particular, with the decrease in the energy gap between the HOMO-LUMO orbitals of the two reactants.

If the catalyst interacts with the electron donor species (Nu^- = nucleophile; Figure 1. 4-a), this increases the energy associated with the HOMO, which leads to a destabilisation of the energy level itself.

On the contrary, if the catalyst interacts with an electron-withdrawing substrate (E^+ = electrophile; Figure 1. 4-b), the LUMO will be stabilised by the interaction with the catalyst and will therefore be more inclined to accept electrons.

A chiral catalyst not only decreases the energy gap leading to the formation of the product (at the thermodynamic level) but is also able to promote the formation of a single enantiomer and will produce a diastereomorphic transition state when interacting with the substrate.

If in the process being considered leads to the formation of two enantiomers and an achiral catalyst is used (in absence of any other asymmetric induction) the two transition states will be degenerate in energy (Figure 1. 5 highlighted in blue line). This will imply that the two enantiomers, (R) and (S), will be synthesised in equal quantities (in the form of racemate) as there is an equiprobability of surpassing both activation barriers.

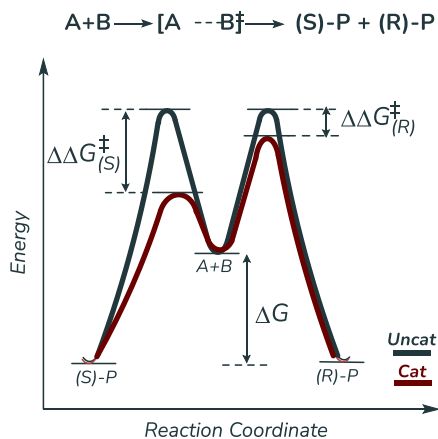
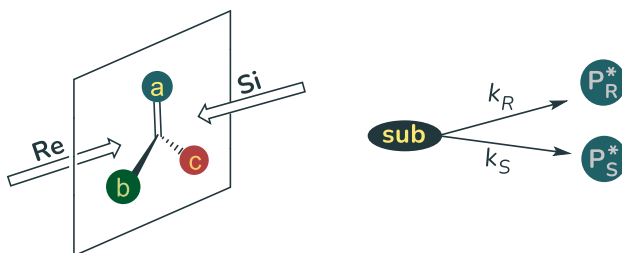


Figure 1. 5 Degenerate transition state (blue) and diastereomorphic transition states (red)

If we consider the process promoted by using a chiral catalyst, we can see how both barriers of transition states will undergo a decrease in activation energy ($\Delta\Delta G^\ddagger$ (R) or (S)), but not in equal amounts ($\Delta\Delta G^\ddagger_{(S)} > \Delta\Delta G^\ddagger_{(R)}$) by generating a diastereomorphic transition state. This predominant energy decrease will promote the major stabilisation of only one activated complex (as shown in Figure 1. 5; red line) for the (S)-enantiomer, which will evolve to products in greater amounts.

By using chiral catalyst to desymmetrising the considered system, is it possible to evaluate the enantioselection as the ratio between the concentrations of the two enantiomers, (R) and (S). By considering the Arrhenius equation (reported in Figure 1. 6), the energy gap produced by the catalyst itself will therefore be proportional to the ratio of the rate constants at which the products are formed.



$$\frac{[P_S^*]}{[P_R^*]} = \frac{[k_S]}{[k_R]}$$

where $k_S = Ae^{-E_S/RT}$; $k_R = Ae^{-E_R/RT}$

$$\frac{[P_S^*]}{[P_R^*]} = e^{-(E_S - E_R)/RT} = e^{-(\Delta E)/RT}$$

Figure 1. 6 Enantiofacial approach and Arrhenius equations

Another parameter in the equation, but an experimental one this time, that enhances the enantioselectivity of a reaction is temperature. Decreasing the reaction temperature could lead to an increase in the enantiomeric excess. However, this is not always guaranteed mainly for two reasons. The first is because not all reactions succeed in converting reagents into products within a reasonable time at low temperatures as the probability of an effective impact is reduced. The second effect that could occur is due to the possibility of promoting different reactive pathways leading to the formation of side products. For this reason, a right compromise must always be found between reactivity and selectivity of the reaction under consideration.

From a chemical point of view, a chiral catalyst can stabilise the formation of a single diastereomorphic transition state most effectively when it is able to shield, for example, a stereogenic face by avoiding an equiprobable approach by the second reactant.

There are different types of catalysts that differ on the basis of the type of interaction with the reagent.¹⁶

1.2 Asymmetric organocatalysis: types of activations

As mentioned above in paragraph 1.1, the use of catalysts based on purely organic compounds was a relatively poorly explored aspect of catalysis. In fact, over the last century, several Nobel prizes have been awarded for catalysis but using transition metal catalysts. We mention for instance the Nobel prize in 1963 won by Karl W. Ziegler and Giulio Natta,¹⁷ who succeeded in using their catalysts to polymerise α -olefins, thus making it possible to obtain isotactic or syndiotactic polymers. In 2001 William S. Knowles and Ryoji Noyori for asymmetric hydrogenation, and K. Barry Sharpless for enantioselective oxidation, and K. Barry Sharpless for enantioselective oxidation.¹⁸

For about another thirty years, this branch of asymmetric synthesis was not explored very much. It is well known that the new rediscovery of modern asymmetric organocatalysis is due to the contribution of two pioneers, Benjamin List and David MacMillan, who independently published, in the same volume in the *Journal of the American Chemical Society*, two works in which the new conceptualisation of organo catalysis was brought to light.

Organocatalysts are indeed small organic molecules (MW<1000), mainly containing carbon, nitrogen, oxygen, sulfur, and phosphorus atoms. The molecules commonly used as catalysts are often derived from the chiral pool, which gives the use of this strategy several advantages. The first derives from the fact that by operating appropriate functionalisation or demolition-type chemistry, pre-existing chiral centres on the compound

¹⁶ G. Quinkert, H. Stark, *Angew. Chem. Int. Ed. Engl.* **1983**, 22, 637.

¹⁷ Nobel Lectures, Chemistry 1963-1970, Elsevier Publishing Company, Amsterdam, 1972; <https://www.nobelprize.org/prizes/chemistry/1963/natta/lecture/>

¹⁸ MLA style: The Nobel Prize in Chemistry 2001. NobelPrize.org. Nobel Prize Outreach AB 2021. Wed. 8 Dec 2021. <<https://www.nobelprize.org/prizes/chemistry/2001/summary/>>

skeleton are exploited. In many cases, these molecules are also directly extracted from natural sources in the form of a single enantiomer (such as α -amino acids, alkaloids, or carbohydrates) which gives them an advantage in their use as they are often found in nature in different enantiopure forms and are not very expensive.

The first distinction is made based on the type of interaction that the catalyst establishes with the substrate to be activated. We are referring to non-covalent catalysis if the interaction established involves the formation of a weak bond or covalent catalysis if the catalyst forms a covalent bond with the substrate to be activated.

1.2.1 Non-covalent catalysis

In this type of activation, the possible weak interactions established between the catalyst and the substrate to be activated can be hydrogen bonding or electrostatic interaction (ca. <5 kcal/mol).

Although the intermolecular forces involved are considerably more flexible and less directional than in covalent interactions, good enantioselection can also be achieved using this type of approach because the stereochemical information is in any case efficiently transmitted to the product by forces acting through space rather than through bonds. This type of activation can be further subdivided into different methods that differ according to the class of catalysts employed:

- general acid catalysis (weak or via hydrogen bonding)
- specific acid/base catalysis (Bronsted acid/base)
- Phase Transfer Catalysis

H-bonding catalysis, or anionic bonding catalysis, occurs when the catalyst (donor) stabilises the transition state of the reactant involved in the chemical reaction through a dense network of hydrogen bonds which pre-organise the approach between the two reactants with a geometry complementary to the catalyst itself (even if the reactive centre is located at a distance from the catalyst). In this manner, a supramolecular chiral interaction was established, and for example, the generated anion could react with the electrophile site. This behaviour is analogous to the

oxyanion hole in the enzyme in which a stabilising cooperative organisation is established between amino acid residues and substrates (acceptors or H-bond donors). In this case, however, the chiral information has transferred at the resultant compound by exploiting the whole chiral environment confining the reagents themselves.

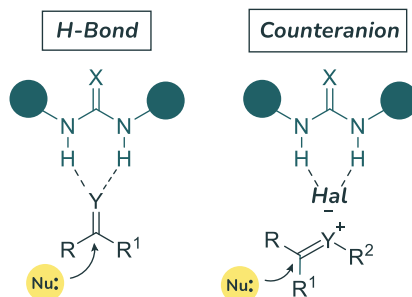


Figure 1. 7 Examples of stabilization of electrophilic reagents by hydrogen bond formation or chiral ion pair generation.

A subclass of this activation is represented by the **counteranion catalysis**, which is involved stabilisation of the counteranion of the transient acyl-iminium ion and oxocarbenium ion. The halides ion is efficiently stabilised from the donor of H-bonds donor catalyst and the resulting activated cation forms a tight ion pair with the catalyst itself that guarantees the enantioselective shield toward the nucleophilic attack.

In order to use specific acid catalysis (or **Brønsted acid catalysis**), by inspiring from the confinant properties of the enzyme, vast numbers of acid catalysts were designed. The increase of the acidity, with consequent lowering pKa value of catalyst, made the activation of substrates possible via protonation-deprotonation. A beautiful example was reported in **Errore. L'origine riferimento non è stata trovata.**, in which the phosphoric acid BINOL-derived can coordinate the starting material with the hydroxylic group to destabilise the ground state while the oxygen bonded to the phosphorous atom stabilises the positive charge during the transition state formation. To improve the enantioselectivity it is important the use of non-coordinating solvent so that the stabilisation of

the counterion arises from the catalyst itself (that will offer a more proximal chiral environment) and not from the reaction medium.

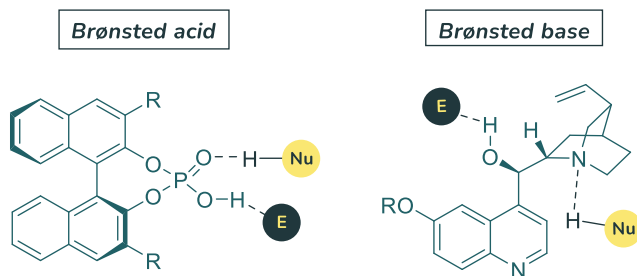


Figure 1. 8 Specific acid/base catalysis respectively via chiral Brønsted acid or base

As regards activation by deprotonation of a substrate, via **Brønsted bases**, we can find activation by tertiary chiral amines (for substrates to be protonated with pK_a less than 10-11) or quaternary ammonium salts (for substrates with pK_a between 10 and 20). Also, in this case, a tight chiral ionic pair is created between the deprotonated compound and catalyst that is able to shield a stereogenic face, directing the approach of the second reagent with good enantioselection. The most exploited chiral bases are derived from Cinchona alkaloids. These are present in nature in the form of pseudoenantiomers, as result they are extremely versatile since they make both enantiomers of the product accessible with good enantioselectivity. An example of organocatalysis, worth mentioning is the first asymmetric synthesis that was made by Bredig and Fiske¹¹ in 1912 by using Cinchona alkaloids as catalyst for the enantioselective hydrocyanation to aldehydes (Fig.1-D). The quaternary nitrogen in the quinuclidinic ring provides a Brønsted-basic site capable of deprotonating hydrogen cyanide and forming with it an ion pair capable of directing a nucleophilic attack with the second reagent with a well-determined topicity.

The other activation mode is **Phase Transfer Catalysis (PTC)**. The term PTC was coined by Starks in 1971¹⁹ to introduce the role of the organic

¹⁹ C. M. Starks, *J. Am. Chem. Soc.* **1971**, 93, 1, 195.

salt catalyst (tetraalkylammonium or tetraalkylphosphonium salts) in the reaction where two different reagents are located in two immiscible solvents. The experimental procedure requires simple and mild reaction conditions, reagents and solvents are well tolerated from the perspective of green chemistry; this ensures that this strategy can be applied on a large scale by the industries.

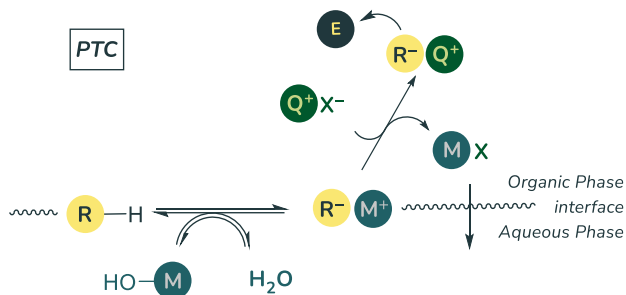


Figure 1. 9 PTC Mechanism

1.2.2 Covalent catalysis

When a catalyst interacts with a substrate by forming a covalent bond, it produces an intermediate in which the asymmetric induction is more tightly structural-dependent on the chiral catalyst than in the intermediate resulting from the non-covalent approach. This firstly results because the generated intermediate will assume mainly the most stable conformation in the tridimensional space. In this way, the structure of the catalyst, based on its steric and electronic effects that are produced on the starting reagent, will force the partner to orientate itself correctly. This is because it exposes only one stereogenic face for the subsequent approach with the second reagent.

However, precisely because the formation of a covalent bond is required, the catalysts have to contain suitable functional groups to be able to bind the substrates to be activated. In addition, the catalysts must be sufficiently stable under the reaction conditions and simultaneously labile after the reaction with the second reactant.

Also in this case, depending on the different functional groups, we can distinguish different catalysis methods.

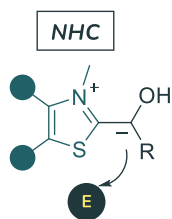


Figure 1. 10 Example of activation via NHC catalysis

A versatile organo-catalytic strategy to perform umpolung on the aldehydic compounds is represented by **N-Heterocyclic-Carbene (NHC)**. This strategy allows varying the natural electrophilic behaviour of carbonyl compounds, causing energy raises of the HOMO orbital, making it more inclined to act as a nucleophile in addition reactions in the conjugate positions.

The following three examples are merged in the larger activation class by primary or secondary amino compound, the aminocatalysis. This branch of asymmetric synthesis is extensively exploited to activate the carbonyl compounds, saturated and unsaturated, in the conjugated positions. The considerable number of reactions performed by using this strategy had highlighted its extraordinary versatility.

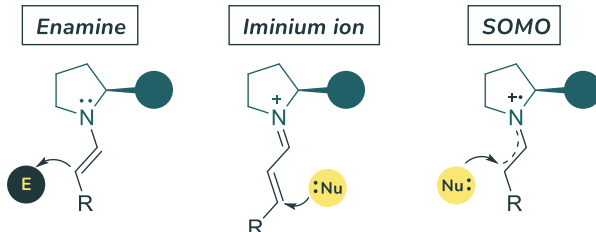


Figure 1. 11 Carbonyl compounds activation via HOMO-raising (enamine), LUMO-lowering (iminium ion), and SOMO catalysis.

The **enamine** activation mechanism involves the first condensation between chiral amine and the saturated carbonyl compound in which a C-C double bond is formed. In this way, the HOMO orbital energy is decreased and the resulting electron density on the C in alpha position is ready to carry out a nucleophilic attack on an electrophilic species.

The **iminium ion** activation instead is performed to activate unsaturated carbonyl compounds, which don't have an enolizable proton in the alpha position. A pre-equilibrium with the correspondent enamine is generated,

but, in this case, the iminium ion specie is mostly stabilised from the vicinal π -system. In this case, the active species has a positive formal charge on the nitrogen heteroatom which recalls the electrons of the conjugated double bond by lowering the energy of the LUMO orbital. In this way, the beta position is activated towards an attack by a nucleophilic species. This strategy is quite similar to the activation via Lewis acid in which the coordination of the transition metal catalyst on the oxygen of the carbonyl compound increases the acidity, by LUMO orbital decreasing energy.

Lastly, **SOMO** activation is a strategy (introduced in 2006) in which is it possible to perform α -functionalisation of an unsaturated carbonyl compound (such as for the enamine), but in this case through a nucleophilic attack of a second reagent partner. For this reason, SOMO activation is considered complementary to the enamine approach. The mechanism involves a mono-electron oxidation of an electron-rich enamine that generates a highly reactive cation radical with three p -electrons. The electron is located in a singly occupied molecular orbital (SOMO, from which the name derives). The latter intermediate, in the presence of a nucleophilic species in solution, forms a C-C bond in the alfa position.

1.3 Amino-organocatalysis: proline and its derivatives

The conceptualisation of the term “organocatalysis”, as mentioned above, was introduced at the beginning of the century thanks to two reactions using catalysis performed with chiral secondary amines, therefore via amino-organocatalysis. Both proposed a mechanism for the activation of carbonyl compounds through the employment of chiral organo-aminocatalysts. In the first case, the L-Proline was chosen for the enamine activation of ketones towards electrophilic substrates; in the second case, the imidazolidinone was employed to activate the α,β -unsaturated aldehydes via iminium ion to perform the first highly enantioselective organocatalytic Diels-Alder reaction.

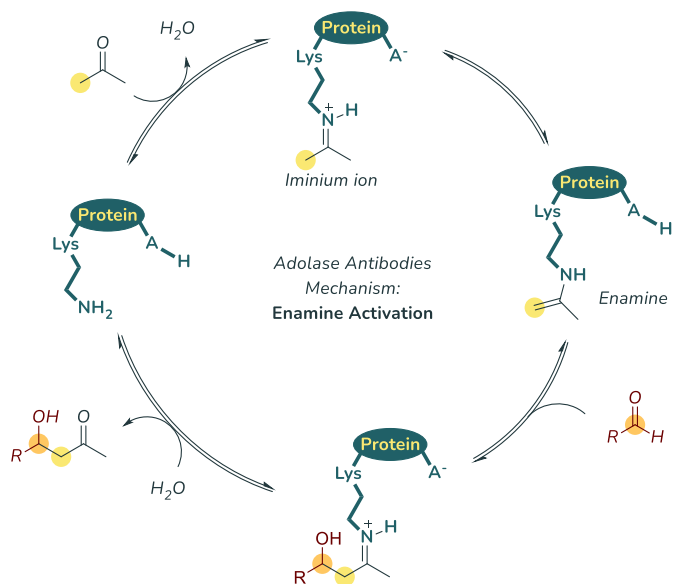
The first (chosen only because of the page number of the reference article) is Benjamin List, who at that time was studying numerous

enzyme-catalysed asymmetric reactions and was particularly interested in understanding the perfect enantioselective mechanism of Aldolase Antibodies.²⁰ As he explained excellently during his Nobel lecture,²¹ at that time, he wondered how an enzyme could create such a perfect chiral environment to drive a reaction enantioselectively. As was already known, enzyme sites consist of protein material in which only a few amino acid residues, located in the optimal geometric position, were directly involved in catalysis.

For example, as shown in **Scheme 1. 7**, the primary amine group of the Lysine (Lys) residue, assisted simultaneously by the acid group of Tyrosine (Tyr), it activates acetone via iminium ion by a bifunctional mechanism. After a rapid equilibrium that interconverts the iminium ion into an enamine, the electrophilic species undergoes a nucleophilic attack to form the aldol addition compound. This positively charged intermediate is once again stabilised by the presence of the deprotonated acid group of the Tyr residue before undergoing hydrolysis to form the product by regenerating the catalyst.

²⁰ T. Hoffmann, G. Zhong, B. List, D. Shabat, J. Anderson, S. Gramatikova, R. A. Lerner, C. F. Barbas III, *J. Am. Chem. Soc.* **1998**, *120*, 2768.

²¹ <https://www.youtube.com/watch?v=IW4zgOHhefc>



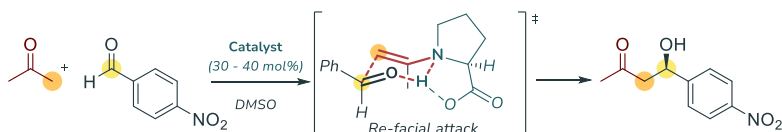
Scheme 1.7 Enamine Mechanism of Aldolase Antibodies

Because of this previous expertise, List decided to study the reactivity of a rudimentary and highly simplified enzyme system identified in the L-Proline residue (Scheme 1. 8). To overcome the use of enzymatic catalysts, the authors of the presented article initially decided to perform a catalyst screening in an aldol addition reaction between acetone and *p*-NO₂-benzaldehyde using only commercially available amino acids (at 30-40 mol%) free in solution.²² They first tried primary and acyclic amino acids as catalysts, which resulted in the product being obtained with poor conversion (<10%). They then considered proline and other cyclic amino acids (homologues of proline itself or functionalised prolines).

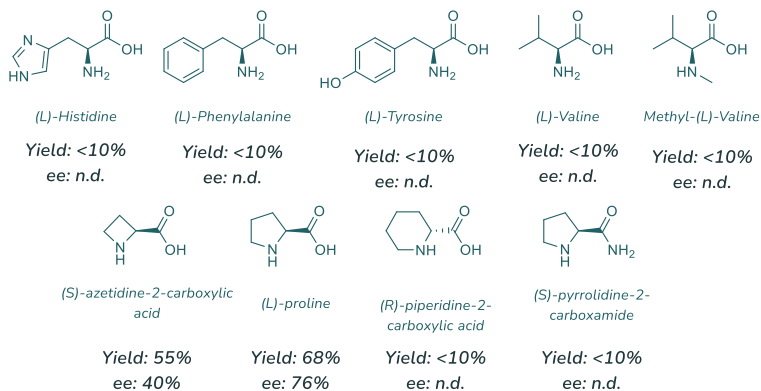
Interestingly, the four-term cyclic compound (2-azetidincaroxylic acid) was efficient in forming the product, albeit with a lower enantioselection than when proline was employed. In contrast, the six-terminal cyclic

²² B. List, R. A. Lerner, C. F. Barbas III, *J. Am. Chem. Soc.* **2000**, *122*, 2395.

(*pipecolic acid*) and 2-pyrrolidine carboxamide (thus with protected hydroxyl function) were unable to catalyse the reaction.



Catalysts Screening



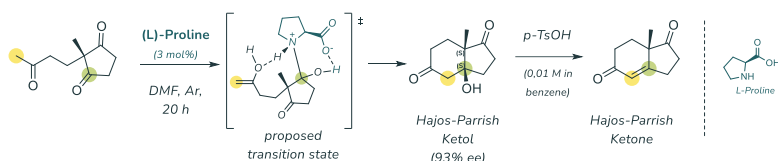
Scheme 1. 8 Aldol reaction performed with different catalysts by List and co-workers.

The reason for this resides in the geometry of the molecule, in which only the five-term pyrrolidine cycle of the proline assumes a conformation appropriate towards the vicinal hydroxyl group, which is able to orientate the electrophile, ensuring a well-defined enantiofacial approach.

The mechanistic hypothesis proposed by the authors, supported by experimental evidence, show that during the formation of the transition state, in addition to activation via enamine, there was also the double stabilisation of the second reagent by the con-participated hydroxyl group of the C-terminal portion of the amino acid and the pyrrolidine nitrogen. The extensive stabilisation form a sort of six-member ring in which the phenylic group in the prochiral centre of the electrophile assumes the equatorial position (avoiding steric 1,3-diaxial interactions, according to Zimmerman-Traxler model) encountering the *Re*-facial

approach, which determines the stereochemistry observed in the product. It is interesting to underline that, although List brought to light the enamine catalysis, the catalyst loading used to perform the reaction was relatively high for such modest yields (68% yield with 30 mol% of catalyst).

Although earlier studies had already reported that Proline could function as a “primordial enzyme”, List and co-workers were able to identify the correct reaction mechanism. In fact, in the article reported in 1974 by Hajos and Parrish,²³ they had already mentioned that proline had the correct geometry to explain the mechanism, since it contains a stereogenic centre very proximal to the catalytic site, and, in addition, the nitrogen atom is part of a five-term cycle, which gives the catalytic system extreme rigidity (Scheme 1. 9).



Scheme 1. 9 Intramolecular aldolic condensation performed by Hajos and Parrish

Unfortunately, the proposed transition state was wrong. In addition, considering the aldolic reaction leading to the formation of a versatile synthetic chiral scaffold, they identified Proline as an interesting catalyst with biomimetic potential.

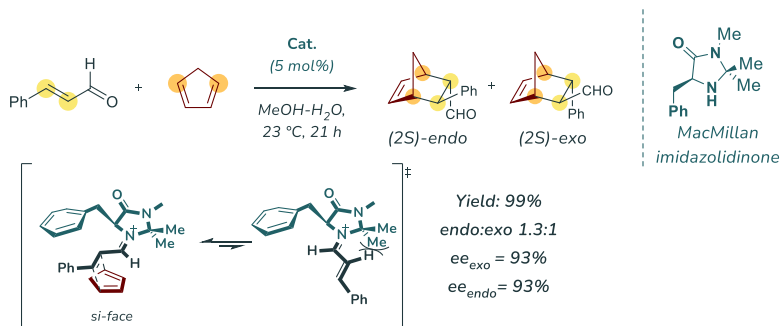
While List has explained the mechanism of the enamine reaction, the other pioneer David MacMillan coined with extreme elegance and vigour the term organocatalysis in his landmark article.²⁴ Additionally, he presented the enantioselective Diels-Alder performed with the imidazolidinone, a synthetic aminocatalyst extremely versatile.

In this remarkable work, the electrophilic position in the considered substrate has been activated via iminium ion (LUMO activation). The

²³ Z. G. Hajos, and D.R. Parrish, *J. Org. Chem.* **1974**, 39, 12.

²⁴ A. Kateri Ahrendt, C. J. Borths, D. W. C. MacMillan, *J. Am. Chem. Soc.* **2000**, 122, 4243.

iminium ion has the amine portion in the imidazolidinone positively charged and manages to attract to itself electrons of the condensed cinnamaldehyde by forming the dienophile in a conjugated position, that in presence of a diene (cyclopentadiene) undergoes a concerted electronic rearrangement to obtain the substituted norbornene (Scheme 1. 10).



Scheme 1. 10 First Highly Enantioselective Organocatalytic Diels-Alder Reaction

The high level of enantioselection of both products was validated with molecular modelling calculation in which is it possible to observe the steric hindrance of the benzylic group, that efficiently shields the possible approach from the front by the dienophile. This effect is further highlighted by the spatial arrangement of the iminium ion. In this case, the iminium ion assumes the *E* conformation to limit the additional steric interaction established with the two methyl groups in the alpha position.

Also as concerns the yield of the desired product, the MacMillan catalyst results more efficient than the proline used by List, in fact in the presented work, the catalyst loading was decreased at 5 mol% instead of the 30 mol%.

After these publications, which were considered milestones, asymmetric aminocatalysis assumed an enormous interest in the scientific community. In a very short time, impressive results were achieved such that, after a few years, this field of research was recognised as an independent area of organic chemistry.⁸

The ambitious goals that followed over the years focused not only on studying the applicability of these catalysts in synthesising

enantioenriched molecules but also on obtaining catalysts that were increasingly performing from the point of view of yield and enantioselection, or by found the optimal reaction conditions to perform it.

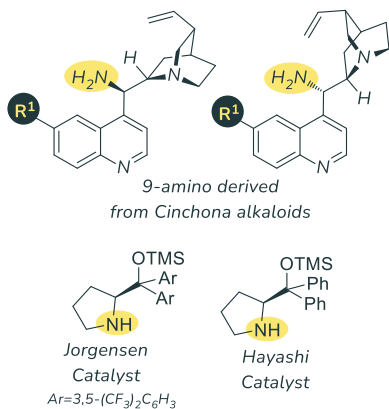


Figure 1. 12 Other aminocatalyst derived from Cinchona alkaloids or prolinols

activate two reactive partners in order to localise them more closely in a smaller reactive space (Figure 1. 12).

Worthy of mention are the bifunctional 9-amino-derivatives of Cinchona alkaloids catalyst. The primary amine function is employed to activate the ketones. The use of these alkaloids functionalised on stereocentre 9 with an amine group ensures the desired asymmetric induction in the final product as they are commercially available, and inexpensively, in their pseudo-enantiomeric forms. Other catalysts largely employed in asymmetric catalysis are represented from the Jorgensen-Hayashi catalysts, α,α -diphenyl prolinols ethers, in which is present the pyrrolidine ring as proline but with high hindering power derived from the presence of two phenyl groups.

The main difference between the use of proline or pyrrolidine derivatives, which are cluttered and functionalised on the hydroxyl group, lies in the geometry assumed by the transition state during the reaction. It is well

For this reason, a new generation of catalysts was synthesised. Derivatives of sterically encumbered natural compounds, for example, induce a more pronounced enantiofacial approach because the reactive intermediate formed by catalyst and substrate is more prone to react through a preferential spatial approach of the non-activated reagent. Or, still with biomimetic catalysis in perspective, bi- or multi-functional catalysts have been designed that can simultaneously

known that when using proline in a Michael addition reaction, for example, an intramolecular hydrogen bond is generated with the hydroxyl portion of the carbonyl acid of the amino acid (Figure 1. 13-A). This causes the activated compound to assume a predominantly *Re* facial geometry.

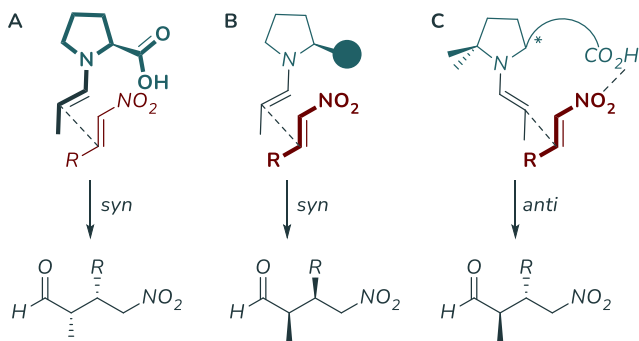


Figure 1. 13 Different approach with proline or its derivatives.

On the other hand, by using more cluttered catalysts or proline derivatives in which the hydroxyl group is protected, the enantioselection obtained is the opposite in that the steric interaction is favoured. In both cases, however, a *syn*-type addition is created between the two approaching reagents (Figure 1. 13-B).

In a recent article, Prof. Helma Wennemers' group reported a Michael reaction in which an *anti*-addition is observed. The peptide sequence used as an amino catalyst consists of a non-natural first proline residue in which the α^1 - position of the pyrrolidine ring is functionalised with two methyl groups. An *anti* addition is observed with this catalyst, because the generated enamine prefers to assume the *s-cis* conformation instead of the normal *s-trans* conformation (Figure 1. 13-C).

1.4 Organocatalysis drawbacks: how to overcome it and aim of the thesis

This thesis will discuss some of the strengths of asymmetric organocatalysis (in particular aminocatalysis) as a viable approach for the

synthesis of chiral compounds, focusing on possible ways to overcome some of the critical issues associated with the use of this synthetic approach.

Despite all the technological advances, there are still some critical points to overcome which are often found in the use of organocatalysis. In most cases, this effect is due to low substrate activation as catalysts exhibit low catalytic efficiency, or low turnover numbers (TON) and turnover frequencies (TOF) especially when it comes to covalent catalysis.²⁵

In the enamine activation, for example, the determinant kinetic step concerns the hydrolysis of the desired product and subsequent restoration of the catalyst to its active form. To encourage this step, an acidic co-catalyst is often added to increase the rate of hydrolysis by nitrogen protonation of the secondary base.²⁶ But this is only one of several approaches that have been tried. In another approach we can see the improvement of the catalytic performance, by using the bifunctional catalysts. The introduction of a second catalytic functional group into the chiral scaffold of the catalyst, that can interact and activate the second reactive partner, may provide a good improvement. The power of these catalysts is due to the proximity factors that direct the reactants to interact through a preferential stereo-approach. The only limitation is that these catalysts can only activate a restricted number of substrates as self-quenching reactions (e.g., acid-base reactions) may occur. Furthermore, not all catalyst combinations were synthesized to satisfy synthetic requirements, without considering these catalysts are often commercially available, but not very economical. To further expand the field of catalysis, many research groups have attempted to merely merge two, or more, reactive pathways by simultaneously employing two, or more, different catalysts that are capable of activating their respective reactive partners to provide an adequate activation of both intermediate

²⁵ X. Companyó, J. Burés, *J. Am. Chem. Soc.* **2017**, *139*, 8432.

²⁶ a) K. Patora-Komisarska, M. Benohoud, H. Ishikawa, D. Seebach, Y. Hayashi, *Helv. Chim. Acta.* **2011**, *94*, 719. b) X. Companyó, J. Bures, *J. Am. Chem. Soc.* **2017**, *139*, 8432.

to obtain this result (HOMO-LUMO activation).²⁷ This type of catalysis is called synergistic catalysis and supplies an alternative and complementary approach compared to bifunctional catalysis. The activated species can rapidly react, making reactions possible, that would otherwise be inefficient or even impossible with traditional mono- or bifunctional catalysis methods.

Because of this strategy, in addition to not having to synthesize the catalyst with the two different functionalities desired in the same structure, it is possible to expand the number of combinations between catalysts, to optimize the reaction under investigation. This approach, which is extremely versatile because of its rapidity of use, also shows how two different catalytic approaches can be used to form increasingly complex molecules. The merging of multiple catalytic paths, such as metal-organocatalysis, photo-organocatalysis, or organo-organocatalysis, opens indeed

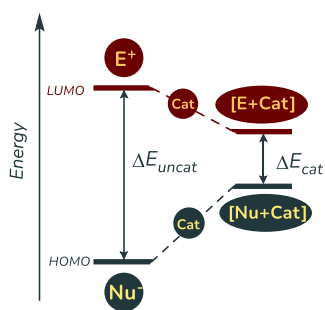


Figure 1. 14 Bi-catalysis HOMO-LUMO activation or synergistic activation

the possibility to screen several combinations of a wide range of catalysts for a particular reaction (Figure 1. 14).

In the chapter 2, was reported a study that concerns the increasing of catalytic efficiency by using peptidic heterogeneous phase organocatalysts that self-assemble in aqueous media, by exploiting supramolecular interaction.²⁸ Fibrils as supramolecular systems offer a good chiral environment to perform asymmetric reactions, as hydrophobic pockets are created between the different peptide monomers, allowing the reactants to locate themselves closer to the catalyst and approach it in a more enantioselective manner. The ease with which this catalyst can be prepared, from sequence synthesis to self-assembly, opens up the

²⁷ A. Sinibaldi, V. Nori, A. Baschieri, F. Fini, A. Arcadi, A. Carlone, *Catalysts* **2019**, 9, 928.

²⁸ A. Sinibaldi, F. Della Penna, M. Ponzetti, F. Fini, S. Marchesan, A. Baschieri, F. Pesciaioi, A. Carlone, *Eur. J. Org. Chem.* **2021**, 39, 5403.

possibility of exploring a whole range of organocatalysed reactions. In addition, aqueous media, used in this case as solvent and for triggering the fibrils self-assembly process, was also chosen to try to solve the problem related to the green aspects because it is an important aspect that the chemical society is turning its attention to is precisely the environmental impact of organic reactions. Green chemistry is a branch of organic chemistry, which emerged around the same time as organocatalysis, and has been developing considerably in recent years.²⁹ The renewed attention is due to the demand from governments to promote increasingly environmentally sustainable protocols requires a more comprehensive knowledge of this issue. Organocatalysis offers a good starting point in this instance, thanks to the intrinsic properties of many organocatalysts of high air and moisture tolerance, it has been possible to exploit these characteristics by carrying out the reactions in more eco-friendly solvents than those commonly used in organic synthesis, such as aqueous solvents. When water is used as a solvent, a positive increase in the kinetics of the organic reaction is most often observed. This is because organic reagents, which are hydrophobic, are prone to self-solvation in an attempt to limit their interactions with the aqueous medium. This leads to an increase in the local concentration of the reactants, which tend to occupy a limited volume instead of diffusing freely in the bulk solvent.

In Chapter 3 the optimisation of a synthetic process leading to the formation of a drug precursor, thus potentially applicable on an industrial scale, using water as the reaction solvent was reported.³⁰ In order to further emphasise the green aspect of the screening of the reaction conditions, was used a method that allows the identification of the optimal experimental condition through a limited number of experiments. More specifically, the strategy used relies on chemometric methods to

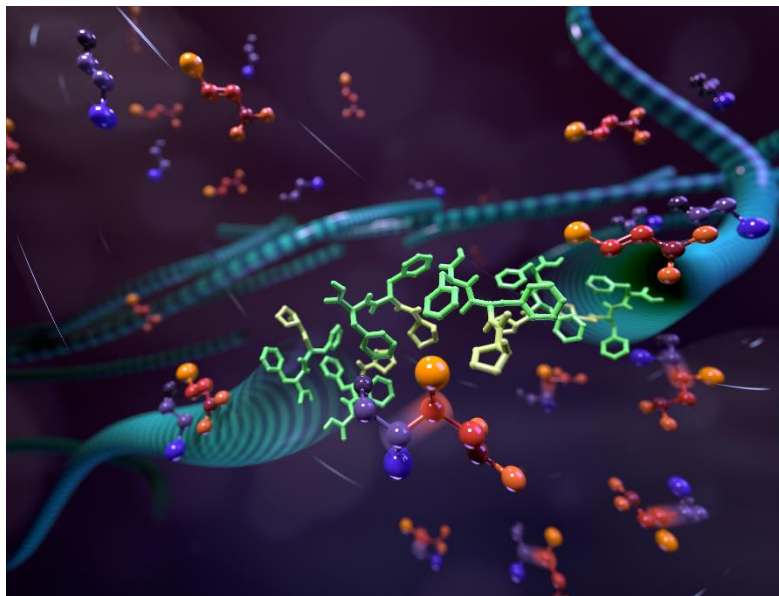
²⁹ A. Antenucci, S. Dughera, P. Renzi, *ChemSusChem* **2021**, *14*, 2785.

³⁰ V. Nori, A. Sinibaldi, G. Giorgianni, F. Pescioli, E. Di Cocco, F. Di Donato, A. Biancolillo, A. Landa, A. Carlone, *Chem. Eur. J.* **2022**, e202104524.

rationally explore the influence of selected experimental variables through the experimental design or DoE.

As a concluding chapter, we will see another strategy concerning the immobilisation of the catalyst on inert supports. Supported catalysis represents a valid approach to performing heterogeneous catalysis. This way, the catalyst could be subsequently reused and recycled. Generally, however, the activity of supported catalysts is lower than the one of their homogeneous counterpart. To gain a better understanding, the adsorption phenomena between the support-reagent that may affect catalysis were taken into account. The study of the T_1/T_2 ratio proved to be a robust NMR parameter for characterising the interactions between differently substituted molecules and solid surfaces.

Chapter 2: Asymmetric Organocatalysis Accelerated via Self-Assembled Minimal Structures



The following chapter reports an original research work in which the self-assembly was exploited to increase the catalytic efficiency of a supramolecular catalyst. With the goal of extremely simplifying biomimetic catalytic systems, the formation of tidy supramolecular structures from tripeptide sequences was found to be an efficient strategy. Starting, therefore, with a description of the peptide sequences used in asymmetric organocatalysis, the phenomena leading to the formation of supramolecular structures will subsequently be described and based on this, and limitations of organocatalysis, we thought we could exploit self-assembly to accelerate reactions.

2.1 Peptidic sequences in organocatalysis

Over the past decades, several research groups have focused their attention on the development of peptides as effective and useful asymmetric catalysts for various organic reactions.¹ The employment of short peptide sequences is a versatile alternative to the use of biocatalysis. The use of the latter strategy, as mentioned in chapter 1, for the synthesis of optically pure compounds is not at all trivial. Despite the high performance of enzymatic catalytic systems in terms of activity and enantiospecificity, their use is often confined to a limited range of applicability in terms of substrates and experimental conditions.²

A factor that significantly determines the catalytic efficiency of an enzymatic system is certainly the structural complementarity between substrates and the active catalytic site. When the catalytic sites, are in their native state in the correct folding, they expose the functional groups present in the side chains of the α -amino acid residues. This way the starting material can be activated and oriented in the chiral environment, therefore being at the appropriate distance to react. The complex folding that constitutes the active site allows α -amino acid residues, that are quite remote at the level of the primary structure, to be extremely close to each other in three-dimensional space so as to fulfil the catalytic function.³ The simplification of enzymatic systems is the subject of continuous study by many research groups, who have created an extensive library of peptide sequences that emulate the catalytic functions of enzymes satisfyingly but not of course with the catalytic perfection that distinguishes them. The chiral microenvironment and proximity factors are less stringent in the case of peptide catalysts, which

¹ H. Wennemers, *Chem. Commun.* **2011**, 47, 12036.

² T. Hoffmann, G. Zhong, B. List, D. Shabat, J. Anderson, S. Gramatikova, R. A. Lerner, C. F. Barbas III, *J. Am. Chem. Soc.* **1998**, 120, 2768.

³ M. Dias Gomes, *J. M. Woodley Molecules*, **2019**, 24, 3573.

allows the active site to be more accessible to a wider range of substrates to be activated.⁴

The structural control of the chiral pocket has been refined over the years through continuous studies of particular sequences that generate well-defined structural motifs. The use of peptides, besides favoring different types of activation by exploiting the different catalytic functionalities present in the side chains (such as acidic, basic, or coordinating functional groups), can lead to the formation of different structural motifs. These structural motifs mimic the secondary structure (α -helices and β -strands) of an enzyme. For example, there are extensively characterised peptidic sequences containing for example the dimer of dimethyl-glycine,⁵ or the sequence D-Proline-L-Proline,⁶ which can promote the β -turn motif.

Currently, peptide-mimesis *a priori* succeeds in designing prototypes of low molecular weight pseudo-enzyme structures, containing these conformational folds obtained from particular α -amino acid sequences,⁷ with the help of modern combinatorial techniques that at the computational level predict their folding.⁸ In addition, the simplicity of synthesising peptide chains at the chemical level has made them good candidates for the use in catalysis. The large structural variability, given by the 21 natural α -amino acids and the synthetic one, can give access to an unlimited number of sequences that can cover a wide spectrum of synthetic action not only limited to the formation of C-C bonds. Before the new era of asymmetric organocatalysis, several works have been

⁴ I. Rivilla, M. Odriozola-Gimeno, A. Aires, A. Gimeno, J. J. Barbero, M. Torrent-Sucarrat, A. L. Cortajarena, F. P. Cossio *J. Am. Chem. Soc.* **2020**, *142*, 2, 762.

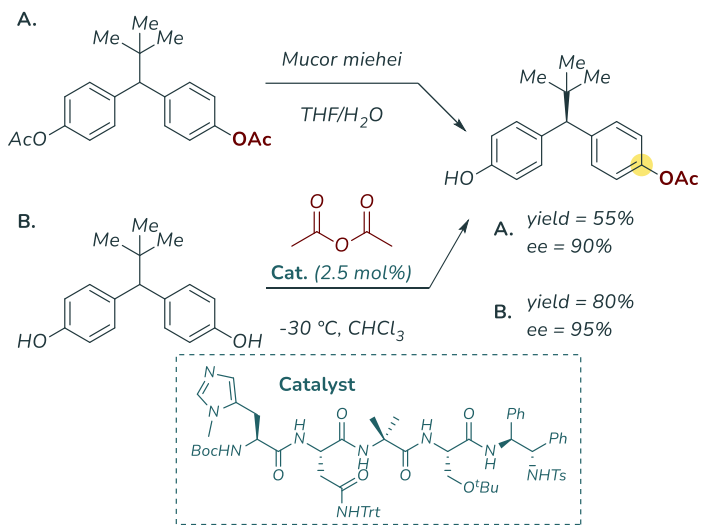
⁵ A. Buchberger, C. R. Simmons, N. E. Fahmi, R. Freeman, N. Stephanopoulos *J. Am. Chem. Soc.* **2020**, *142*, 3, 1406.

⁶ M. Wiesner, M. Neuburger, H. Wennemers, *Chem. Eur. J.* **2009**, *15*, 10103.

⁷ a) E. A. Colby Davie, S. M. Mennen, Y. Xu, S. J. Miller, *Chemical Reviews* **2007**, *107*, 12; b) H. Wennemers, R. T. Raines, *Curr. Opin. Chem. Biol.*, **2008**, *12*, 690.

⁸ J. D. Revell and H. Wennemers *Current Opinion in Chemical Biology* **2007**, *11*, 269.

published aiming at using peptide sequences such as, for example, in asymmetric hydrocyanation reactions⁹ or Julià-Colonna epoxidations.¹⁰



Scheme 2. 1 Desymmetrisation performed with peptide sequence

The rudimentary peptide structures were refined over the years in an attempt to increase their catalytic performance while decreasing the catalyst loading. Peptides are also employed for the desymmetrisation process, such as a key intermediate as pharmaceutical drug candidate.¹¹ Miller and co-workers, reported the discovery process employed a powerful peptide-based to lead asymmetric remote acylation reaction on a prochiral stereocentre (distance larger than than 5.7 Å; Scheme 2. 1).

⁹ J.I. Oku, N. Ito, S. Inoue, *Makromol Chem* **1979**, 180, 1089.

¹⁰ S. Julià, J. Guixer, J. Masana, J. Rocas, S. Colonna, R. Annunziata, H. Molinari, *J Chem Soc Perkin Trans I* **1982**, 1317.

¹¹ a) C. A. Lewis, A. Chiu, M. Kubryk, J. Balsells, D. Pollard, C. K. Esser, J. Murry, R. A. Reamer, K. B. Hansen, S. J. Miller, *J. Am. Chem. Soc.* **2006**, 128, 16454; b) C. A. Lewis, J. L. Gustafson, A. Chiu, J. Balsells, D. Pollard, J. Murry, R. A. Reamer, K. B. Hansen, S. J. Miller, *J. Am. Chem. Soc.* **2008**, 130, 16358.

The first example of an enantioselective bromination mediated by a tetrapeptide as a catalyst, in which there is a tertiary amine acting as a Brønsted base, was also reported by Miller in 2013.¹² This catalyst was able to promote the formation of atropoisomers with two chiral axes. However, tertiary benzamides were appropriately chosen as the starting substrate, as they have sufficiently high barriers to racemisation after ortho functionalisation (Scheme 2. 2).

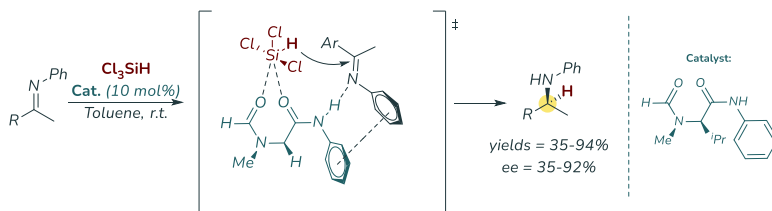


Scheme 2. 2 Enantioselective bromination mediated by a tetrapeptide

In presence of several H-bond acceptor and donor sites, peptides can also be exploited to catalyse reactions via weak interactions. An example, reported by in 2004,¹³ in regards to the use of an unnatural dipeptide that promotes the asymmetric reduction of ketimines (Scheme 2. 3). The catalyst succeeds to activate the reactive partners through three different weak interactions instead of a covalent interaction: the amidic proton of the catalyst forms a hydrogen bond with the nitrogen of the ketimine and a π - π staking interaction with the aromatic portion, while the two oxygen atoms coordinate the hydride donor. The spatial rearrangement ensures good enantioselectivity of the desired product.

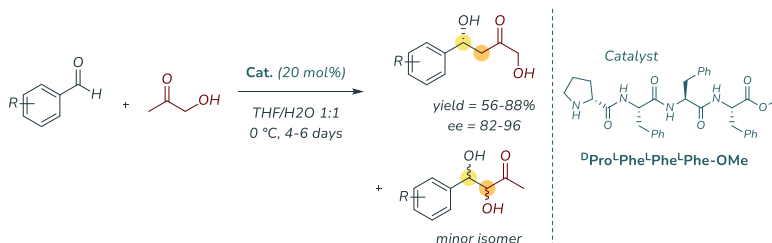
¹² a) K. T. Barrett, S. J. Miller *J. Am. Chem. Soc.* **2013**, *135*, 2963; b) K. T. Barrett, A. J. Metrano, P. R. Rablen, S. J. Miller, *Nature* **2014**, *509*, 71

¹³ A. V. Malkov, A. Mariani, K. N. MacDougall, P. Kocovsky *Org. Lett.* **2004**, *6*, 13, 2253.



Scheme 2. 3 asymmetric reduction of ketimines mediated by weak interactions.

As concerning the C-C bond formation, Gong et al synthesised a peptide sequence containing a proline residue linked to three phenylalanine residues in which the C-terminal portion was protected as an ester.¹⁴ The reaction shown in Scheme 2. 4, is an aldolic reaction between hydroxyacetone and differently substituted benzaldehydes on the aromatic ring. The predominant obtained product is the 1,4 adduct. In addition to providing good enantioselection, it is quite interesting as the peptide catalyst manages to address with good regioselective control. In fact, by using proline as a catalyst the formation as a major adduct the product derived by the 1,2 attack (minority product obtained from Gong) is observed with values >20:1 of regioselectivity.¹⁵⁻



Scheme 2. 4 Aldol reaction with formation of majority adduct 1,4.

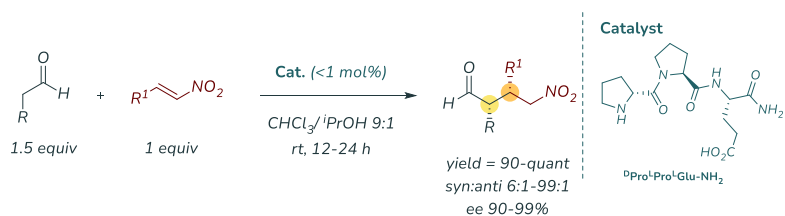
A noteworthy example was reported by Wennemers research group. For years they have shown a strong interest in catalytic systems containing peptides with heterochiral sequences that can promote 1,4-addition reactions between aldehydes and nitro-olefines in organic solvent

¹⁴ Z. Tang, Z.-H. Yang, L.-F. Cun, L.-Z. Gong, A.-Q. Mi and Y.-Z. Jiang, *Org. Lett.* **2004**, *6*, 2285.

¹⁵ W. Notz, B. List, *J. Am. Chem. Soc.* **2000**, *122*, 7386.

mixtures. A particular sequence, resulting from a perfect balance of structural complementarity characteristics, has been thoroughly studied as it showed a high catalytic efficiency, the ^DPro^L-Pro^L-Glu-NH₂ (Scheme 2. 5).

The sequence studied can establish three intramolecular hydrogen bonds (observed with NMR techniques¹⁶ thanks to the presence of a single terminal residual of β-amino acid (Glu)¹⁷ in which the amino-terminal group is present. The resulting stabilization considerably stiffens the tertiary structure by folding the tripeptide into a β-sheet motif.



Scheme 2. 5 Michael addition performed with heterochiral peptide sequence

The excellent catalytic performance of the peptide ^DPro^L-Pro^L-Glu-NH₂ when it is used in the asymmetric 1,4-addition reaction of aldehydes to nitro-olefines, is the result of numerous optimization studies involving solvent, ionic strength, and additives used as co-catalysts.¹⁸ This has implied a drastic reduction in catalyst loading which was reduced by up to $\leq 1\text{ mol}\%$.¹⁹ An extremely low value when compared to the catalyst loading required to carry out the same reaction using proline as an asymmetric organocatalyst.²⁰

¹⁶ C. Rigling, J. K. Kisunzu, J. Duschmalé, D. Häussinger, M. Wiesner, M. O. Ebert, H. Wennemers, *J. Am. Chem. Soc.* **2018**, 140, 10829.

¹⁷ T. Schnitzera, H. Wennemers, *Helv. Chim. Acta* **2019**, 102, e1900070

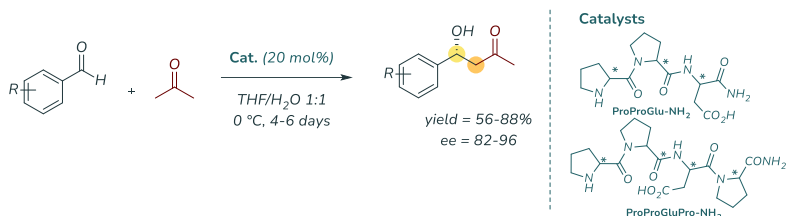
¹⁸ M. Wiesner, M. Neuburger, H. Wennemers, *Chem. Eur. J.* **2009**, 15, 10103.

¹⁹ M. Wieser, G. Upert, G. Angelici, H. Wennemers, *J. Am. Chem. Soc.* **2010**, 132, 1, 6.

²⁰ T. Schnitzer, M. Wiesner, P. Krattiger, H. Wennemers, *Org. Biomol. Chem* **2017**, 15, 5877.

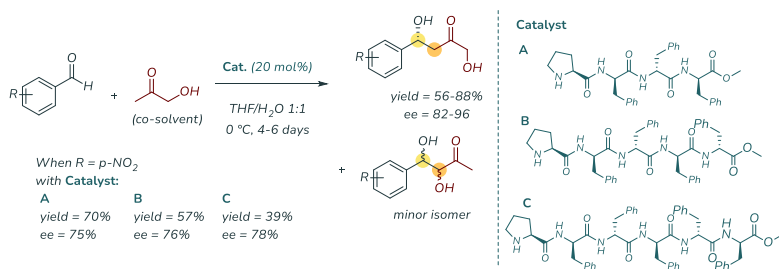
However, increasing structural complexity, starting from reactions in which proline as a monomer is used at high loading (often more than 10 mol%) towards the use of increasingly refined peptide structures, frequently does not lead to an improvement of catalytic performance. Indeed it further demonstrates the power of the optimised structure identified by Wennemers group, a study conducted in her laboratory has reported all possible diastereoisomers of related tri- and tetrapeptidic catalysts of the type *H*-Pro-Pro-Glu/Asp-NH₂ and *H*-Pro-Pro-Glu/Asp-Pro-NH₂ in which they compared their catalytic performance in aldol and conjugated addition reaction (Table 2. 1). In each reported case, the peptidic sequences showed an increase of yield compared to a single amino acid proline, but only the tripeptide ProProGlu-NH₂ has the structural requirements for high catalytic efficiency.

Table 2. 1 Aldol reaction: Effect of different chiral centres on catalyst performance



Entry	Peptide	Conv.	(S)-ee%
1	LLL	Quant. (4h)	80
2	LLLL	Quant. (6h)	75
3	LLLD	Quant. (6h)	74
4	DLL	50	-45
5	DLLL	10	-40
6	LDDL	5	-40
7	LDL	50	31
8	LDLL	10	17
9	LDLD	5	11
10	DDL	50	-46
11	LLDL	10	46
12	LLDD	5	30

Another example was reported in 2004 by Jiang and coworkers.²¹ They published an interesting paper regarding an enantioselective direct aldol reaction (the same one shown in Scheme 2. 4), in which the catalytic effect of homologous peptide series was considered. Using an N-terminal Proline sequence bonded to three, four, or five residues of phenylalanine, different substituted benzaldehydes and hydroxyacetone were screened (Scheme 2. 6). In each reported entry, by using tetrapeptide as a catalyst, the yield was higher than by employing penta- or hexapeptide, while a comparable enantiomeric excess was obtained. Moreover, also the reaction time was longer for the superior homologues catalysts.



Scheme 2. 6 Aldol reaction: Effect on performance for a series of homologous catalysts

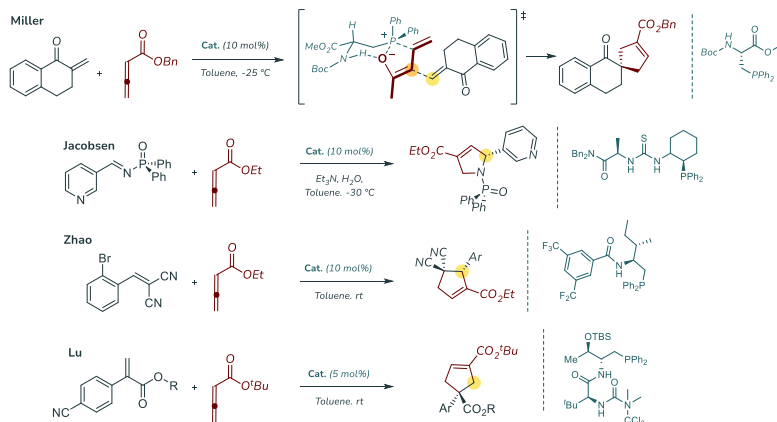
By using different functionalised amino acids, synthetically produced, many research groups focused their study on the bifunctional activation. For example, the β -amidophosphines as catalyst, are widely used to promote the [3+2]-cycloadditions reaction with a high level of stereocontrol. This result was rationalised by Houk research group supported by computational studies.²² The theoric reported all models for the transition state that showed the instauration of intermolecular hydrogen bond between the N-amino portion of the derived amino acid and electrophile (or nucleophile reagent in the case of Miller study)²³ the

²¹ Z. Tang, Z.H. Yang, L.-F. Cun, L.-Z. Gong, A.-Q. Mi, Y. Z. Jiang, *Org. Lett.* **2004**, 6, 13, 2285.

²² Y.-H. Lam, M. N. Grayson, M. C. Holland, A. Simon, K. N. Houk, *Acc. Chem. Res.* **2016**, 49, 750.

²³ B. J. Cowen, S. J. Miller, *J. Am. Chem. Soc.* **2007**, 129, 10988.

stabilisation of the negative charge of the generated enolate mediated by the phosphines moiety (Scheme 2. 7).²⁴



Scheme 2. 7 Selected examples of bifunctional catalysts containing α -aminoacidic residues

It is important to note that the excellent enantioselectivity is due to the high catalyst loading (in almost all cases reported, the percentage is 10 molar) and the low temperature, which guarantees a good conversion into the desired result product.

2.2 Self-assembly and supramolecular structures

Self-assembly is generically defined as a process in which a disordered system of monomeric components forms an organised structure with a considerable degree of order in three spatial dimensions.

The self-assembly process can occur in several ways: co-assembly, direct self-assembly or step-wise self-assembly. In all of these, there is always an initial pre-organisation in which the building blocks form a first-order

²⁴ a) H. Xiao, Z. Chai, C.-W. Zheng, Y.-Q. Yang, W. Liu, J.-K. Zhang, G. Zhao, *Angew. Chem. Int. Ed.* **2010**, 49, 4467. b) Y. Q. Fang, E. N. Jacobsen, *J. Am. Chem. Soc.* **2008**, 130, 5660. c) X. Han, Y. Wang, F. Zhong, Y. Lu, *J. Am. Chem. Soc.* **2011**, 133, 1726. d) H.-P. Deng, D. Wang, Y. Wei, M. Shi, *Beilstein J. Org. Chem.* **2012**, 8, 1098.

structural motif that subsequently organises into increasingly complex structures.

When the self-assembly process is triggered by an external stimulus, the system under consideration proceeds from a state of non-equilibrium to a state of thermodynamic equilibrium in which the Gibbs free energy of the individual isolated molecules is greater than that of the self-assembled structure.²⁵

The types of trigger can be manifold, depending on the properties of the monomer unit under consideration. The driving force is the variation of electrostatic interaction, which can give rise to long- and short-range interactions, even at the nanometric scale, that defines the degree of cross-linking of the self-assembled compound. This in turn can be modified by making appropriate solvents, pH, and counterion changes that stabilise the net, or partial, charges that are generated during the assembly process.

A source of stabilisation in the self-assembly process is due to the interaction with the solvent medium. By using polar solvent, the stabilisation of the charges is also affected by this, but if the solvent is apolar, the stabilisation only involves the subunits of building blocks, which attempts to minimise solvophobic interactions, and form a dense network of weak non-covalent bonds between themselves. The degree of hydration of the monomers also clearly influences the anisotropy of the system, since the first hydration sphere will also be involved in the stabilisation process.²⁶

The pH variation is exploited when a protonable or deprotonable functional group is present in the monomer unit, such as the N-terminal and C-terminal groups of peptide chains. For example, by increasing the pH of a solution in which there are residues containing carboxyl groups,

²⁵ N. Singh, M. Kumar, J. F. Miravet, R. V. Ulijn, B. Escuder, *Chem. Eur. J.* **2017**, *29*, 981.

²⁶ H. Jin, Y. Zhou, W. Huang, D. Yan, *Langmuir* **2010**, *26*, 18, 14512.

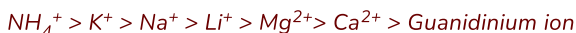
it is possible to maximise electrostatic repulsion, while decreasing the pH will encourage these monomer units to move closer together.²⁷

The appropriate choice of counteranions, on the other hand, stabilises the positive or negative charge by forming a tight ion pair. As is well known in the literature, the stabilisation of a protein is a concept that has been classified using the Hofmeister series (or lyotropic series) by which the ability of the protein to salting-in and salting-out is measured. Generally anions have a stronger ability than cations to solubilise (salting-in) and stabilise the peptide, or protein, when dissolved in aqueous solvents.²⁸ This is because the lyotropic effect increases when the radius of the counterion decreases, as closer ionic pairs are generated.

Anion



Radius



Cation

Figure 2. 1 Hofmeister Liotropic Series

For instance, to observe protein precipitation in an aqueous medium, the presence of sulphate and phosphate ions (kosmotropes agents) can promote salting-out as these ions are strongly solvated by the medium (Figure 2. 1). This favours the folding of the proteins themselves, which tend to elude the hydrophobic effect by auto-solvating on their own.

In the biological molecules, the self-assembly follows a refined hierarchical structure operated in millennia of evolution. In the artificial

²⁷ M. Tena-Solsona, B. Escuder, J. F. Miravet, Chem. Mater. **2015**, 27, 3358.

²⁸ a) J. Paterová, K. B. Rembert, J. Heyda, Y. Kurra, H. I. Okur, W. R. Liu, C. Hilty, P. S. Cremer, P. Jungwirth, J. Phys. Chem. B **2013**, 117, 8150. b) S. Roy, N. Javid, P. W. J. M. Frederix, D. A. Lamprou, A. J. Urquhart, N. T. Hunt, P. J. Halling, R. V. Uljij, Chem. Eur. J. **2012**, 18, 11723.

system, the hierarchical organization is less efficient since the complex equilibrium of various driving forces is not compensated excellently.²⁹

The advancement of the study of proteins as macromolecules and their characterization has taken place through sophisticated sequencing and imaging techniques (mainly X-rays) that allowed us to evaluate which structural correlations occurred between the α -amino acid sequence and the tertiary and quaternary structure. This has made it accessible to chemists to study numerous strategies to maximize the probability to obtain short synthetic sequences, derived from bio-molecules, that can self-assemble by non-covalent interactions trying to recreate what happens in biological molecules.

By examining, for example, the use of a short peptide sequence as a self-assembling system rather than an enzyme, the main difference found concerns molecular polydispersion in the solvent bulk. The interactions that bind monomers to each other are generally of a non-covalent supramolecular nature, and it is therefore very difficult to control the length and size of supramolecular aggregates. In the latter, there are many translational and rotational degrees of freedom compared to enzymes, and this results in a large number of metastable states that offer the possibility of interconverting into different conformations as they possess low kinetic barriers.³⁰

2.2.1 Selected examples

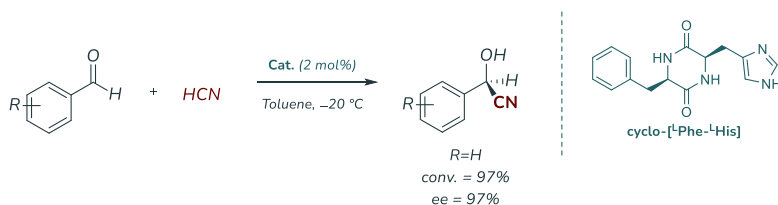
Many research groups today have been fascinated by the possibility of recreating a self-assembled minimalist catalytic system as an intermediate evolutionary system between homogeneous catalysis using low molecular weight molecules and enzymes, in combination with the possibility to study them as simplified models of enzymes in order to understand their complex functioning.³¹

²⁹ Y. Lu, J. Lin, L. Wang, L. Zhang, C. Cai, *Chem. Rev.* **2020**, *120*, 9, 4111.

³⁰ N. Singh, M. Kumar, J. F. Miravet, R. V. Uljijn, B. Escuder, *Chem. Eur. J.* **2017**, *23*, 981.

³¹ G. Gulseren, M. A. B. Tekinay, M. O. Guler, *J. Mater. Chem. B* **2016**, *4*, 4605.

In an early study of supramolecular chemistry in 1990 Inoue and co-workers reported the using of a cyclic dipeptide as a catalyst, which consisted of phenylalanine and histidine.³² It was employed in the asymmetric addition reaction of hydrogen cyanide on substituted benzaldehydes **Scheme 2. 8**). In this study, the authors reported that, in the experimental conditions under which they operated, a gel is formed and that the formation of this gel generated an increase in the enantioselection of the reaction.



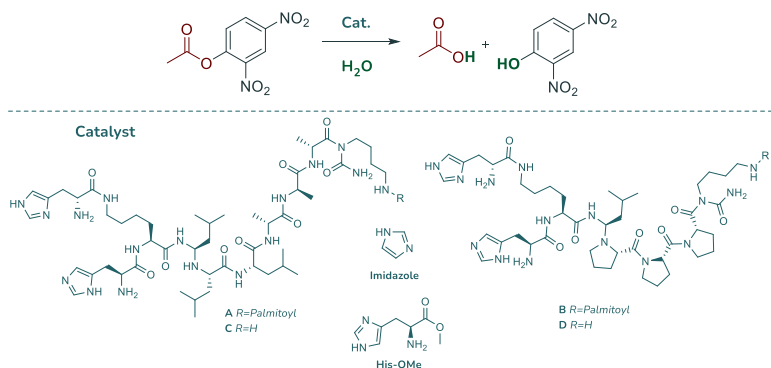
Scheme 2. 8 Asymmetric addition reaction of hydrogen cyanide on substituted benzaldehydes

They observed an increase in the racemization of the product when the reaction mixture underwent a gel-to-sol transition, which they did not notice when the reaction was set at lower temperatures. They obtained (S)-(+)-mandelonitrile in 95% yield with ee of 93% in toluene, although the supramolecular structure was not extensively characterised.

The first example of catalysis aimed at obtaining a supramolecular catalyst that was a valid bridge between enzymatic catalysis was reported by Guler and Stupp.³³ In this article, the authors synthesised a library of amphiphilic peptide catalysts capable of self-assembling into nanostructures, in which a histidine-core is present, in an attempt to mimic a hydrolytic enzyme. 2,4-dinitrophenyl acetate was chosen as a model substrate and conversion was assessed through kinetic studies. By comparing the yield of hydrolysis with the different catalysts, the authors observed a significant increase in the desired product when the system considered had a higher level of order (Scheme 2. 9).

³² K. Tanaka, A. Mori, S. Inoue, *J. Org. Chem.* **1990**, *55*, 181.

³³ M. O. Guler, S. I. Stupp, *J. Am. Chem. Soc.* **2007**, *129*, 12082.



Scheme 2.9 Biomimicking of a hydrolytic enzyme performed with peptide sequences

In particular, with catalyst **A** that formed supramolecular nanofibres internally ordered as catalytic particles, they found a higher reaction rate compared with the use of catalysts that were capable of forming spherical aggregates (**B**, **C**, and **D**) with less supramolecular order or the homogeneous catalysts (**His-OMe** and **Imidazole**).

In a subsequent study, even more minimal sequences were investigated to assess the catalytic efficiency of co-assembled supramolecular systems in the above-mentioned hydrolysis reaction.³⁴

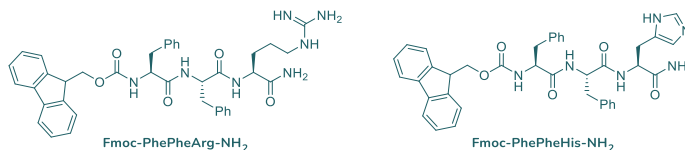


Figure 2.2 Monomeric units of α -amino acids to obtain a co-assembled supramolecular structure

The sequences in question are *Fmoc* tripeptides protected in the *N*-terminal residue in which the *C*-terminal amide residue has been varied

³⁴ Z. Huang, S. Guan, Y. Wang, G. Shi, L. Cao, Y. Gao, Z. Dong, J. Xu, Q. Luo, J. Liu, *J. Mater. Chem. B* **2013**, *1*, 2297.

(Figure 2. 2). In the first sequence we find a histidine (as in the case reported by Stupp) and in the second one an arginine.

When these two units are co-assembled in the appropriate ratio, nanotubes are generated in which there is a double activation. This supramolecular structure was drawn specifically to obtain an extremely efficient catalytic system since the catalytic centre (His) and the guanidyl groups stabilise the transition state of the hydrolytic reaction even more strongly than if the two sequences were used individually, thus that the supramolecular PepNTs-His-Argmax structure was able to accelerate the hydrolysis reaction markedly enough to show a saturation kinetic behaviour typical of that of natural enzymes.

Very often the examples reported in the literature of self-assembled systems containing amino acids possess a polar head, consisting of one residues of amino acid or a short peptide sequence, linked to long alkyl chains. These amphipathic units have been used to generate supramolecular structures because they are able to aggregate supramolecularly using the desire to escape from the solvent medium as a driving force.

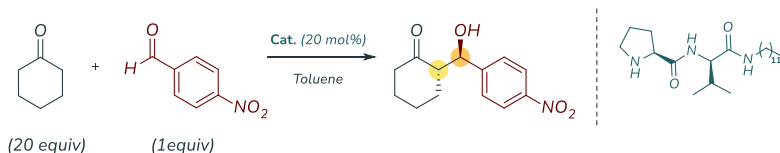
In a 2009 paper, Escuder reported an L-proline-based supramolecular hydrogel that is capable of self-assembling to form double layers that were used as an efficient organocatalyst for the direct aldol reaction with high stereoselection.³⁵

The sequence, previously optimised by the same group to improve the morphological characteristics of the gel, showed excellent organocatalytic properties in terms of yield and enantioselection only when the reaction was conducted by decreasing the temperature (from 25 °C to 5 °C) with the addition of an organic co-solvent layered above the gel surface. When the reagents were placed in direct contact with the gel (formed by the peptide and water), although the NMR yield was greater than 99%, the asymmetric induction obtained was very low (dr

³⁵ F. Rodríguez-Llansola, J. F. Miravet, B. Escuder, *Chem. Commun.* **2009**, 7303.

75:25; ee = 12%). When the reagents were previously dissolved in toluene, however, only the diastereomeric ratio increased.

Table 2. 2 Aldol reaction performed with L-proline-based supramolecular hydrogel



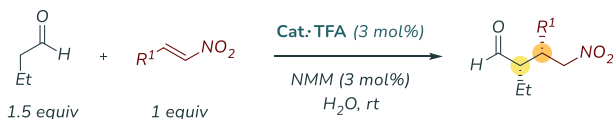
Entry	T (°C)	t (h)	Yield	anti:syn	ee
1 ^a	25	36	>99%	75:25	12
2	25	16	>99%	91:9	18
3	5	24	98%	92:8	88
4 ^b	5	24	>99%	93:7	87
5 ^c	5	24	>99%	92:8	90

^aWithout Toluene; ^b entry 3 second run; ^c entry 3 third run.

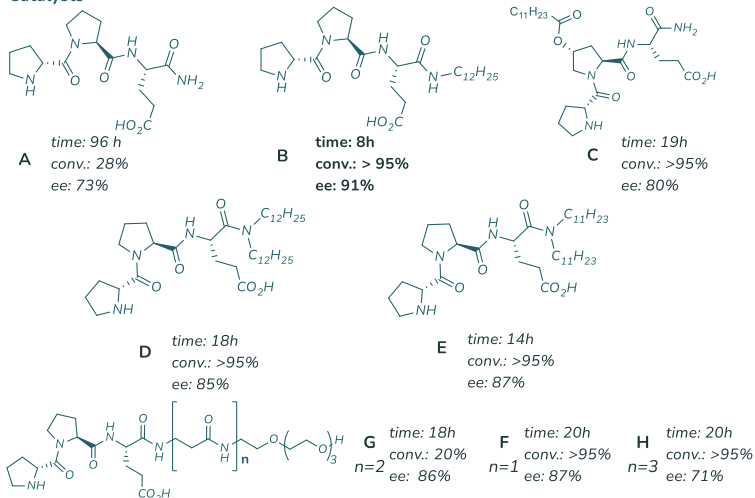
The combined effect of temperature and organic co-solvent led to the formation of the desired product with an excellent enantiomeric excess. The same authors reported the importance of the organic co-solvent in facilitating the diffusion of the *para*-nitro benzaldehyde, which is poorly soluble in water, within the hydrophobic region of the gel to penetrate better the catalytic sites where cyclohexanone is bound as enamine. Furthermore, the use of these solid-like heterogeneous phase catalysts has the advantage that they can be reused for at least three cycles.

Also the catalytic behaviour of some peptide sequences as a catalyst that are capable in the water of forming emulsions has been studied as a catalyst.³⁶ The catalysts examined are short peptide sequences functionalised in the C-terminal portion in the form of amides with long alkyl or polyoxygenated chains (Scheme 2. 10).

³⁶ J. Duschmalé, S. Kohrt, H. Wennemers, *Chem. Commun.* **2014**, 50, 8109.



Catalysts



Scheme 2. 10 Michael reaction performed with different peptides containing alkyl or polyoxygenated chains

The long apolar chains inserted into the structural motif are inclined to arrange themselves in contact with each other, forming micellar aggregates that generate a chiral hydrophobic microenvironment. This results in the stabilisation of the reagents, which tend to confine themselves to a much smaller space than the entire solvent bulk, with a consequent increase in local concentration. Operating under these conditions, and by comparing the same reaction performed in water with a catalytic system in which only the peptidic $^D\text{ProProGlu}$ sequence is present (in which the aliphatic chain is not present), an increase in reactivity has been observed, with good results also concerning enantiomeric excess. To try to optimise these results, experiments were also carried out by varying the pH of the solvent medium or by adding organic co-solvents. For pH variation, an acidic environment (NaHSO_4

1M) inhibited the reaction, while a basic pH (pH >8) decreased the enantioselection for the base-catalysed background racemisation reaction.³⁷ On the other hand, the addition of organic co-solvents increased the enantioselection of the reaction (ee=95% with a mixture 85:15 of H₂O/CHCl₃).

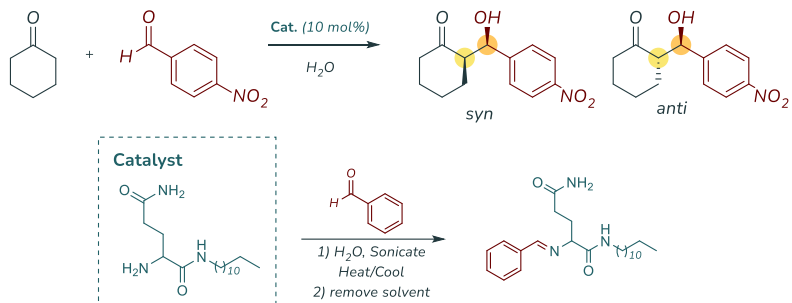
Very often, however, it is not so simple to carry out catalysis with these catalytic systems and in a recent example reported in the literature has shown how the use of gels made up of low molecular weight of a glutamine amide derivative is extremely difficult to use because the three-dimensional structure of the gel may not be stable under the chosen reaction conditions.³⁸

In the cited example, the authors initially showed the optimisation of the triggering conditions in different solvents (gelators) at different concentrations, which led to the sol-gel transition of a glutamine amide derivative. (Scheme 2. 11) The solvents that triggered partial gel formation were acetonitrile, tetrahydrofuran, and toluene, whereas, the formation of gel resistant even to vial inversion was found using cyclohexane and water.

The formed gel was exploited for its catalytic potential in the aldolic reaction between *p*-nitrobenzaldehyde and cyclohexanone. The catalyst generated the desired product in good yield (98%) but with a low enantioselection (ee_{anti}=32%, ee_{syn}=11%, d.r.=1.3:1). The authors themselves report that the gel is not stable and reproducible for catalysis because the system is highly heterogeneous.

³⁷ F. Rodríguez-Llansola, B. Escuder, J. F. Miravet, *Org. Biomol. Chem.* **2009**, *7*, 3091.

³⁸ K. Hawkins, A. K. Patterson, P. A. Clarke, D. K. Smith, *J. Am. Chem. Soc.* **2020**, *142*, 4379.



Scheme 2. 11 Aldol reaction and collateral reaction

In an attempt to verify the stability conditions of the gel, the authors examined the interaction between the gel and the two reagents separately. Only the addition of benzaldehyde promoted gel formation, but not cyclohexanone, since the *para*-nitrobenzaldehyde forms a Schiff base with the *N*-terminal residue, thus forming a two-component gel in dynamic equilibrium with the non-bonded form.

However, it was only by performing heating-cooling cycles that they noticed that the stability and reproducibility of this gel were increased.

Abstract: Self-assembling minimalistic peptides embedded with an organocatalytic moiety were designed. By controlling the formation of fibrils via external intervention, it was shown that the activation is accelerated when the organocatalyst is in its supramolecular state. The effect of the accelerated catalysis was demonstrated in a Michael benchmark reaction.

2.3 Target of the project

Recently, a different approach to organocatalysis has been devised at the supramolecular level; with a range of different designs, and inspired by the catalytic systems previously developed, molecular machines, embedded with organocatalytic moieties, have been used for controlling chemical reactions.³⁹ Within these systems, mechanical motion impressively enabled the control of catalysis, albeit at a level that cannot compete with the typical molecular catalysis. Additionally, besides the reactivity and enantiocontrol of the system, the complexity of assembling a molecular machine makes the development of new efficient catalysts an enormous challenge. On the other hand, self-assembling short peptides have attracted great interest in recent years as versatile building blocks for functional nanostructures in a variety of applications.⁴⁰ Derivatives of the dipeptide Phe-Phe stand out amongst other structural motifs, thanks to the high propensity towards fibrillization in a variety of solvents, and the finding that many aromatic N-caps template self-assembly, giving scope for chemical diversity of the building blocks.⁴¹ This kind of building blocks typically associates into β -structures, which are held together by the ordered hydrogen bonding

³⁹ For selected examples, please see: a) V. Blanco, A. Carlone, K. D. Hänni, D. A. Leigh, B. Lewandowski, *Angew. Chem. Int. Ed.* **2012**, *51*, 5166; b) L. van Dijk, M. J. Tilby, R. Szpera, O. A. Smith, H. A. P. Bunce, S. P. Fletcher, *Nat. Rev. Chem.* **2018**, *2*, 0117; c) C. Biagini, S. Di Stefano, *Angew. Chem. Int. Ed.* **2020**, *59*, 8344; d) G. Olivo, G. Capocasa, D. Del Giudice, O. Lanzalunga, S. Di Stefano, *Chem. Soc. Rev.* **2021**, *50*, 7681.

⁴⁰ J. Raeburn, A. Z. Cardoso, D. J. Adams, *Chem. Soc. Rev.* **2013**, *42*, 5143.

⁴¹ S. Marchesan, A. V. Vargiu, K. E. Styan, *Molecules* **2015**, *20*, 19775.

between peptide amides, hydrophobic interactions and π -stacking.^{41,42} The tendency to undergo self-assembly of an oligopeptide is strictly dependent on its structure, since ordered aggregation is the result of a careful balance between hydrophobic and hydrophilic forces.⁴³

We surmised that self-assembling minimalistic peptides embedded with an organocatalytic moiety could be designed. This way, an easily prepared peptide could function as an enhanced organocatalyst in its supramolecular assembly, exhibiting features that typical catalysts do not possess, by creating a lipophilic pocket, and by excluding water from its structure. Furthermore, it may improve the activation of organic reagents by the cooperative interaction of different functions of the structure, or its activity be switched on and off, or from one type of catalysis to another.⁴⁴ It must be noted that there are examples, albeit limited, of simple catalytic activity, that is displayed at appreciable rates once the self-assembled structure is created.^{45,46}

Therefore, through the creation of self-assembling organocatalysts, which consist of short peptide derivatives made with amino acids with natural side chains, it is possible to create a new generation of enzyme mimetic catalysts with supramolecular hydrophobic pockets that may

⁴² X. Du, J. Zhou, J. Shi, Bing Xu *Chem. Rev.* **2015**, *115*, 13165.

⁴³ a) A. M. Garcia, D. Iglesias, E. Parisi, K. E. Styan, L. J. Waddington, C. Deganutti, R. De Zorzi, M. Grassi, M. Melchionna, A. V. Vargiu, S. Marchesan, *Chem* **2018**, *4*, 1; b) S. Panja, D. J. Adams, *Chem. Soc. Rev.* **2021**, *50*, 5165.; c) A. Lampel, *Chem* **2020**, *6*, 1222.

⁴⁴ O. Zozulia, M. A. Dolan, I. V. Korendovych, *Chem. Soc. Rev.* **2018**, *47*, 3621.

⁴⁵ a) A. M. Garcia, M. Kurbasic, S. Kralj, M. Melchionna, S. Marchesan, *Chem. Commun.* **2017**, *53*, 8110; b) C. Zhang, R. Shafi, A. Lampel, D. MacPherson, C. G. Pappas, V. Narang, T. Wang, C. Maldarelli, R. V. Uljin, *Angew. Chem. Int. Ed.* **2017**, *56*, 14511; c) W. Fang, Y. Zhang, J. Wu, C. Liu, H. Zhu, T. Tu, *Chem. Asian J.* **2018**, *13*, 712; d) A. Reja, S. P. Afrose, D. Das, *Angew. Chem. Int. Ed.* **2020**, *59*, 4329; e) O. Zozulia, L. R. Marshall, I. Kim, E. M. Kohn, I. V. Korendovych, *Chem. Eur. J.* **2021**, *27*, 5388; f) M. Díaz-Caballero, S. Navarro, M. Nuez-Martínez, F. Peccati, L. Rodríguez-Santiago, M. Sodupe, F. Teixidor, S. Ventura *ACS Catalysis*, **2021**, *11*, 2, 595.

⁴⁶ For an interesting report of a catalytic heterochiral peptide system in organic solvent mixtures, that does not seem to display enhanced catalytic activity in its supramolecular structure, please see: M. Wiesner, M. Neuburger, H. Wennemers, *Chem. Eur. J.* **2009**, *15*, 10103.

bind and activate substrates also in non-conventional water-based solvents, through the creation of microenvironments able to host organic reagents.

In particular, proline is a useful building block in light of its prominent role in organocatalysis. Amphiphiles containing this amino acid were studied for their ability to catalyse Mannich reactions in their assembled state.⁴⁷ Combined with cinchona alkaloids, proline yielded supramolecular catalysts for diastereoselective and enantioselective domino Mannich/aza-Michael/aldol reaction.⁴⁸ A self-assembling lipopeptide featuring proline residues was also applied to the catalysis of a model aldol reaction.⁴⁹ However, all these examples rely on moderately complex structures that require several synthetic steps. Simpler catalysts composed of just a few amino acids are attractive alternatives, as they can be easily prepared taking advantage of well-established peptide synthesis protocols. In particular, tripeptides can be accessed also by liquid-phase methods at low cost, on a large scale to aid future implementation in industrial processes. For example, Wennemers et al. described elegant examples of proline-based tripeptides for asymmetric addition reactions of aldehydes to nitroalkenes with excellent selectivities in their molecular state.⁵⁰ We reasoned that coupling the organocatalytic proline with the self-assembling propensity of Phe-Phe could provide an interesting strategy to access supramolecular catalysts. Herein, to the best of our knowledge, we report the first proof of concept of supramolecular fibril organocatalysts, composed solely of a tripeptide,

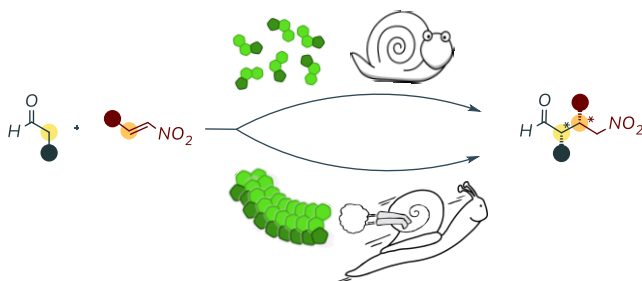
⁴⁷ N. Singh, B. Escuder *Chem. Eur. J.* **2017**, *23*, 9946.

⁴⁸ S. Jakkampudi, S. Konda, H. Arman, J. C.-G. Zhao, *Adv. Synth. Catal.* **2020**, *362*, 2419.

⁴⁹ J. N.B.D. Pelin, C. J. C. Edwards-Gayle, V. Castelletto, A. M. Aguilar, W. A. Alves, J. Seitsonen, J. Ruokolainen, I. W. Hamley *ACS Applied Materials & Interfaces*, **2020**, *12*, 12, 13671.

⁵⁰ a) P. Krattiger, R. Kovasy, J. D. Revell, S. Ivan, H. Wennemers *Org. Lett.* **2005**, *7*, 1101. b) J. Duschmalé, H. Wennemers, *Chem. Eur. J.* **2012**, *18*, 1111; c) R. Kastl, H. Wennemers *Angew. Chem. Int. Ed.* **2013**, *52*, 7228; d) C. E. Grünenfelder, J. K. Kisunzu, H. Wennemers *Angew. Chem. Int. Ed.* **2016**, *55*, 8571; e) T. Schnitzer, H. Wennemers *J. Am. Chem. Soc.* **2017**, *139*, 15356; f) T. Schnitzer, A. Budinská, H. Wennemers *Nat. Catal.* **2020**, *3*, 143.

that exhibit higher efficiency and activity than their non-self-assembled structures in the Michael reaction of aldehydes **1** to nitroalkenes **2** (Scheme 2. 12).



Scheme 2. 12 Enhancement of catalytic activity in a Michael reaction via a self-assembled organocatalyst.

D-Pro-*L*-Phe-*L*-Phe (**^oPFF**) was selected for this study for the strategic presence of a *N*-terminal proline residue that would allow the system to promote aminocatalysis in aqueous media. The stereoconfiguration was chosen based on a recent study on *Pro*-Phe-Phe isomers, of which the *D*-*L*-*L* stereoconfiguration (or its *L*-*D*-*D* enantiomer) provided the strongest propensity to self-organise in supramolecular fibrils, which, above a critical concentration, formed macroscopic hydrogels.⁵¹ In line of principle, **^oPFF** could thus yield both nanofibrillar catalysts to be used in solution, or macroscopic functional materials. Furthermore, the choice for the *D*-*L*-*L* stereoconfiguration was supported also by the finding that, for His-Phe-Phe, esterase-like activity emerged only in the supramolecular state, thus offering the possibility to switch on/off the supramolecular catalyst with its assembly/disassembly.^{39a} We surmised that its design, and the supramolecular self-assembly guaranteed by the tripeptide sequence (two residues of phenylalanine), like natural enzymatic systems, create an organic microenvironment that brings the reagents closer to each other and, more importantly, to the catalytic site (the proline moiety). We

⁵¹ A. M. Garcia, M. Melchionna, O. Bellotto, S. Kralj, S. Semeraro, E. Parisi, D. Iglesias, P. D'Andrea, R. De Zorzi, A. V. Vargiu, S. Marchesan, *ACS Nano* **2021**, *15*, 2, 3015.

speculated that, using this approach, the catalytic activity would be enhanced when the tripeptide is in its self-assembled form.

2.4 Results and discussion

Synthesis and characterisation of organocatalytic fibrils

⁰PFF was synthesised via homogeneous phase synthesis in five steps with an overall yield of 71%. The chosen synthetic route is based on an orthogonal protecting/deprotecting approach, starting from commercial NBoc-^DPro and ^LPheOMe and yielding the TFA salt of the desired peptide. Using the same procedure, the epimer peptide ^LProPhePhe (^LPFF) was also synthesised to evaluate the effects of supramolecular organization on catalysis, since it was reported to form amorphous aggregates under the same experimental conditions at which ⁰PFF fibrillated.⁵¹ In addition, ^DProPhe (^DPF) was also synthesised to confirm the positive impact of ⁰PFF on catalysis (*vide infra*).

We first focused on self-assembly conditions of ⁰PFF. While, as expected, fibrils were unable to assemble in pure water, we were able to detect their formation both in HFIP/H₂O solution (1:10 v/v) and in a phosphate buffer saline solution (PBS) 0.15 M at pH = 7.4. Using these conditions, after few minutes under mild agitation, we observed the presence of fibrils at different concentrations (see Experimental section). In contrast, in the same experimental conditions in which ⁰PFF fibrils were observed, homochiral analogue ^LPFF only yielded amorphous aggregates, accordingly to what was previously observed.^{51,52} The same behaviour is observed for the ^DPF derivative, showing only amorphous aggregates in both aqueous solutions. ⁰PFF and ^LPFF divergent supramolecular behaviour has been recently characterised in detail.⁵¹ In this work, fibrils assembly was confirmed by means of brightfield and

⁵² P. Frederix, G. Scott, Y. M. Abul-Hajja, D. Kalafatovic, C. G. Pappas, N. Javid, N. T. Hunt, R. V. Ulijn, T. Tuttle, *Nature Chem* **2015**, 7, 30.

fluorescence microscopy in absence or presence of Thioflavin T as a fluorescent probe (Figure 2. 3).

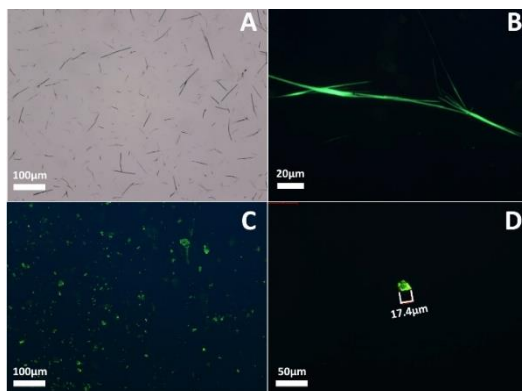


Figure 2. 3 (A) Micrographs of 25 mM ¹⁹PFF fibrils in PBS pH=7.4 observed in bright field (B) or stained with the fluorescent probe Thioflavin T and observed with a FITC band-pass filter; (C and D) ¹⁴PFF amorphous aggregates observed in the same conditions as (B).

Transmission electron microscopy (TEM) analysis confirmed the ability of ¹⁹PFF to self-assemble into fibrils in PBS and HFIP/water (Figure 2. 4). In PBS, fibrils bundled into fibres of heterogeneous diameters, spanning tens, and in a few cases, even hundreds of nanometres (Figure 2. 4 A-B); conversely, in HFIP/water a homogenous population of 10.3 ± 2.3 nm ($n=100$) was observed (Figure 2. 4 C-D).

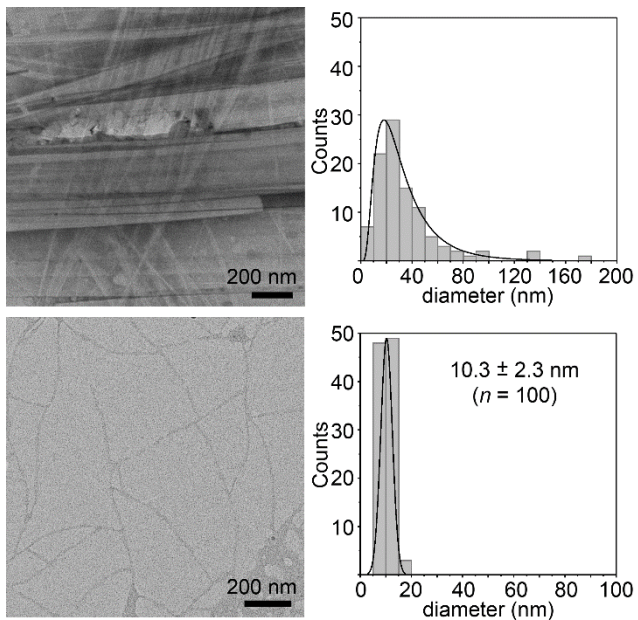


Figure 2. 4 TEM micrographs of ⁹PFF fibrils in PBS (A) and HFIP/water (C) and corresponding fibril diameter distribution (B, D).

Reaction optimisation

One of the most important and broadly utilised reactions to form asymmetric C–C bonds in organic synthesis is the Michael addition,⁵³ usually in combination with chiral secondary amines as catalysts. Among these, proline and its derivatives are extensively used to catalyse the α -addition of carbonylic compounds to various electrophiles via covalent enamine catalysis.

Hence, the addition of isovaleraldehyde **1a** to β -nitrostyrene **2a** was chosen as a benchmark reaction to test the catalytic activity of the tripeptide in aqueous solutions, both assembled in supramolecular fibrils and in its free peptide form. This aldehyde was chosen for its limited reactivity with respect to aliphatic linear aldehydes;⁵⁴ this way, the enhanced catalysis via fibrils could be better appreciated and the optimal reaction conditions eventually found used for other substrates.

The reaction catalysed by ^DPFF in pure water where no fibrils are formed (Table 2. 3, entry 1), was compared with solvent mixtures where the peptide self-assembles (entries 2-3). While the reactions performed in HFIP/H₂O provided poor results, a very encouraging improvement in conversion and ee was observed when run in PBS (51% vs 17% conversion, and 72% vs 69% ee, compared to water). This result was, indeed, the first indication that organocatalysis could be enhanced in fibrils.

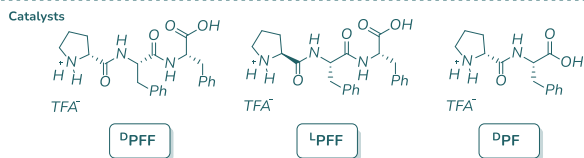
To confirm that the conversion rate was, in fact, affected by the supramolecular state of ^DPFF, first the uncatalysed reaction was tested (entry 4) to assess whether the PBS had any effect on the conversion. Then, the epimer ^LPFF peptide was tested first in pure water and

⁵³ Organocatalytic enantioselective conjugate addition reactions: a powerful tool for the stereocontrolled synthesis of complex molecules, Edited by J. L. Vicario, D. Badía, L. Carrillo, E. Reyes, Ed. RSC Publishing, Cambridge 2010.

⁵⁴ M. Marigo, P. Melchiorre, ChemCatChem 2010, 2, 621.

subsequently in PBS, where it forms agglomerates (entries 5 and 6), and showed only a small increase in conversion.

Table 2. 3 Optimisation of reaction conditions for the addition of isovaleraldehyde **1a** to β -nitrostyrene **2a**.^a



entry	Cat	cat (%)	solvent	conv. (%) ^b	ee (%) ^{c,d}
1	^D PFF	5	H ₂ O	17	69
2	^D PFF	5	HFIP/H ₂ O	7	53
3	^D PFF	5	PBS	51	72
4	-	-	PBS	< 1	n.d.
5	^L PFF	5	H ₂ O	22	-43
6	^L PFF	5	PBS	33	-48
7	^D PFF	10	PBS	49	71
8	^D PFF	15	PBS	44	71
9 ^e	^D PFF	5	PBS	64	69
10 ^{e,f}	^D PFF	5	PBS	74	66
11 ^{e,f}	^D PFF	5	H ₂ O	41	69
12 ^{e,f}	^L PFF	5	PBS	56	-50
13 ^{e,f}	^D PF	5	H ₂ O	8	70
14 ^{e,f}	^D PF	5	PBS	12	71

^aReaction conditions: isovaleraldehyde **1a** (0.34 mmol, 1 equiv.), β -nitrostyrene **2a** (0.34 mmol, 1 equiv.), d.r. >94:6 *syn/anti* in all cases; ^b conversion was determined by ¹H NMR spectroscopy; ^c ee reported of *syn* (major) diastereomer; ^d the ee value was determined by HPLC on a chiral stationary phase; ^e reaction performed at 35 °C ^f reaction performed with 2 equiv. of **1a**.

Then, the effect of the catalyst loading of ^DPFF was evaluated. It was observed that the best results were obtained with 5% catalyst loading (entries 3, 7-8). Albeit counterintuitive at a first glance, this result should not mislead. In fact, using a lower catalyst loading at the same concentration of catalyst means that less solvent is used in the reaction, hence a higher concentration of reagents. Increasing the temperature to 35 °C resulted in a higher conversion without significantly affecting the ee (entries 3 vs 9), an outcome that is further improved using two equivalents of isovaleraldehyde **1a** (entry 10). Before progressing with these optimised conditions, they were also compared when run in water and with the non-self-assembling epimer ^LPFF in PBS at 35 °C; to our delight, the beneficial effect of fibrils for organocatalytic activity is still evident at this temperature (74% vs 41% and 56% conversion, entries 10-12), supporting the idea that the higher conversion is not merely due to the higher temperature.

Bearing in mind that comparing ⁰PFF with ⁴PFF to deconvolute the effect of fibrils for catalysis is not entirely correct, ⁰PF the inferior analogue of ⁰PFF, that does not form fibrils, was also tested in water and PBS (entries 13-14) and it showed a neglectable increase in conversion (8% vs 12%). This further set of experiment was needed to rule out the effect of PBS alone on the catalysis and to further prove that the supramolecular assembly affected the conversion rate, underpinning the initial concept that we set out to prove. Therefore, the scope of the reaction was investigated with the optimised conditions shown in Table 1, entry 10.

Acceleration of the organocatalytic reaction promoted by the ⁰PFF fibrils

Based on the collected investigation results, we wished to evaluate the impact of the ⁰PFF on the enamine addition of aldehydes **1a-g** with nitroalkenes **2a-i** in PBS at the 24h timepoint, using ⁰PFF as supramolecular peptide-like fibril organocatalyst. As expected, nearly all aldehydes proved to be more reactive than isovaleraldehyde **1a**. The catalysis promoted by the organocatalyst in their supramolecular assembly is faster and the acceleration imparted by the fibrils is evident for all aldehydes (Table 2. 4). In fact, there is a 11% to 74% increment in conversion, over 24 h, when using fibrils to promote the reaction.

The improvement in dr and ee of the reactions is marginally interesting in this context; the most interesting aspect, for the purpose of the proof of concept of the enhanced catalysis in fibrils, is the actual improvement in conversion that is evident in all entries.

Nitrostyrene **2a** is the nitroalkene used in benchmark reactions because of its higher reactivity, besides its availability and stability; a range of aldehydes **1a-g** showed increased reactivity with **2a** when fibrils of ⁰PFF catalysed the reaction. Aldehyde **1b**, probably thanks to its smaller size, proved to be the one that benefitted the most from the fibrils (**3ba**, 26% conv. in H₂O vs quant. conv. in PBS), whereas hydrocinnamaldehyde **1g** showed the smallest enhancement (**3ga**, 73% conv. in H₂O vs 84% conv. in PBS), supposedly because of the effect of the larger substituent and its higher difficulty to insert and interact within the fibrils.

Aldehyde **1c** was chosen to evaluate a range of nitroalkenes **2a-i**. In general, the acceleration of the reaction is comparable for all nitroalkenes, around 40% increase in conversion, regardless of whether they are aromatic with electron-withdrawing or electron-donating groups (**3ca**, **3cb-3cf**), or aliphatic with substituents of different sizes (**3cg-3ci**) (Table 2. 4).

Table 2. 4 Enhanced catalysis of fibril organocatalyst ^oPFF in the reaction of aldehydes **1a-g** with β -nitroalkenes **2a-i**.^a

H ₂ O: 28%	26%	56%	51%	53%
PBS: 61%	>95%	93%	93%	92%
H ₂ O: 36%	73%	49%	17%	33%
PBS: 81%	84%	>95%	61%	74%
H ₂ O: 24%	74%	22%	27%	56%
PBS: 61%	>95%	62%	61%	>95%

^aReaction conditions: aldehyde **1a-g** (0.68 mmol, 2 equiv.), nitroalkenes **2a-i** (0.34 mmol, 1 equiv.), H₂O or PBS, ^oPFF (25mM), 5 mol%; conversion was determined by ¹H NMR spectroscopy.

A comparison of the reactions carried out in absence and in presence of fibrils, i.e.: in water and PBS, for **3aa** is displayed in Figure 2. 5, by plotting the evolution of the conversion versus time. The reaction catalysed in the presence of fibrils is clearly faster from the start, and during the whole 24 h observed, showing a steeper slope; this behavior can be ascribed to

the presence of fibrillar aggregates seen in PBS over amorphous aggregates in water.

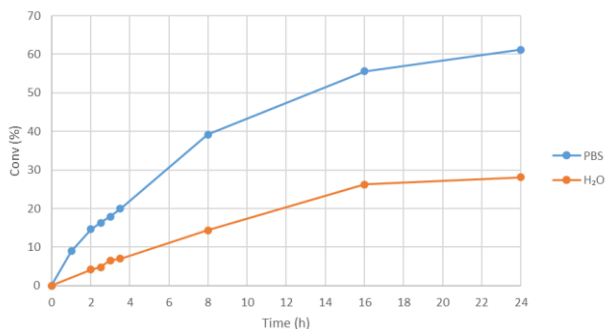


Figure 2. 5 Comparison of the conversion to **3aa** in reactions catalysed by ^oPFF, in PBS and H₂O over 24h.

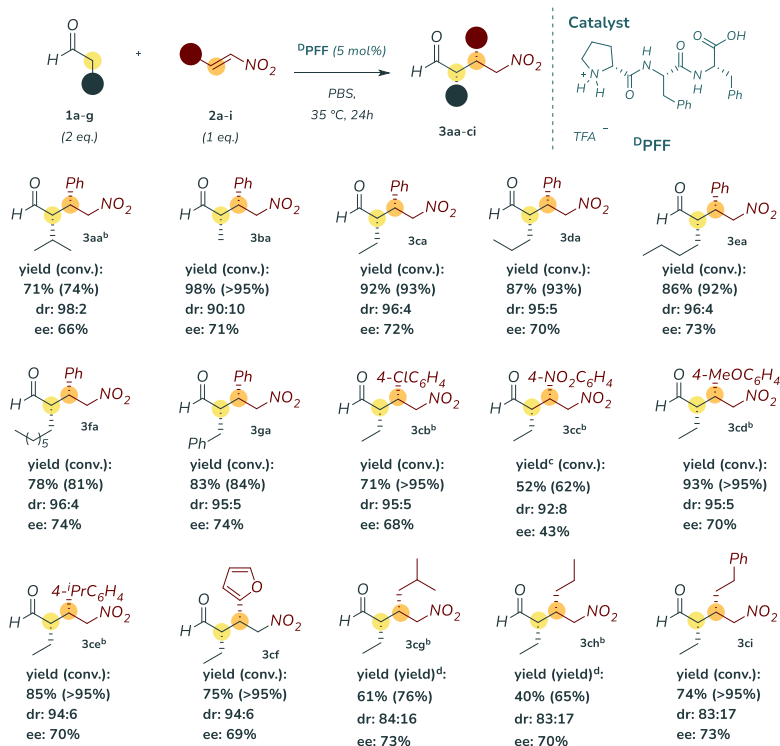
Scope of the Michael reaction promoted by the ^oPFF fibrils

Having established that supramolecular ^oPFF accelerates the Michael reaction as compared to their non-supramolecular counterpart, we evaluated the scope of the organocatalytic reaction between aldehydes **1a-g** and nitroalkenes **2a-i** (Table 2. 5).

Various aldehydes reacted with nitrostyrene **2a** providing the desired products in very good to high yields, with the less steric hindered aldehydes providing higher yields and conversions (e.g.: **3ba** and **3ca** vs **3aa**). On the other hand, a range of nitroalkenes **2a-i** also furnished the desired products in respectable yields when reacted with aldehyde **1c**. Yields of aromatic nitroalkenes with electron-withdrawing groups (**3cb-cc**) were lower than the ones with electron-donating groups (**3cd-ce**). As expected, aliphatic nitroalkenes also proved to be less reactive than nitrostyrene **2a** and provided the desired products in lower yields over the same reaction time.

In general, however, all isolated yields are in good agreement with the conversion (i.e.: no relevant side-products or degradation of the starting material can be expected at this stage).

Table 2. 5 Catalytic asymmetric Michael addition of aldehydes **1a-g to b-nitroalkenes **2a-i**.^a**



^aReaction conditions: aldehyde **1a-g** (0.68 mmol, 2 equiv.), nitroalkenes **2a-i** (0.34 mmol, 1 equiv.), PBS, ^bDPFF (25mM), 5 mol%; conversion was determined by ¹H NMR spectroscopy; dr determined by ¹H NMR analysis of the crude reaction mixture; the ee value was determined by HPLC on a chiral stationary phase; the ee values reported are for the *syn* diastereoisomer, see experimental section for the further data. ^b *t* = 72 h. ^c Yield calculated via qNMR. ^d Yield calculated via qNMR, in place of conversion, due to high volatility.

Conclusions and future perspective

In conclusion, we reported the first proof of concept of a simple tripeptide featuring proline and able to self-assemble into fibrils, that accelerates a Michael-type catalysis in its supramolecular state.

This approach represents a viable option to explore to accelerate catalysis and overcome the low activation often associated with organocatalysis. The catalysis is accelerated when the catalyst is in its supramolecular form; to effect acceleration benign and cost-effective solvents and conditions are employed, rendering the process easy to implement. Furthermore, the self-assembling organocatalyst is a tripeptide; it is, therefore, easy to prepare on bigger scale and at a low cost.

The nature of the self-assembling organocatalyst makes it modular and a range of aminoacids can be chosen to effect the formation of fibrils. Further work is underway for the development of different organocatalytic fibrils that would deploy a range of activations based on their constituents. For this purpose, the peptide sequences, capable of self-assembling in supramolecular structures, already synthesised in our laboratory, and their proposed activations have been reported (Scheme 2. 13).

More precisely, we focused our attention on other peptides sequences able to organise themselves in supramolecular structures to explore different types of organocatalytic activation, taking inspiration from other peptide sequences previously reported⁵⁵ in the literature:

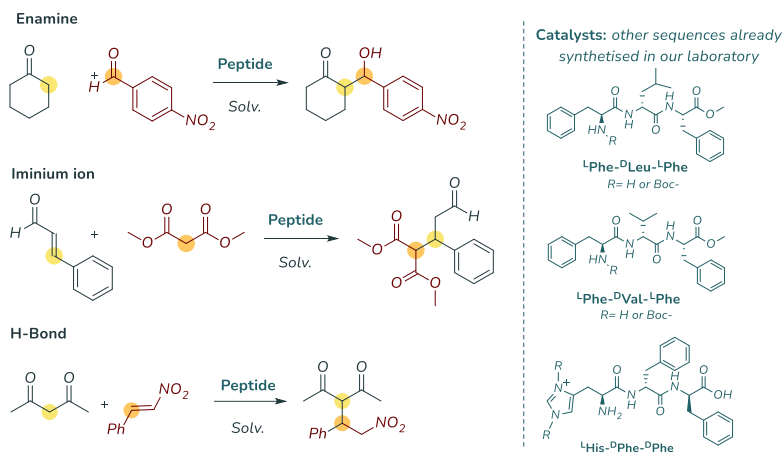
- via enamine or iminium ion activation, with respectively saturated or unsaturated ketones, through the formation of intermediates mediated by primary amine function of N-terminal amino acid (not hindered in α -position like proline residues), verifying and also comparing the steric hindrance effect on how it may affect the enantiomeric excess and hydrophobicity of the considered system.

- via Hydrogen-bond activation to try to improve further the reactivity of the supramolecular system due to the non-covalent interaction between reagents and catalysts. This way, we can expect that the electrostatic

⁵⁵ a) A. M. Garcia, D. Iglesias, E. Parisi, K. E. Styan, L. J. Waddington, C. Deganutti, R. De Zorzi, M. Grassi, M. Melchionna, A. V. Vargiu, S. Marchesan, *Chem* **2018**, 4, 8, 1862. b) A. M. Garcia, M. Kurbasic, S. Kralj, M. Melchionna, S. Marchesan, *Chem. Commun.* **2017**, 53, 8110

interaction between reactants and catalyst to allow faster mass transfer, in order to increase the turnover frequency, and therefore the catalytic efficiency of the catalyst itself.

- $^L\text{His-}^D\text{Phe-}^D\text{Phe}$ due to the presence of the imidazole ring, the N-terminal functionalised histidine residue could act not only as a primary amine, and thus activate ketones, as a base (for the presence of the imidazole group), but also as a possible site to perform the NHC activation.



Scheme 2. 13 Examples of possible activations with catalysts synthesised in our laboratory

2.4.1 Materials and methods

N-Boc-*D*-Proline **I**, *L*-Phenylalanine methyl ester **II**, *N*-Boc-*L*-Proline **VII**, EDC hydrochloride, HOBT monohydrate and all other commercially available reagents were purchased by Merck and Fluorochem and used as received unless otherwise stated. Analytical grade solvents were purchased by Merck and Carlo Erba. Silica Gel 60A (35-70 μ), HPLC solvents, trifluoroacetic acid (TFA) and 0,15 M phosphate buffer saline (PBS: mono- and di-basic phosphate salt 0,01 M, [KCl]=0,0027 M, [NaCl]=0,137 M; prepared by dissolving one tablet – Merck product number P4417 - in 200 mL of deionised water; pH 7.4 at 25 °C) were purchased by Merck. Aldehydes **1a-g**, β -nitrostyrene **2a**, **2f** and internal standards (1,3,5-trimethoxybenzene and 1,2,4,5-tetramethylbenzene) were purchased by Merck. Nitroalkenes **2b-e** and **2g-i** were prepared as previously reported.⁵⁶

Transmission Electron Microscopy (TEM) analysis: *D*-Pro-*L*-Phe-*L*-Phe (**PFF**) self-assembly was performed using the protocol described in section 3. After 30 minutes, samples were carefully dropcasted on TEM grids (copper-supported carbon film), which were previously treated in a UV-Ozone Procleaner Plus for 5 minutes. Samples were dried for 5 minutes, stained with aqueous potassium phosphotungstate (6 mM, pH 7.1) and dried in vacuo overnight. TEM micrographs were acquired on a Philips electron microscope 208 (FEI, Oregon, USA, 100kV) equipped with a Quemesa camera (Olympus, Germany). Images were recorded with RADIUS software and analysed with FIJI software.

Thioflavin-T assay was performed with a Carl Zeiss Axioplan 2 microscope, equipped with an HBO 50 mercury short arc lamp and a 470/40 nm band pass filter (FITC standard filter).

Nuclear magnetic resonance analyses (¹H-, ¹⁹F and ¹³C-NMR spectra) were acquired using a Bruker Advance III 400 MHz spectrophotometer. Chemical shifts (δ) are reported in ppm relative to residual solvent signals

⁵⁶ G. Giorgianni, V. Nori, A. Baschieri, L. Palombi, A. Carlone, *Catalysts*, **2020**, *10*, 1296.

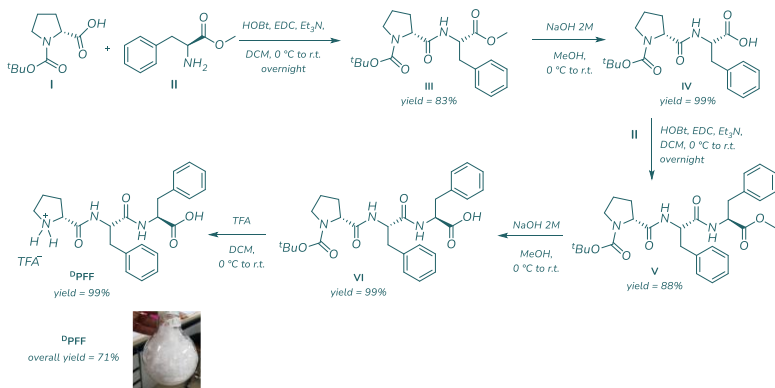
for ^1H - and ^{13}C -NMR (^1H -NMR: 7.26 ppm for CDCl_3 , 2.50 ppm for $(\text{CD}_3)_2\text{SO}$; ^{13}C -NMR: 77.0 ppm for CDCl_3 , 39.5 ppm for $(\text{CD}_3)_2\text{SO}$). ^{19}F -NMR was recorded using fluorobenzene as internal standard ($\delta = -113.15$ ppm in $(\text{CD}_3)_2\text{SO}$). ^{13}C -NMR spectra were acquired with ^1H broadband decoupled mode. Coupling constants are given in Hz. Conformers around the amide bonds are always observed; however, it was possible to determine only the ratio between the major/minor isomers generated around the Pro-Boc amide bond. NMR spectra of compounds **3aa-ci** include traces of the anti diastereoisomer.

Chromatographic purifications of peptides **III** and **V** were performed using automated BÜCHI - Reveleris® X2-UV System. Optical rotations were measured on a ZUZI 412 Digital Polarimeter (tube length: 100 mm). FTIR-ATR analyses were recorded using a Perkin Elmer UATR two spectrophotometer. HPLC analyses were acquired using an Agilent 1220 Infinity II liquid chromatographer equipped with a Phenomenex column - Lux $3\mu\text{m}$ -i-Cellulose 5. Racemic samples were prepared using a racemic mixture of D-Proline and L-Proline as a catalyst at 35 °C in dimethyl sulfoxide (DMSO) overnight. Optical rotations are in agreement with values reported in the literature.

High-resolution mass spectra were recorded on a LC-MS apparatus: Thermo Scientific UHPLC Ultimate 3000 coupled with Q Exactive™ Hybrid Quadrupole-Orbitrap™ Mass Spectrometer via HESI-II heated electrospray ion source.

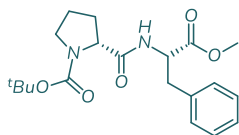
2.4.2 Synthesis of the catalysts.

Synthesis and characterisation of tripeptide ^DPFF



Scheme 2.14 synthetic path for the synthesis of ^DPFF

N-Boc-*D*-proline-*L*-phenylalanine methyl ester III.⁵⁷ Round bottom flask



A: To a solution/dispersion of the *N*-Boc-*D*-proline I (4.65 mmol, 1 g, 1 equiv.) in DCM (0.2 M) at 0°C, 1-hydroxybenzotriazole monohydrate (HOBT, 5.12 mmol, 0.784 g, 1.1 equiv.) was added and the mixture stirred for 5 minutes, after which *N*-(3-dimethylaminopropyl)-*N'*-ethyl carbodiimide hydrochloride (EDC, 5.12 mmol, 0.834 g, 1.1 equiv.) was added. This solution was left under stirring at 0 °C for one hour.

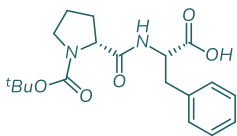
Round bottom flask B: In a second round bottom flask *L*-phenylalanine methyl ester II (5.12 mmol, 1.1 g, 1.1 equiv.) was dissolved in DCM (0.2 M) and triethylamine was added dropwise (18.6 mmol, 2.6 mL, 4 equiv.) at room temperature. The mixture was left under stirring for one hour.

⁵⁷ H. Kessler, H. Matter, G. Gemmecker, A. Kling, M. Kottenhahn, *J. Am. Chem. Soc.* **1991**, 113, 20, 7550

After this period, the solution from round bottom flask B was transferred into the round bottom flask A, rinsing with a small amount of DCM (5 mL). The reaction mixture was stirred at room temperature overnight and the reaction was monitored by TLC (petroleum ether/ethyl acetate 1:2). After the completion of the reaction, the organic phase was extracted three times with HCl (0.1 M), with brine, and then dried over MgSO₄.

The desired product was purified by flash chromatography (eluent in gradient: petroleum ether/ethyl acetate from 80:20 to 0:100). The clean product was obtained as a white foam (3.86 mmol, 1.45 g, yield = 83 %). ¹H-NMR (400 MHz, (CD₃)₂SO): (mixture of conformers, 69:31) major isomer δ = 8.25 - 8.19 (m, 1H), 7.33 - 7.22 (m, 5H), 4.60 - 4.47 (m, 1H), 4.17 - 4.04 (m, 1H), 3.65 (m, 3H), 3.45 - 3.37 (m, 1H), 3.29 - 3.23 (m, 1H), 3.10 (dd, J = 13.9, 5.0 Hz, 1H), 2.97 (dd, J = 13.8, 9.9 Hz, 1H), 2.11 - 1.99 (m, 1H), 1.80 - 1.59 (m, 3H), 1.25 (m, 9H); ¹³C-NMR (100 MHz; (CD₃)₂SO) δ = 172.6 (C), 172.0 (C), 153.4 (C), 137.4 (C), 129.0 (CH), 128.2 (CH), 126.5 (CH), 78.3 (C), 59.5 (CH), 53.3 (CH), 51.8 (CH₃), 46.4 (CH₂), 36.4 (CH₂), 30.7 (CH₂), 27.8 (CH₃), 22.8 (CH₂); HRMS (ESI-QTOF): m/z calcd for [C₂₀H₂₈N₂O₅ + H⁺] 377.2070; found: 377.2067 and m/z calcd for [C₂₀H₂₈N₂O₅ + Na⁺] 399.1890; found: 399.1887; [α]_D²⁵ = -57 (c = 0.17 in methanol).

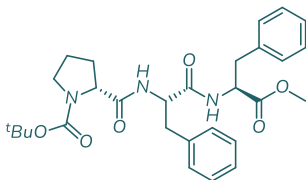
N-Boc-D-proline-L-phenylalanine **IV**. The methoxy protected peptide **III** (3.86 mmol, 1.45 g, 1 equiv.) was dissolved in methanol (0.15 M) and stirred until complete dissolution. The round bottom flask was cooled at 0 °C, then NaOH (2 M) was slowly added to the solution (about 0.2 M with respect to **III**). The reaction mixture was monitored by TLC until the precursor disappeared completely (about 40 minutes). The solution was cooled to 0 °C and acidified with 3 M HCl until pH 2.



Methanol was evaporated under reduced pressure and the residue was partitioned between ethyl acetate and water. The organic phase was dried over MgSO₄. Compound **IV** was obtained quantitatively as a white foam (3.81 mmol, 1.38 g, yield = 99 %). ¹H-NMR (101 MHz, (CD₃)₂SO): (mixture of conformers 70:30) major isomer δ = 12.71 (s, 1H), 8.01 - 7.92 (m, 1H), 7.27 - 7.18 (m, 5H), 4.50 - 4.39 (m, 1H), 4.12 - 4.01 (m, 1H),

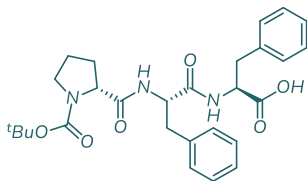
3.38 – 3.32 (m, 1H), 3.21 (dt, $J = 10.1, 6.7$ Hz, 1H), 3.07 (dd, $J = 13.8, 4.5$ Hz, 1H), 2.91 (dd, $J = 13.7, 10.0$ Hz, 1H), 2.02 (dt, $J = 9.1, 6.4$ Hz, 1H), 1.70 (m, 3H), 1.29 (m, 9H); $^{13}\text{C-NMR}$ (100 MHz; $(\text{CD}_3)_2\text{SO}$) $\delta = 173.5$ (C), 172.9 (C), 153.8 (C), 138.2 (C), 129.4 (CH), 128.5 (CH), 126.8 (CH), 78.8 (C), 60.1 (CH), 53.8 (CH), 46.9 (CH_2), 37.0 (CH_2), 31.2 (CH_2), 28.3 (CH_3), 23.3 (CH_2); **HRMS (ESI-QTOF)**: m/z calcd for $[\text{C}_{19}\text{H}_{26}\text{N}_2\text{O}_5 + \text{Na}^+]$ 385.1733; found: 385.1720; $[\alpha]_D^{25} = -38$ ($c = 0.20$ in methanol).

N-Boc-*D*-proline-*L*-phenylalanine-*L*-phenylalanine methyl ester **V**. *N*-Boc-*D*-proline-*L*-phenylalanine-*L*-phenylalanine methyl ester **V** was prepared starting from *N*-Boc-*D*-proline-*L*-phenylalanine **IV** (3.81 mmol, 1.38 g), following the procedure used for the synthesis of **III**. The desired product was purified by flash chromatography



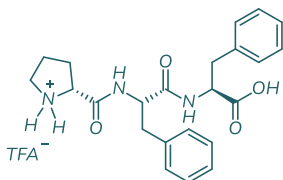
(eluent in gradient: petroleum ether/ethyl acetate from 80:20 to 0:100). The clean product was obtained as a white foam (3.34 mmol, 1.75 g; yield = 88 %). $^1\text{H-NMR}$ (400 MHz; $(\text{CD}_3)_2\text{SO}$): (mixture of conformers 67:33) major isomer $\delta = 8.56$ -8.39 (m, 1H), 8.00 - 7.79 (m, 1H), 7.38 - 7.13 (m, 10H), 4.66-4.51 (m, 2H), 4.11 - 4.00 (m, 1H), 3.67 - 3.61 (m, 3H), 3.36 - 3.30 (m, 1H), 3.28 - 3.22 (m, 1H), 3.16 - 2.91 (m, 3H), 2.89 - 2.74 (m, 1H), 2.08 - 1.88 (m, 1H), 1.75 - 1.55 (m, 3H), 1.30 (m, 9H); $^{13}\text{C-NMR}$ (101 MHz; $(\text{CD}_3)_2\text{SO}$) $\delta = 172.1$ (C), 171.7 (C), 171.4 (C), 153.3 (C), 137.7 (C), 137.0 (C), 129.1 (CH), 129.0 (CH), 128.3 (CH), 127.9 (CH), 126.6 (CH), 126.2 (CH), 78.3 (C), 59.5 (CH), 53.6 (CH), 53.3 (CH), 51.8 (CH_3), 46.4 (CH_2), 37.6 (CH_2), 36.6 (CH_2), 30.7 (CH_2), 27.8 (CH_3), 22.9 (CH_2); **HRMS (ESI-QTOF)**: m/z calcd for $[\text{C}_{29}\text{H}_{37}\text{N}_3\text{O}_6 + \text{H}^+]$ 524.2755; found: 524.2751; $[\alpha]_D^{25} = -54$ ($c = 0.17$ in methanol).

N-Boc-*D*-proline-*L*-phenylalanine-*L*-phenylalanine **VI**. *N*-Boc-*D*-proline-*L*-phenylalanine-*L*-phenylalanine **VI** was prepared starting from *N*-Boc-*D*-proline-*L*-phenylalanine-*L*-phenylalanine methyl ester **V** (3.34 mmol, 1.75 g), following the procedure used for **IV**. Compound **VI** was obtained



quantitatively as a white foam (3.31 mmol, 1.68 g, yield = 99 %). **¹H-NMR** (400 MHz; (CD₃)₂SO) (mixture of conformers 65:35) major isomer δ = 8.46 (d, J = 7.3 Hz, 1H), 7.93 (d, J = 8.9 Hz, 1H), 7.67 (d, J = 8.4 Hz, 1H), 7.32 – 7.03 (m, 10H), 4.78 – 4.32 (m, 2H), 4.10 – 3.89 (m, 1H), 3.25 – 2.76 (m, 5H), 2.69 (dd, J = 13.7, 10.4 Hz, 1H), 2.06 – 1.78 (m, 1H), 1.70 – 1.47 (m, 3H), 1.39 – 1.09 (m, 9H); **¹³C-NMR** (101 MHz; (CD₃)₂SO) δ = 173.0 (C), 172.0 (C), 171.1 (C), 153.4 (C), 137.8 (C), 137.6 (C), 129.2 (2 CH), 128.1 (CH), 127.9 (CH), 126.3 (CH), 126.2 (CH), 78.4 (C), 69.8 (CH), 59.6 (CH), 53.7 (CH), 46.4 (CH₂), 37.6 (CH₂), 36.8 (CH₂), 30.8 (CH₂), 27.8 (CH₃), 22.9 (CH₂); **HRMS (ESI-QTOF)**: m/z calcd for [C₂₈H₃₅N₃O₆ + Na⁺] 532.2418; found: 532.2426; [α]_D²⁵ = –31.2 (c = 0.12 in methanol).

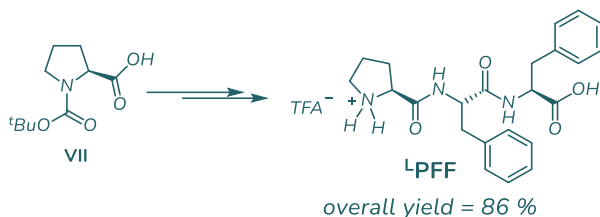
D-proline-L-phenylalanine-L-phenylalanine (TFA⁻ salt) **⁰PFF**. N-Boc-D-proline-L-phenylalanine-L-phenylalanine



VI (3.31 mmol, 1.68 g, 1 equiv.) was dissolved in DCM (0.05 M), the solution was cooled to 0 °C, and TFA was added dropwise (89.4 mmol, 7 mL, 27 equiv.). The reaction mixture was left at room

temperature for one hour. The reaction was monitored via TLC on reverse stationary phase (ACN/H₂O 7:3). The solvent was removed, the crude was dissolved in chloroform and evaporated under reduced pressure in order to remove the excess acid (3.3 mmol, 1.35 g, yield = 99 %). **¹H-NMR** (400 MHz, (CD₃)₂SO) δ = 9.39 (s, 1H), 8.80 (d, J = 9.0 Hz, 1H), 8.66 (d, J = 8.0 Hz, 1H), 8.39 (s, 1H), 7.42 – 7.16 (m, 10H), 4.75 (ddd, J = 11.0, 9.2, 3.7 Hz, 1H), 4.52 (ddd, J = 9.2, 8.2, 5.0 Hz, 1H), 4.14 – 4.08 (m, 1H), 3.18 – 3.10 (m, 4H), 2.98 (dd, J = 13.9, 9.3 Hz, 1H), 2.69 (dd, J = 13.7, 11.1 Hz, 1H), 2.09 (dt, J = 14.5, 7.9 Hz, 1H), 1.82 – 1.70 (m, 1H), 1.60 – 1.50 (m, 1H), 1.27 (td, J = 14.5, 7.1 Hz, 1H); **¹³C-NMR** (101 MHz; (CD₃)₂SO) δ = 173.6 (C), 171.7 (C), 168.5 (C), 158.7 (CO, q, J_{CF} = 32.1 Hz), 138.5 (C), 138.3 (C), 130.3 (CH), 130.0 (CH), 129.2 (CH), 128.9 (CH), 127.4 (CH), 127.3 (CH), 117.4 (CF₃, q, J_{CF} = 294.7 Hz), 59.9 (CH), 54.6 (CH), 54.4 (CH), 46.4 (CH₂), 39.1 (CH₂), 37.5 (CH₂), 30.6 (CH₂), 24.0 (CH₂); **¹⁹F-NMR** (376 MHz; (CD₃)₂SO) δ = –73.7 (s, 3F); **FTIR-ATR**: 3065, 1650, 1545, 1497, 1456, 1179, 1133, 1030, 835, 797, 728, 698, 492, 411 cm⁻¹; **ESI-MS**: 410 [M⁺]; **HRMS (ESI-QTOF)**: m/z calcd for [C₂₃H₂₈N₃O₄]⁺ 410.2074; found: 410.2075; [α]_D²⁵ = +24 (c = 0.14 in methanol).

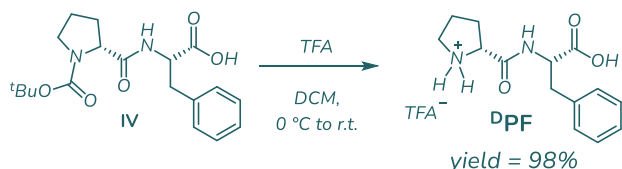
Synthesis of tripeptide ^LPFF



L-proline-*L*-phenylalanine-*L*-phenylalanine (TFA⁻ salt) ^LPFF⁵⁸ *N*-Boc-*L*-proline **VII** was used instead of *N*-Boc-*D*-proline **I**, and *L*-proline-*L*-phenylalanine-*L*-phenylalanine (TFA⁻ salt) ^LPFF was prepared following the synthetic steps used for the heterochiral tripeptide ^DPFF (4.22 mmol, 1.73 g, overall yield = 86 %). ¹H-NMR (400 MHz, (CD₃)₂SO) δ = 12.65 (s, 1H), 9.25 (s, 1H), 8.71 (d, *J* = 8.5 Hz, 1H), 8.50 (d, *J* = 7.9 Hz, 1H), 7.43 – 6.77 (m, 10H), 4.59 (td, *J* = 9.9, 4.2 Hz, 1H), 4.46 (td, *J* = 9.0, 5.0 Hz, 1H), 4.05 (t, *J* = 7.4 Hz, 1H), 3.23 – 2.99 (m, 4H), 2.92 (dd, *J* = 13.9, 9.2 Hz, 1H), 2.73 (dd, *J* = 13.9, 10.1 Hz, 1H), 2.29 – 2.18 (m, 1H), 1.91 – 1.66 (m, 3H); ¹³C-NMR (100 MHz; (CD₃)₂SO) δ = 172.7 (C), 170.6 (C), 167.9 (C), 157.8 (CO, *q*, *J*_{CF}31.0 Hz), 137.5 (2xC), 129.1 (2xCH), 128.2 (CH), 128.1 (CH), 126.4 (2xCH), 117.32 (CF₃, *q*, *J*_{CF} = 300.8 Hz), 58.7 (CH), 54.1 (CH), 53.6 (CH), 45.7 (CH₂), 37.5 (CH₂), 36.6 (CH₂), 29.5 (CH₂), 23.4 (CH₂); ¹⁹F-NMR (376 MHz; (CD₃)₂SO) δ = -73.5 (s, 3F); HRMS (ESI-QTOF): *m/z* calcd for [C₂₃H₂₈N₃O₄]⁺ 410.2074; found: 410.2126; [α]_D²⁵ = -15.3 (*c* = 0.18 in methanol).

⁵⁸ a) E. Morisset, A. Chardon, J. Rouden, J. Blanchet, *Eur. J. Org. Chem.* **2020**, 3, 388, b) G. K. Min, D. Hernández, A. T. Lindhardt, T. Skrydstrup, *Org. Lett.* **2010**, 12, 4716. c) A. Mollica, R. Costante, A. Stefanucci, F. Pinnen, G. Luisi, S. Pieretti, A. Borsodi, E. Bojnik, S. Benyhe, *Eur. J. Med. Chem.* **2013**, 68, 167. d) M. Freund, S. Schenker, S. B. Tsogoeva, *Org. Biomol. Chem.* **2009**, 7, 4279.

Synthesis of dipeptide ⁰PF



D-proline-*L*-phenylalanine (TFA⁻ salt) ⁰PF. Starting from intermediate IV (1.38 mmol, 500 mg), the procedure used for the synthesis of *D*-proline-*L*-phenylalanine-*L*-phenylalanine (TFA⁻ salt) ⁰PFF was also used for the synthesis of *D*-proline-*L*-phenylalanine (TFA⁻ salt) ⁰PF (1.36 mmol, 356 mg, yield = 98 %). ¹H-NMR (400 MHz, (CD₃)₂SO) δ = 9.51 (s, 1H), 8.91 (d, *J* = 8.6 Hz, 1H), 8.46 (s, 1H), 7.33 – 7.16 (m, 5H), 4.58 (ddd, *J* = 10.2, 8.7, 4.4 Hz, 1H), 4.15 (s, 1H), 3.22 – 3.05 (m, 3H), 2.84 (dd, *J* = 13.7, 10.4 Hz, 1H), 2.12 (dq, *J* = 14.3, 7.9 Hz, 1H), 1.78 (dp, *J* = 14.4, 7.3 Hz, 1H), 1.61 (dp, *J* = 13.8, 7.3 Hz, 1H), 1.38 (dq, *J* = 13.4, 7.2 Hz, 1H). ¹³C-NMR (100 MHz; (CD₃)₂SO): δ = 172.3 (C), 167.8 (C), 158.3 (CO, *q*, *J*_{CF} = 31.9 Hz), 137.2 (C), 129.2 (CH), 128.2 (CH), 126.6 (CH), 116.9 (CF₃, *q*, *J*_{CF} = 298.0 Hz), 58.9 (CH), 53.4 (CH), 45.5 (CH₂), 36.9 (CH₂), 29.6 (CH₂), 23.2 (CH₂); ¹⁹F-NMR (376 MHz; (CD₃)₂SO) δ = -73.7 (s, 3F); HRMS (ESI-QTOF): *m/z* calcd for [C₁₄H₁₉N₂O₃]⁺ 263.1390; found: 263.1431; [α]_D²⁵ = +36 (*c* = 0.23 in methanol).

Fibrils formation tests.

Table 2. 6 Fibrils formation test in different solvents, varying the concentration of ^oPFF

Solvent(s)	Final concentration of ^o PFF [mM]	mg/mL solvent	Fibrils formed
H ₂ O	25	13	No
	10	5	No
HFIP/H ₂ O (1:9)	60	31	Yes (Hydrogel)
	25	13	Yes
	10	5	Yes
PBS	25	13	Yes
	10	5	Yes

H₂O: ^oPFF was dissolved in the required amount of water to obtain a 25 mM or 10 mM solution. After complete dissolution, no fibrils could be detected. The same solution was sonicated for 40 minutes, yielding amorphous aggregates visible to the naked eye. The absence of fibrils was confirmed by microscope analysis.

HFIP/H₂O: ^oPFF was dissolved in the required amount of hexafluoro-2-propanol (HFIP) to obtain a solution 10 times more concentrated than the final molarity of the solutions. After complete dissolution, 100 μ L of this solution was diluted with water to reach the desired concentration; an opalescent solution is obtained. Fibrils could be detected after about ten minutes; their presence was confirmed afterwards by microscope analysis.

PBS: ^oPFF was dissolved in the required amount of aqueous PBS in order to obtain 10 mM and 25 mM solutions. When ^oPFF was used, fibrils could be detected after about five minutes; their presence was confirmed

afterwards by microscope analysis. On the contrary, when ^LPFF was used, in the same conditions, no fibrillar structures could be detected by microscope. When the same solution was sonicated for 40 minutes, amorphous aggregates were still visible with the naked eye; a later microscope inspection of such solution confirmed the presence of no fibrils. The absence of fibrils has also been confirmed for compound ^DPF.

Microscopy.

Fibrils assembly was confirmed by means of brightfield and fluorescence microscopy in absence or presence of Thioflavin T as a fluorescent probe (Figure 2. 6).

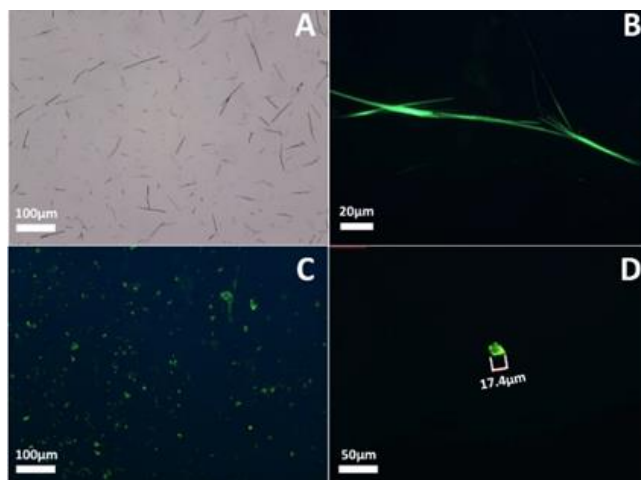


Figure 2. 6 Micrographs of 25 mM ^DPF fibrils in PBS pH = 7.4 observed in bright field (A) or stained with the fluorescent probe Thioflavin T and observed with a FITC band-pass filter (B); ^LPFF amorphous aggregates observed in the same conditions as B (C and D).

Thioflavin-T assay: An aliquot of 12,5 μ l of the fibrils-containing solution was placed on a non-autofluorescent microscope slide. 25 μ l of Thioflavine-T solution (20 mM in glycine-NaOH, pH 7.5, previously filtered with a regenerated cellulose filter 0.2 μ m) were taken from the vial and placed on the slide. After 15 minutes, microscope analysis showed the fibrils at λ_{ex} = 450 nm and λ_{em} = 470-600 nm.

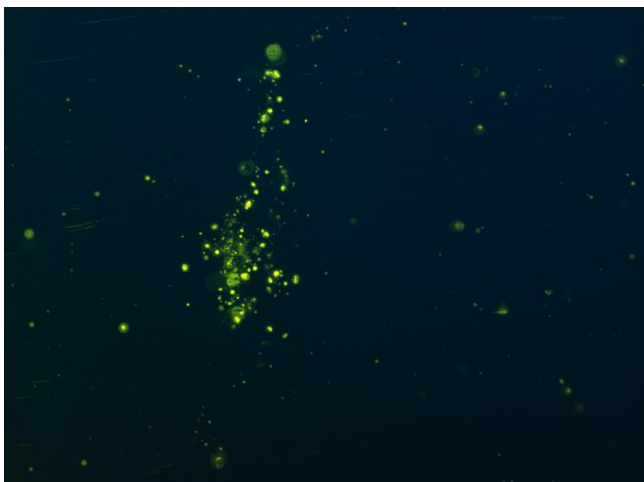


Figure 2. 7 Microscope analysis of ⁹PF in water

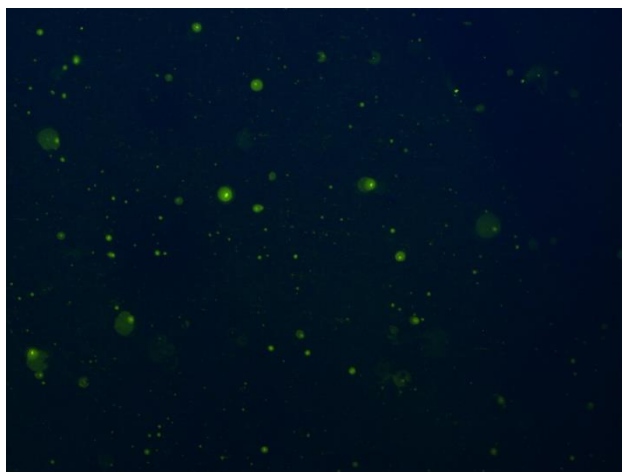


Figure 2. 8 Microscope analysis of ⁹PF in PBS solution.

Transmission electron microscopy (TEM) analysis confirmed the ability of ⁹PF to self-assemble into fibrils in PBS and HFIP/H₂O (Figure 2. 9). In PBS, fibrils bundled into fibres of heterogeneous diameters, spanning tens, and in a few cases, even hundreds of nanometres (Figure A-B);

conversely, in HFIP/water a homogenous population of 10.3 ± 2.3 nm ($n=100$) was observed (Figure C-D).

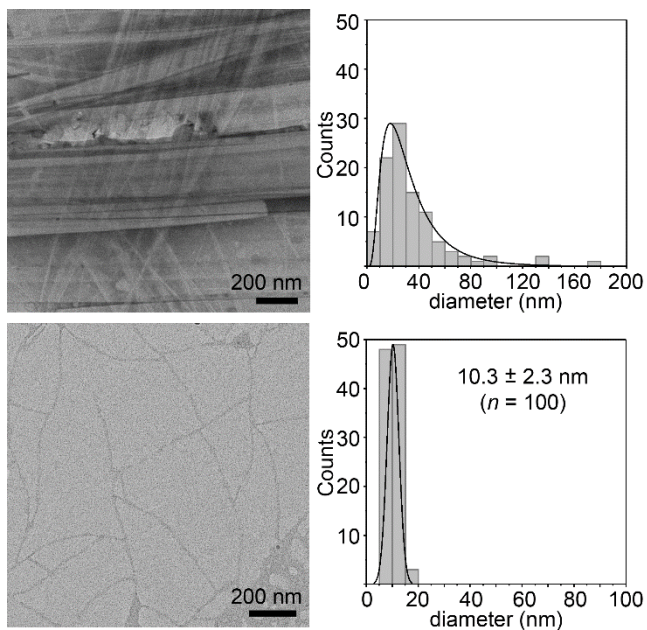


Figure 2. 9 TEM micrographs of ¹⁹PFF fibrils in PBS (A) and HFIP/water (C) and corresponding fibril diameter distribution (B, D).

Reaction optimisation

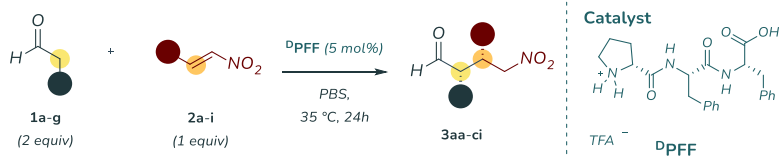
General procedure for Michael addition of isovaleraldehyde to trans- β -nitrostyrene. In a vial containing the appropriate amount of solvent such as water, HFIP/H₂O solution, or PBS solution (phosphate buffer 0.01 M, KCl 0.0027 M, NaCl 0.137 M, pH = 7.4), the catalyst was added to have a final concentration of 10 or 25 mM. The loading of the catalyst ranged from 5 to 15 %. After 10 minutes under gentle stirring, isovaleraldehyde **1a** (0.34 or 0.68 mmol, 36 or 72 μ L, 1 or 2 equiv.) was added, and after additional 10 minutes trans- β -nitrostyrene **2a** (0.34 mmol, 50 mg, 1 equiv.) was added. If required by the experiment, the appropriate amount of acidic co-catalyst was added (from 0 to 1 eq) and the solution was stirred at 100 rpm for 72 h at the desired temperature. The aqueous phase was extracted with ethyl acetate, dried over MgSO₄, filtered and the solvent was evaporated under reduced pressure. The d.r. was determined by ¹H-NMR analysis of the crude mixture and the product was isolated by flash chromatography (eluent in gradient: petroleum ether/ ethyl acetate from 90:10 to 0:100).

General procedure for the reported catalytic reaction.

Michael addition of aldehydes to nitroalkenes via self-assembled minimal structures. In a vial containing 670 μL of PBS solution (phosphate buffer 0.01 M, KCl 0.0027 M, NaCl 0.137 M, pH = 7.4), fibrils of catalyst $^{\text{D}}$ PFF have been prepared (0,05 equiv., 8.8 mg; 25 mM) and the final solution was stirred at 100 rpm at 35°C. After 10 minutes aldehydes **1a-g** (0.68 mmol, 2 equiv.) and nitroalkenes **2a-i** (0.34 mmol, 1equiv.) were added. The aqueous phase was extracted with ethyl acetate or diethyl ether in case of low boiling point products (**3cg**, **3ch**), dried over MgSO_4 , filtered and the solvent was evaporated under reduced pressure. The d.r. was determined by $^1\text{H-NMR}$ analysis of the crude mixture and the products were isolated by flash chromatography (eluent in gradient: petroleum ether/ ethyl acetate from 90:10 to 0:100 or petroleum ether/dichloromethane from 70:30 to 0:100). NMR spectra of previously reported compounds were in agreement with those of the authentic samples and/or available literature data. The enantiomeric excess was determined by chiral-stationary-phase HPLC analysis through comparison with the authentic racemic material. The syn/anti ratio of compound **3aa** was determined by comparison with the data reported in the literature.⁵⁹ The absolute configuration of compounds was determined by comparison with its optical rotation with literature data.

⁵⁹ S. Zhu, S. Yu, D. Ma, *Angew. Chem. Int. Ed.* **2008**, *47*, 545.

Table 2. 8 Catalytic asymmetric Michael addition of aldehydes **1a-g** to α -nitroalkenes **2a-i**.^a



entry	3	Conv (%)	Yield (%)	dr (Syn:Anti)	ee (%)	Syn(Anti)
1	3aa ^b	74	71	98:2	66	(55)
2	3ba	>95	98	90:10	71	(63)
3	3ca	93	92	96:4	72	(50)
4	3da	93	87	95:5	70	(58)
5	3ea	92	86	96:4	73	(47)
6	3fa	81	78	96:4	74	(67)
7	3ga	84	83	95:5	74	(67)
8	3cb ^b	>95	71	95:5	68	(60)
9	3cc ^b	>95	52 (62 ^c)	92:8	43	(40)
10	3cd ^b	>95	93	95:5	70	(51)
11	3ce ^b	>95	85	94:6	70	(50)
12	3cf	>95	75	94:6	69	(73)
13	3cg ^b	76 ^d	61	84:16	73	(68)
14	3ch ^b	65 ^d	52	83:17	70	(62)
15	3ci	>95	74	83:17	73	(69)

^a Reaction conditions: aldehyde **1a-g** (0.68 mmol, 2 equiv.), nitroalkenes **2a-i** (0.34 mmol, 1 equiv.), H₂O or PBS, DPFF (25mM), 5 mol%; conversion was determined by ¹H NMR spectroscopy; yield of isolated product; dr determined by ¹H NMR analysis of the crude reaction mixture; the ee value was determined by HPLC on a chiral stationary phase. ^b t = 72 h. ^c Yield was calculated via qNMR using internal standard 1,2,4,5-tetramethylbenzene. ^d Quantitative yield was calculated via qNMR using internal standard 1,3,5-trimethoxybenzene.

Comparison of the conversion to 3aa in reactions catalysed by ^oPFF, in PBS and H₂O over 24h.

Following the general procedure, and employing **1a** (0.68 mmol, 72 μ L, 2 equiv.) and **2a** (0.34 mmol, 50 mg, 1 equiv.), eight reactions were performed and stopped at different time points. Each experiment was performed in triplicate, and conversion was determined by ¹H-NMR spectroscopy integrating signals at 8.02 ppm (d, *J* = 13.7 Hz, 1H – starting material) and 4.67 (dd, *J* = 12.5, 4.4 Hz, 1H - product).

Table 2. 9 Conversion for the PBS profile recorded at different time point

Time (h)	Run 1	Run 2	Run 3	Average
0	0,00	0,00	0,00	0,00
1	9,69	8,51	8,65	8,95
2	15,94	13,98	14,11	14,67
2.5	16,32	16,02	16,73	16,36
3	18,29	16,57	18,81	17,89
3.5	18,84	20,27	20,64	19,92
8	40,24	36,45	40,88	39,19
16	57,44	55,32	53,78	55,61
24	62,83	63,14	59,61	61,22

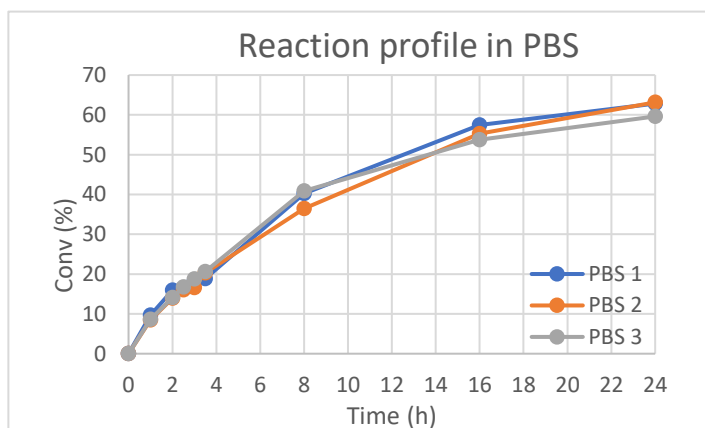
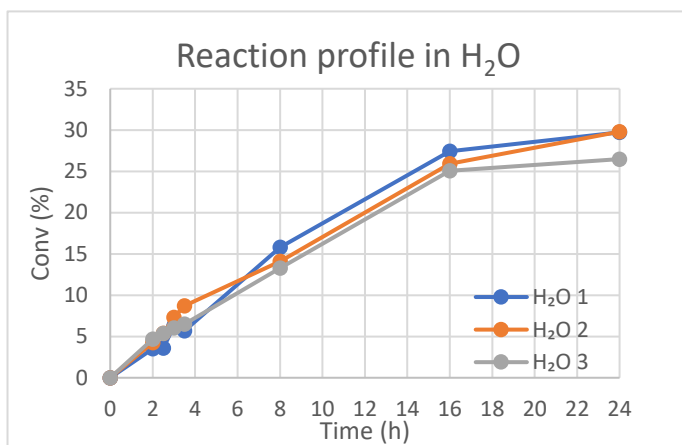


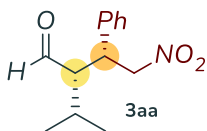
Table 2. 10 Conversion for the H₂O profile recorded at different time point

Time (h)	run 1	run 2	run 3	Average
0	0,00	0,00	0,00	0,00
2	3,52	4,26	4,68	4,15
2,5	3,57	5,39	5,36	4,77
3	6,27	7,31	6,04	6,54
3,5	5,69	8,72	6,49	6,97
8	15,81	14,12	13,27	14,39
16	27,43	25,91	25,08	26,25
24	29,72	29,83	26,48	28,11



2.4.3 Characterisation data for compounds 3aa-ci.

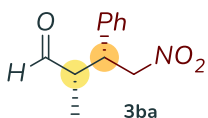
(2*S*,3*R*)-2-isopropyl-4-nitro-3-phenylbutanal **3aa**.⁵²



Synthesised in agreement with general procedure of asymmetric Michael addition of aldehydes to nitroalkenes via self-assembled minimal structures using fibrils of catalyst ^oPFF (8.8 mg, 0.0167 mmol), isovaleraldehyde (56.6 mg, 0.68 mmol), *trans*- β -nitrostyrene (50 mg, 0.34 mmol). The reaction mixture was stirred at 35 °C for 72h, to furnish the crude product [*dr* = 98:2, determined by integration of one set of ¹H NMR signal (δ_{major} 9.93 ppm, δ_{minor} 9.80 ppm - d)]. The title compound was isolated as a yellow oil by flash chromatography (eluent in gradient: petroleum ether/ ethyl acetate from 90:10 to 0:100) in 71% yield (0.23 mmol, 56 mg) and 66% ee.

¹H-NMR (400 MHz, CDCl₃) Syn product: δ = 9.93 (d, *J* = 2.4 Hz, 1H), 7.38 – 7.30 (m, 3H), 7.21 – 7.16 (m, 2H), 4.67 (dd, *J* = 12.5, 4.4 Hz, 1H), 4.58 (dd, *J* = 12.5, 9.9 Hz, 1H), 3.95 – 3.85 (m, 1H), 2.77 (ddd, *J* = 10.7, 4.1, 2.4 Hz, 1H), 1.72 (dtd, *J* = 14.1, 7.1, 4.2 Hz, 1H), 1.10 (d, *J* = 7.2 Hz, 3H), 0.89 (d, *J* = 7.0 Hz, 3H); ¹³C-NMR (101 MHz, CDCl₃) δ = 204.3 (CHO), 137.1 (C), 129.1 (2 x CH), 128.0 (CH), 127.7 (2 x CH), 78.9 (CH₂), 58.8 (CH), 41.9 (CH), 27.9 (CH), 21.6(CH₃), 16.9 (CH₃); [α]_D²⁵ = -40.2 (c = 0.48 in chloroform, 66% ee); HPLC (Lux 3 μ m-cellulose 5, Hexane/*i*-Propanol 85:15, flow: 0.4 mL/min, λ =210 nm) Syn stereoisomers (*t*_{major}: 15.96 min.; *t*_{minor}: 17.74 min.); Anti stereoisomers (*t*_{major}: 9.10 min.; *t*_{minor}: 11.18 min.).

(2*S*,3*R*)-2-methyl-4-nitro-3-phenylbutanal **3ba**.⁶⁰



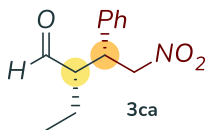
Synthesised in agreement with general procedure of asymmetric Michael addition of aldehydes to nitroalkenes via self-assembled minimal structures using fibrils of catalyst ^oPFF (8.8 mg, 0.0167 mmol), propionaldehyde (39.5 mg, 0.68 mmol),

⁶⁰ K. Patora-Komisarskaa, M. Benohouda, H. Ishikawaa, D. Seebach, Y. Hayashi, *Helv. Chim. Acta*, **2011**, 94, 719.

trans- β -nitrostyrene (50 mg, 0.34 mmol). The reaction mixture was stirred at 35 °C for 24h, to furnish the crude product [*dr* = 90:10, determined by integration of one set of ^1H NMR signal (δ_{major} 9.70 ppm, δ_{minor} 9.53 ppm - d)]. The title compound was isolated as a pale yellow oil by flash chromatography (eluent in gradient: petroleum ether/ ethyl acetate from 90:10 to 0:100) in 98% yield (68 mg, 0.32 mmol) and 71% ee.

$^1\text{H-NMR}$ (400 MHz, CDCl_3) Syn product: δ = 9.70 (d, J = 1.7 Hz, 1H), 7.37 – 7.26 (m, 3H), 7.22 – 7.14 (m, 2H), 4.80 (dd, J = 12.6, 5.6 Hz, 1H), 4.68 (dd, J = 12.7, 9.4 Hz, 1H), 3.88 – 3.77 (m, 1H), 2.88 – 2.71 (m, 1H), 0.99 (d, J = 7.3 Hz, 2H); $^{13}\text{C-NMR}$ (101 MHz, CDCl_3) δ = 202.19 (CHO), 136.57 (C), 129.07 (CH), 129.02 (2 x CH), 128.08 (CH), 128.03 (2 x CH), 78.07 (CH_2), 48.41 (CH), 44.03 (CH), 12.06 (CH_3); $[\alpha]_{\text{D}}^{25}$ = -13.4 (c = 0.37 in chloroform, 71% ee); **HPLC** (Lux $3\mu\text{m}$ -cellulose 5, Hexane/*i*-Propanol 85:15, flow: 0.4 mL/min, λ =210 nm) Syn stereoisomers (t_{major} : 24.62 min.; t_{minor} : 28.72 min.); Anti stereoisomers (t_{major} : 32.77 min.; t_{minor} : 17.09 min.).

(2*S*,3*R*)-2-ethyl-4-nitro-3-phenylbutanal **3ca**.⁸⁶¹



Synthesised in agreement with general procedure of asymmetric Michael addition of aldehydes to nitroalkenes via self-assembled minimal structures using fibrils of catalyst **PFF** (8.8 mg, 0.0167 mmol), butyraldehyde (49.0 mg, 0.68 mmol), *trans*-

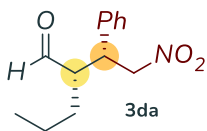
β -nitrostyrene (50 mg, 0.34 mmol). The reaction mixture was stirred at 35 °C for 24h, to furnish the crude product [*dr* = 96:4, determined by integration of one set of ^1H NMR signal (δ_{major} 9.72 ppm, δ_{minor} 9.49 ppm - d)]. The title compound was isolated as a pale yellow oil by flash chromatography (eluent in gradient: petroleum ether/ ethyl acetate from 90:10 to 0:100) in 92% yield (0.31 mmol, 69 mg) and 72% ee.

$^1\text{H-NMR}$ (400 MHz, CDCl_3) Syn product: δ = 9.72 (d, J = 2.6 Hz, 1H), 7.37 – 7.25 (m, 3H), 7.20 – 7.16 (m, 2H), 4.72 (dd, J = 12.7, 5.0 Hz, 1H), 4.63 (dd, J = 12.7, 9.7 Hz, 1H), 3.85 – 3.76 (m, 1H), 2.68 (dddd, J = 10.1, 7.5,

⁶¹ K. Patora-Komisarskaa, M. Benohouda, H. Ishikawaa, D. Seebach, Y. Hayashi, *Helv. Chim. Acta*, **2011**, 94, 719.

4.9, 2.6 Hz, 1H), 1.51 (m, 2H), 0.83 (t, $J = 7.5$ Hz, 3H); $^{13}\text{C-NMR}$ $\delta =$ (101 MHz, CDCl_3) 203.1 (CHO), 136.8 (C), 129.0 (2 x CH), 128.1 (CH), 128.0 (2 x CH), 78.5 (CH_2), 55.0 (CH), 42.7 (CH), 20.3 (CH_2), 10.6 (CH_3); $[\alpha]_{\text{D}}^{25} = -28.2$ ($c = 0.51$ in chloroform, 72% ee); **HPLC** (Lux $3\mu\text{m}$ -cellulose 5, Hexane/*i*-Propanol 85:15, flow: 0.4 mL/min, $\lambda = 210$ nm) Syn stereoisomers (t_{major} : 22.33 min.; t_{minor} : 24.55 min.); Anti stereoisomers (t_{major} : 19.19 min.; t_{minor} : 14.68 min.).

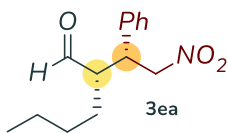
(*S*)-2-((*R*)-2-nitro-1-phenylethyl)pentanal **3da**.⁵³



Synthesised in agreement with general procedure of asymmetric Michael addition of aldehydes to nitroalkenes via self-assembled minimal structures using fibrils of catalyst $^{\text{D}}\text{PFF}$ (8.8 mg, 0.0167 mmol), valeraldehyde (58.6 mg, 0.68 mmol), *trans*- β -nitrostyrene (50 mg, 0.34 mmol). The reaction mixture was stirred at 35 °C for 24h, to furnish the crude product [$dr = 95:5$, determined by integration of one set of ^1H NMR signal (δ_{major} 9.70 ppm, δ_{minor} 9.47 ppm - d)]. The title compound was isolated as a pale yellow oil by flash chromatography (eluent in gradient: petroleum ether/ ethyl acetate from 90:10 to 0:100) in 87% yield (69 mg, 0.29 mmol) and 70% ee.

$^1\text{H-NMR}$ (400 MHz, CDCl_3) Syn product: $\delta = 9.71$ (d, $J = 2.8$ Hz, 1H), 7.38 – 7.27 (m, 4H), 7.20 – 7.15 (m, 2H), 4.70 (dd, $J = 12.8, 5.4$ Hz, 1H), 4.65 (dd, $J = 12.7, 9.4$ Hz, 1H), 3.77 (td, $J = 9.5, 5.4$ Hz, 1H), 2.70 (tt, $J = 9.5, 3.1$ Hz, 1H), 1.54 – 1.12 (m, 4H), 0.80 (t, $J = 7.1$ Hz, 3H); $^{13}\text{C-NMR}$ (101 MHz, CDCl_3) $\delta =$ 203.2 (CHO), 136.8 (C), 129.1 (2 x CH), 128.1 (CH), 128.0 (2 x CH), 78.4 (CH_2), 53.8 (CH), 43.2 (CH), 29.4 (CH_2), 19.7 (CH_2), 13.8 (CH_3); $[\alpha]_{\text{D}}^{25} = -7.9$ ($c = 0.58$ in chloroform, 70% ee); **HPLC** Lux $3\mu\text{m}$ -cellulose 5, Hexane/*i*-Propanol 85:15, flow: 0.4 mL/min, $\lambda = 210$ nm Syn (t_{major} : 19.02 min; t_{minor} : 21.24 min); Anti stereoisomers (t_{major} : 16.85 min.; t_{minor} : 13.01 min.).

(S)-2-((R)-2-nitro-1-phenylethyl)hexanal **3ea**.⁶²



Synthesised in agreement with general procedure of asymmetric Michael addition of aldehydes to nitroalkenes via self-assembled minimal structures using fibrils of catalyst **PFF** (8.8 mg, 0.0167 mmol), hexanal (68.1 mg, 0.68 mmol), *trans*- β -nitrostyrene (50 mg, 0.34 mmol). The reaction mixture was stirred at 35 °C for 24h, to furnish the crude product [*dr* = 96:4, determined by integration of one set of ¹H NMR signal (δ_{major} 9.69 ppm, δ_{minor} 9.48 ppm - d)]. The title compound was isolated as a pale yellow oil by flash chromatography (eluent in gradient: petroleum ether/ ethyl acetate from 90:10 to 0:100) in 86% yield (72 mg, 0.29 mmol) and 73% ee.

¹H-NMR (400 MHz, CDCl₃) Syn product: δ = 9.71 (d, *J* = 2.8 Hz, 1H), 7.39 – 7.27 (m, 3H), 7.21 – 7.14 (m, 2H), 4.71 (dd, *J* = 12.8, 5.2 Hz, 1H), 4.64 (dd, *J* = 12.7, 9.5 Hz, 1H), 3.77 (td, *J* = 9.6, 5.3 Hz, 1H), 2.69 (tt, *J* = 9.3, 3.6 Hz, 1H), 1.55 – 1.45 (m, 1H), 1.44 – 1.35 (m, 1H), 1.30 – 1.09 (m, 4H), 0.78 (t, *J* = 6.8 Hz, 3H); ¹³C-NMR (101 MHz, CDCl₃) δ = 203.2 (CHO), 136.8 (C), 129.1 (2 x CH), 128.1 (CH), 128.0 (2 x CH), 78.4 (CH₂), 53.9 (CH), 43.1 (CH), 28.5 (CH₂), 27.0 (CH₂), 22.5 (CH₂), 13.6 (CH₃); [α]_D²⁵ = -16.1 (*c* = 0.39 in chloroform, 73% ee); HPLC (Lux 3 μ m-cellulose 5, Hexane/*i*-Propanol 85:15, flow: 0.4 mL/min., λ =210 nm) Syn stereoisomers (*t*_{major}: 20.58 min.; *t*_{minor}: 22.95 min.); Anti stereoisomers (*t*_{major}: 19.25 min.; *t*_{minor}: 13.75 min.).

(S)-2-((R)-2-nitro-1-phenylethyl)nonanal **3fa**.⁶³



Synthesised in agreement with general procedure of asymmetric Michael addition of aldehydes to nitroalkenes via self-assembled minimal structures using fibrils of catalyst **PFF** (8.8 mg, 0.0167

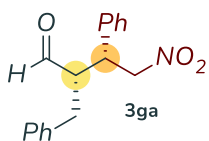
⁶² J. M. Betancort, C. F. Barbas, *Org. Lett.* **2001**, 3, 3737.

⁶³ Z. Zheng, B. L. Perkins, B. Ni, *J. Am. Chem. Soc.* **2010**, 132, 1, 50

mmol), nonanal (96.7 mg, 0.68 mmol), *trans*- β -nitrostyrene (50 mg, 0.34 mmol). The reaction mixture was stirred at 35 °C for 24h, to furnish the crude product [*dr* = 92:8, determined by integration of one set of ^1H NMR signal (δ_{major} 9.67 ppm, δ_{minor} 9.50 ppm - d)]. The title compound was isolated as a pale yellow oil by flash chromatography (eluent in gradient: petroleum ether/ ethyl acetate from 90:10 to 0:100) in 78% yield (76 mg, 0.26 mmol) and 74% ee.

$^1\text{H-NMR}$ (400 MHz, CDCl_3) Syn product: δ = 9.67 (d, J = 2.7 Hz, 1H), 7.35 – 7.24 (m, 3H), 7.16 – 7.14 (m, 2H), 4.70 (dd, J = 12.8, 5.2 Hz, 1H), 4.63 (dd, J = 12.8, 9.6 Hz, 1H), 3.77 (td, J = 9.6, 5.2 Hz, 1H), 2.70 – 2.64 (m, 1H), 1.47 – 1.13 (m, 12H), 0.82 (t, J = 7.0 Hz, 3H); $^{13}\text{C-NMR}$ (101 MHz, CDCl_3) δ = 203.2 (CHO), 136.8 (C), 129.0 (2 X CH), 128.1 (CH), 128.0 (2 X CH), 78.4 (CH_2), 53.9 (CH), 43.1 (CH), 31.5 (CH_2), 29.3 (CH_2), 28.7 (CH_2), 27.3 (CH_2), 26.3 (CH_2), 22.5 (CH_2), 13.9 (CH_3); $[\alpha]_{\text{D}}^{25}$ = -25.3 (c = 0.55 in chloroform, 74% ee); **HPLC** (Lux 3 μm -cellulose 5, Hexane/*i*-Propanol 95:5, flow: 0.4 mL/min., λ =210 nm) Syn stereoisomers (t_{major} : 26.85 min.; t_{minor} : 31.29 min.); Anti stereoisomers (t_{major} : 23.05 min.; t_{minor} : 17.12 min.).

(2*S*,3*R*)-2-benzyl-4-nitro-3-phenylbutanal **3ga**.⁶⁴



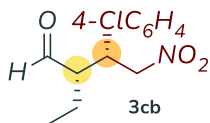
Synthesised in agreement with general procedure of asymmetric Michael addition of aldehydes to nitroalkenes via self-assembled minimal structures using fibrils of catalyst $^{\text{D}}\text{PFF}$ (8.8 mg, 0.0167 mmol), hydrocinnamaldehyde (91.24 mg, 0.68

mmol), *trans*- β -nitrostyrene (50 mg, 0.34 mmol). The reaction mixture was stirred at 35 °C for 24h, to furnish the crude product [*dr* = 95:5, determined by integration of one set of ^1H NMR signal (δ_{major} 9.71 ppm, δ_{minor} 9.56 ppm - d)]. The title compound was isolated as a yellow oil by flash chromatography (eluent in gradient: petroleum ether/ ethyl acetate from 90:10 to 0:100) in 83% yield (79 mg, 0.28 mmol) and 74% ee.

⁶⁴ M. Wiesner, G. Upert, G. Angelici, H. Wennemers, *J. Am. Chem. Soc.* **2010**, 132, 6.

¹H-NMR (400 MHz, CDCl₃) Syn product: δ = 9.71 (d, J = 2.3 Hz, 1H), 7.41 – 7.12 (m, 8H), 7.05 – 7.03 (m, 2H), 4.77 – 4.68 (m, 2H), 3.84 (td, J = 8.6, 6.1 Hz, 1H), 3.12 (tdd, J = 8.7, 5.8, 2.3 Hz, 1H), 2.77 (dd, J = 7.3, 3.6 Hz, 2H); **¹³C-NMR** (101 MHz, CDCl₃) δ = 202.9 (CHO), 137.2 (C), 136.7 (C), 129.2 (2x CH), 128.8 (2 x CH), 128.7 (2 x CH), 128.3 (CH), 128.1 (2 x CH), 126.9 (CH), 78.0 (CH₂), 55.3 (CH), 43.5 (CH), 34.2 (CH₂); [α]_D²⁵ = -2.15 (c = 0.74 in chloroform, 74% ee); **HPLC** (Lux 3μm-cellulose 5, Hexane/*i*-Propanol 85:15, flow: 0.4 mL/min., λ=210 nm) Syn stereoisomers (t_{major}: 18.85 min.; t_{minor}: 23.86 min.); Anti stereoisomers (t_{major}: 20.23 min.; t_{minor}: 13.84 min.).

(2S,3R)-3-(4-chlorophenyl)-2-ethyl-4-nitrobutanal **3cb**.⁶⁵



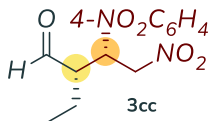
Synthesised in agreement with general procedure of asymmetric Michael addition of aldehydes to nitroalkenes via self-assembled minimal structures using fibrils of catalyst **^DPFF** (8.8 mg, 0.0167 mmol), butyraldehyde (49.0 mg, 0.68 mmol), *trans*-4-Chloro-β-nitrostyrene (62.4 mg, 0.34 mmol). The reaction mixture was stirred at 35 °C for 72h, to furnish the crude product [dr = 95:5, determined by integration of one set of ¹H NMR signal (δ_{major} 9.71 ppm, δ_{minor} 9.48 ppm - d)]. The title compound was isolated as a pale yellow oil by flash chromatography (eluent in gradient: petroleum ether/ethyl acetate from 90:10 to 0:100) in 71% yield (61 mg, 0.24 mmol) and 68% ee.

¹H-NMR (400 MHz, CDCl₃) Syn product: δ = 9.71 (d, J = 2.4 Hz, 1H), 7.34 – 7.31 (m, 2H), 7.14 – 7.11 (m, 2H), 4.72 (dd, J = 12.8, 4.8 Hz, 1H), 4.59 (dd, J = 12.8, 9.9 Hz, 1H), 3.78 (td, J = 9.9, 4.8 Hz, 1H), 2.66 (tdd, J = 8.1, 4.3, 2.1 Hz, 1H), 1.57 – 1.46 (m, 2H), 0.83 (t, J = 7.5 Hz, 3H). **¹³C-NMR** (101 MHz, CDCl₃) δ = 202.7 (CHO), 135.4 (C), 134.1 (C), 129.4 (2 x CH), 129.3 (2 x CH), 78.3 (CH₂), 54.7 (CH), 42.1 (CH), 20.3 (CH₂), 10.5 (CH₃). [α]_D²⁵ = -13.3 (c = 0.24 in chloroform, 68% ee); **HPLC** (Lux 3μm-cellulose 5, Hexane/*i*-Propanol 90:10, flow: 0.5 mL/min., λ=230 nm) Syn

⁶⁵ Y. Wang, J. Lin, K. Wei, *Tetrahedron Asymmetry*, **2014**, *25*, 1599

stereoisomers (t_{major} : 23.65 min.; t_{minor} : 25.43 min.); Anti stereoisomers (t_{major} : 20.57 min.; t_{minor} : 15.30 min.).

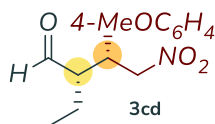
(2*S*,3*R*)-2-ethyl-4-nitro-3-(4-nitrophenyl)butanal **3cc**.



Synthesised in agreement with general procedure of asymmetric Michael addition of aldehydes to nitroalkenes via self-assembled minimal structures using fibrils of catalyst **^oPFF** (8.8 mg, 0.0167 mmol), butyraldehyde (49.0 mg, 0.68 mmol), (*E*)-1-nitro-4-(2-nitrovinyl)benzene (66.1 mg, 0.34 mmol). The reaction mixture was stirred at 35 °C for 72h, to furnish the crude product [$dr = 95:5$, determined by integration of one set of ^1H NMR signal (δ_{major} 9.74 ppm, δ_{minor} 9.53 ppm - *d*)]. The title compound was isolated as a pale yellow oil by flash chromatography (eluent in gradient: petroleum ether/ ethyl acetate from 90:10 to 0:100) in 52% yield (46 mg, 0.17 mmol) and 43% ee.

$^1\text{H-NMR}$ (400 MHz, CDCl_3) Syn product $\delta = 9.74$ (*d*, $J = 2.0$ Hz, 1H), 8.25 – 8.21 (*m*, 2H), 7.42 – 7.39 (*m*, 2H), 4.80 (*dd*, $J = 13.1$, 4.6 Hz, 1H), 4.68 (*dd*, $J = 13.1$, 10.0 Hz, 1H), 3.95 (*td*, $J = 10.0$, 4.6 Hz, 1H), 2.78 (*dddd*, $J = 10.0$, 8.1, 4.2, 1.9 Hz, 1H), 1.56 – 1.43 (*m*, 2H), 0.87 (*t*, $J = 7.5$ Hz, 3H). $^{13}\text{C-NMR}$ (101 MHz, CDCl_3) $\delta = 201.9$ (CHO), 147.7 (C), 144.5 (C), 129.1 (2 x CH), 124.3 (2 x CH), 77.8 (CH_2), 54.3 (CH), 42.2 (CH), 20.4 (CH_2), 10.4 (CH_3). **HRMS (ESI-QTOF)**: m/z calc. for $[\text{C}_{12}\text{H}_{14}\text{N}_2\text{O}_5 + \text{H}^+] = 264.0975$; found: 264.0973; $[\alpha]_{\text{D}}^{25} = -4.5$ ($c = 0.38$ in chloroform, 43% ee); **HPLC** (Lux 3 μm -cellulose 5, Hexane/*i*-Propanol 85:15, flow: 0.7 mL/min., $\lambda = 210$ nm) Syn stereoisomers (t_{major} : 30.94 min.; t_{minor} : 33.09 min.); Anti stereoisomers (t_{major} : 35.20 min.; t_{minor} : 26.39 min.).

(2*S*,3*R*)-2-ethyl-3-(4-methoxyphenyl)-4-nitrobutanal **3cd**.⁵⁷



Synthesised in agreement with general procedure of asymmetric Michael addition of aldehydes to nitroalkenes via self-assembled minimal structures using fibrils of catalyst **^oPFF** (8.8 mg, 0.0167 mmol), butyraldehyde (49.0 mg, 0.68 mmol), *trans*-4-Methoxy- β -nitrostyrene (60.9 mg, 0.34 mmol). The

reaction mixture was stirred at 35 °C for 72h, to furnish the crude product [*dr* = 95:5, determined by integration of one set of ¹H NMR signal (δ_{major} 9.71 ppm, δ_{minor} 9.47 ppm - d)]. The title compound was isolated as a pale yellow oil by flash chromatography (eluent in gradient: petroleum ether/ ethyl acetate from 90:10 to 0:100) in 93% yield (78 mg, 0.31 mmol) and 70% ee.

¹H-NMR (400 MHz, CDCl₃) Syn product: δ = 9.71 (d, *J* = 2.6 Hz, 1H), 7.09 (d, *J* = 8.7 Hz, 2H), 6.86 (d, *J* = 8.7 Hz, 2H), 4.68 (dd, *J* = 12.5, 5.0 Hz, 1H), 4.58 (dd, *J* = 12.5, 9.8 Hz, 1H), 3.78 (s, 3H), 3.74 (td, *J* = 9.5, 4.6 Hz, 1H), 2.62 (dddd, *J* = 10.1, 7.6, 4.8, 2.6 Hz, 2H), 1.55 – 1.47 (m, 2H), 0.83 (t, *J* = 7.5 Hz, 3H); ¹³C-NMR (101 MHz, CDCl₃) δ = 203.1 (CHO), 159.3 (C), 129.0 (2 x CH), 128.6 (C), 114.5 (2 x CH), 78.7 (CH₂), 55.2 (CH), 42.1 (CH), 20.5 (CH₂), 10.7 (CH₃); [α]_D²⁵ = -28.4 (*c* = 0.15 in chloroform, 70% ee); HPLC (Lux 3 μ m-cellulose 5, Hexane/*i*-Propanol 85:15, flow: 0.5 mL/min., λ =210 nm) Syn stereoisomers (*t*_{major}: 26.07 min.; *t*_{minor}: 28.50 min.); Anti stereoisomers (*t*_{major}: 21.94 min.; *t*_{minor}: 18.28 min.).

(2*S*,3*R*)-2-ethyl-3-(4-isopropylphenyl)-4-nitrobutanal **3ce**.



Synthesised in agreement with general procedure of asymmetric Michael addition of aldehydes to nitroalkenes via self-assembled minimal structures using fibrils of catalyst ^oPFF (8.8 mg, 0.0167 mmol), butyraldehyde (49.0 mg, 0.68 mmol), *trans*-4-Isopropyl- β -nitrostyrene (65.0 mg, 0.34 mmol). The reaction mixture was stirred at 35 °C for 72h, to furnish the crude product [*dr* = 94:6, determined by integration of one set of ¹H NMR signal (δ_{major} 9.71 ppm, δ_{minor} 9.48 ppm - d)]. The title compound was isolated as a pale yellow oil by flash chromatography (eluent in gradient: petroleum ether/ ethyl acetate from 90:10 to 0:100) in 85% yield (75 mg, 0.28 mmol) and 70% ee.

¹H-NMR (400 MHz, CDCl₃) Syn product: δ = 9.71 (d, *J* = 2.7 Hz, 1H), 7.19 – 7.17 (m, 2H), 7.09 – 7.06 (m, 2H), 4.69 (dd, *J* = 12.7, 5.2 Hz, 1H), 4.62 (dd, *J* = 12.7, 9.5 Hz, 1H), 3.76 (td, *J* = 9.6, 5.2 Hz, 1H), 2.87 (h, *J* = 6.9 Hz, 1H), 2.64 (dddd, *J* = 9.7, 6.9, 5.8, 2.7 Hz, 1H), 1.52 (td, *J* = 14.2, 6.9 Hz, 2H), 1.23 (d, *J* = 6.9 Hz, 6H), 0.84 (t, *J* = 7.5 Hz, 3H). ¹³C-NMR (101 MHz, CDCl₃) δ = 203.4 (CHO), 148.7 (C), 133.9 (C), 127.8 (CH), 127.1 (CH),

78.5 (CH₂), 55.2 (CH), 42.4 (CH), 33.7 (CH), 23.8 (CH), 20.4 (CH₂), 10.8 (CH₃). **HRMS (ESI-QTOF)**: *m/z* calcd for [C₁₅H₂₁NO₃ + H⁺] 264.1594; found: 264.1591; [α]_D²⁵ = -26.1 (*c* = 0.19 in chloroform, 70% ee); **HPLC** (Lux 3 μm-cellulose 5, Hexane/*i*-Propanol 85:15, flow: 0.5 mL/min., λ=210 nm) Syn stereoisomers (*t*_{major}: 16.93 min.; *t*_{minor}: 18.21 min.); Anti stereoisomers (*t*_{major}: 13.36 min.; *t*_{minor}: 10.05 min.).

(2*S*,3*S*)-2-ethyl-3-(furan-2-yl)-4-nitrobutanal **3cf**.⁵⁷



Synthesised in agreement with general procedure of asymmetric Michael addition of aldehydes to nitroalkenes via self-assembled minimal structures using fibrils of catalyst ^DPFF (8.8 mg, 0.0167 mmol), butyraldehyde (49.0 mg, 0.68 mmol), (*E*)-2-(2-nitrovinyl)furan (47.3 mg, 0.34 mmol). The reaction mixture was stirred at 35 °C for 24h, to furnish the crude product [*dr* = 94:6, determined by integration of one set of ¹H NMR signal (δ_{major} 7.70 ppm, δ_{minor} 9.59 ppm - *d*)]. The title compound was isolated as a pale yellow oil by flash chromatography (eluent in gradient: petroleum ether/ethyl acetate from 90:10 to 0:100) in 75% yield (75 mg, 0.25 mmol) and 69% ee.

¹H-NMR (400 MHz, CDCl₃) Syn product: δ = 9.70 (*d*, *J* = 1.8 Hz, 1H), 7.35 (*dd*, *J* = 3.4, 1.6 Hz, 1H), 6.29 (*dd*, *J* = 3.1, 1.8 Hz, 1H), 6.19 (*t*, *J* = 2.6 Hz, 1H), 4.68 (*d*, *J* = 7.3 Hz, 1H), 4.67 – 4.61 (*m*, 1H), 4.05 – 3.93 (*m*, 1H), 2.74 (*dddd*, *J* = 8.8, 7.2, 5.1, 1.8 Hz, 1H), 1.61 – 1.47 (*m*, 2H), 0.88 (*t*, *J* = 7.5 Hz, 3H); ¹³C-NMR (101 MHz, CDCl₃) δ = 202.3 (CHO), 150.1 (CH), 142.6 (CH), 110.4 (CH), 108.7 (CH), 76.1 (CH₂), 53.4 (CH), 36.6 (CH), 20.0 (CH₂), 10.9 (CH₃); [α]_D²⁵ = -10.4 (*c* = 0.43 in chloroform, 69% ee); **HPLC** (Lux 3 μm-cellulose 5, Hexane/*i*-Propanol 85:15, flow: 0.4 mL/min., λ=210 nm) Syn stereoisomers (*t*_{major}: 16.05 min.; *t*_{minor}: 19.95 min.); Anti stereoisomers (*t*_{major}: 18.59 min.; *t*_{minor}: 17.64 min.).

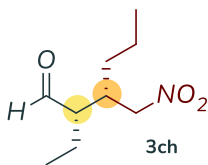
(2S,3S)-2-ethyl-5-methyl-3-(nitromethyl)hexanal **3cg**.⁶⁶



Synthesised in agreement with general procedure of asymmetric Michael addition of aldehydes to nitroalkenes via self-assembled minimal structures using fibrils of catalyst ^DPFF (8.8 mg, 0.0167 mmol), butyraldehyde (49.0 mg, 0.68 mmol), (*E*)-3-methyl-1-nitrobut-1-ene (39.1 mg, 0.34 mmol). The reaction mixture was stirred at 35 °C for 72h, to furnish the crude product [*dr* = 84:16, determined by integration of one set of ¹H NMR signal (δ_{major} 2.76 – 2.68 ppm, δ_{minor} 2.76 – 2.68 ppm, (m, 2H))]. The title compound was isolated as a pale yellow oil by flash chromatography (eluent in gradient: petroleum ether/ dichloromethane from 70:30 to 0:100) from 90:10 to 0:100 or petroleum ether) in 61% yield (41 mg, 0.20 mmol) and 73% ee.

¹H-NMR (400 MHz, CDCl₃) Syn product: δ = 9.71 (d, *J* = 1.2 Hz, 1H), 4.47 (dd, *J* = 12.5, 6.4 Hz, 1H), 4.41 (dd, *J* = 12.5, 6.6 Hz, 1H), 2.76 – 2.68 (m, 2H), 2.42 (dtd, *J* = 9.0, 4.8, 1.2 Hz, 1H), 1.79 (ddq, *J* = 14.7, 8.5, 7.4 Hz, 1H), 1.60 (dp, *J* = 13.3, 6.6 Hz, 1H), 1.49 (dq, *J* = 14.8, 7.5, 5.0 Hz, 1H), 1.22 (ddd, *J* = 7.8, 6.6, 4.6 Hz, 2H), 1.00 (t, *J* = 7.4 Hz, 3H), 0.90 (dd, *J* = 6.5, 5.0 Hz, 6H); ¹³C-NMR (101 MHz, CDCl₃) δ = 203.0 (CHO), 77.2 (CH₂), 54.1 (CH), 38.4 (CH₂), 34.8 (CH), 25.3 (CH), 22.7 (CH₃), 22.1 (CH₃), 18.6 (CH₂), 12.2 (CH₃); [α]_D²⁵ = +3 (*c* = 0.10 in chloroform); HPLC (Lux 3 μ -cellulose 5, Hexane/*i*-Propanol 85:15, flow: 0.5 mL/min., λ =210 nm) Syn stereoisomers (*t*_{major}: 6.32 min.; *t*_{minor}: 8.22 min.); Anti stereoisomers (*t*_{major}: 17.28 min.; *t*_{minor}: 7.77 min.).

(2S,3S)-2-ethyl-3-(nitromethyl)hexanal **3ch**.⁵⁸



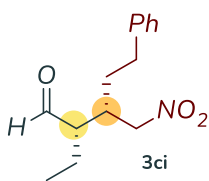
Synthesised in agreement with general procedure of asymmetric Michael addition of aldehydes to nitroalkenes via self-assembled minimal structures using fibrils of catalyst ^DPFF (8.8 mg, 0.0167 mmol), butyraldehyde (49.0 mg, 0.68

⁶⁶ K. S. Feu, A. F. de la Torre, S. Silva, M. A. F. de Moraes Junior, A. G. Corrêa, M. W. Paixão, *Green Chem.* **2014**, *16*, 3169.

mmol), (*E*)-1-nitropent-1-ene (39.1 mg, 0.34 mmol). The reaction mixture was stirred at 35 °C for 72h, to furnish the crude product [*dr* = 83:17, determined by integration of one set of ¹H NMR signal (δ_{major} 2.43 – 2.31 ppm, δ_{minor} 2.27 – 2.22 ppm, (*m*, 1H))]. The title compound was isolated as a pale yellow oil by flash chromatography (eluent in gradient: petroleum ether/ dichloromethane from 70:30 to 0:100) in 40% yield (25 mg, 0.13 mmol) and 70% ee.

¹H-NMR (400 MHz, CDCl₃) Syn product: δ = 9.70 (d, *J* = 1.4 Hz, 1H), 4.50 – 4.29 (m, 2H), 2.70 – 2.54 (m, 1H), 2.43 – 2.31 (m, 1H), 1.77 (ddt, *J* = 14.0, 7.3, 5.2 Hz, 1H), 1.60 – 1.29 (m, 5H), 0.99 (td, *J* = 7.4, 3.6 Hz, 3H), 0.91 (p, *J* = 5.9, 5.2 Hz, 3H); ¹³C-NMR (101 MHz, CDCl₃) δ = 203.2 (CHO), 77.0 (CH₂), 53.9 (CH), 36.6 (CH), 31.3 (CH₂), 20.0 (CH₂), 18.6 (CH₂), 13.9 (CH₃), 12.1 (CH₃); [α]_D²⁵ = –2.8 (*c* = 0.14 in chloroform, 70% ee); HPLC (Lux 3 μ m-cellulose 5, Hexane/*i*-Propanol 85:15, flow: 0.5 mL/min., λ =210 nm) Syn stereoisomers (*t*_{major}: 7.99 min.; *t*_{minor}: 11.01 min.); Anti stereoisomers (*t*_{major}: 17.07 min.; *t*_{minor}: 9.31 min.).

(2*S*,3*S*)-2-ethyl-3-(nitromethyl)-5-phenylpentanal **3ci**.⁶⁷



Synthesised in agreement with general procedure of asymmetric Michael addition of aldehydes to nitroalkenes via self-assembled minimal structures using fibrils of catalyst ⁰PFF (8.8 mg, 0.0167 mmol), butyraldehyde (49.0 mg, 0.68 mmol), (*E*)-(4-nitrobut-3-en-1-yl)benzene (60 mg, 0.34 mmol). The reaction mixture was stirred at 35 °C for 24h, to furnish the crude product [*dr* = 83:17, determined by integration of one set of ¹H NMR signal (δ_{major} 9.68 ppm, δ_{minor} 9.66 ppm - d)]. The title compound was isolated as a pale yellow oil by flash chromatography (eluent in gradient: petroleum ether/ ethyl acetate from 90:10 to 0:100) in 74% yield (62 mg, 0.25 mmol) and 73% ee.

¹H-NMR (400 MHz, CDCl₃) Syn product: δ = 9.68 (d, *J* = 1.4 Hz, 1H), 7.31 – 7.14 (m, 5H), 4.53 (dd, *J* = 12.5, 6.8 Hz, 1H), 4.47 (dd, *J* = 12.6, 6.2 Hz,

⁶⁷ Y. Wang, S. Ji, K. Wei, J. Lin, RSC Adv., 2014, 4, 30850

1H), 2.78 – 2.58 (m, 3H), 2.46 (dtd, $J = 8.6, 5.0, 1.4$ Hz, 1H), 1.85 – 1.65 (m, 3H), 1.60 – 1.49 (m, 1H), 0.98 (t, $J = 7.5$ Hz, 3H); $^{13}\text{C-NMR}$ (101 MHz, CDCl_3) $\delta = 202.9$ (CHO), 140.5 (C), 128.6 (2 x CH), 128.2 (2 x CH), 126.3 (CH), 76.8 (CH_2), 53.8 (CH), 36.2 (CH), 33.0 (CH_2), 31.0 (CH_2), 18.7 (CH_2), 11.9 (CH_3); $[\alpha]_{\text{D}}^{25} = -13.4$ ($c = 0.26$ in chloroform, 73% ee); **HPLC** (Lux $3\mu\text{m}$ -cellulose 5, Hexane/*i*-Propanol 90:10, flow: 0.5 mL/min., $\lambda = 230$ nm) Syn stereoisomers (t_{major} : 11.79 min.; t_{minor} : 16.07 min.); Anti stereoisomers (t_{major} : 23.41 min.; t_{minor} : 13.09 min.).

Chapter 3: DoE-driven development of an organocatalytic protocol for the enantioselective preparation of γ -amino acids precursors in water



In this chapter, I will focus on two main aspects, that converge in the same direction, for the optimisation of a potentially applicable industry process. It was decided to improve a synthetic process leading to the formation of γ -amino acid precursors that are attractive pharmaceutical targets. The optimisation process involved the use of water as solvent medium. In order to carry out an optimisation of a reaction in water, switching from an organic solvent to an aqueous one. It was clear from the start that a significant number of experimental variables would have had to be taken into account. To better evaluate all the parameters that can affect the increase of the response rationally and efficiently, the optimisation of this work was carried out via Design of Experiment (DoE) (which will be discussed in more detail in the next section). Before starting the discussion, however, I would like to highlight the class of catalysts used for successful optimisation.

3.1 Dialkylprolinol ethers: water-compatible catalysts

The rapid development of organic reactions performed in water as a solvent is a topic that has interested many research groups in both academia and industry.¹ This is because, especially in industry, enormous efforts have been made to rationalise production and waste disposal costs in order to move in the direction of an increasingly competitive and ecologically aware market.

In fact, despite the unique physical properties of this solvent, that is economical and widely available, and the absence of risk in its manipulation, its use can present some disadvantages. For example, many catalysts establish a dense network of hydrogen bonds or other polar interactions with substrates to direct the approach of the second reagent. If water is used, all these interactions may be lost.²

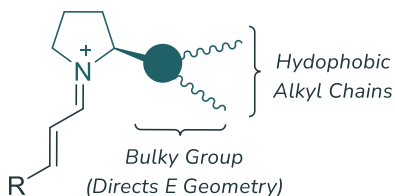


Figure 3. 1 Prolinols derived with alkyl chains

In 2007 the research group of Claudio Palomo synthesised a new class of prolinols derivatives able to ensure asymmetric induction in water solvents.³ They designed such organocatalysts by considering the bulky group near the aminic

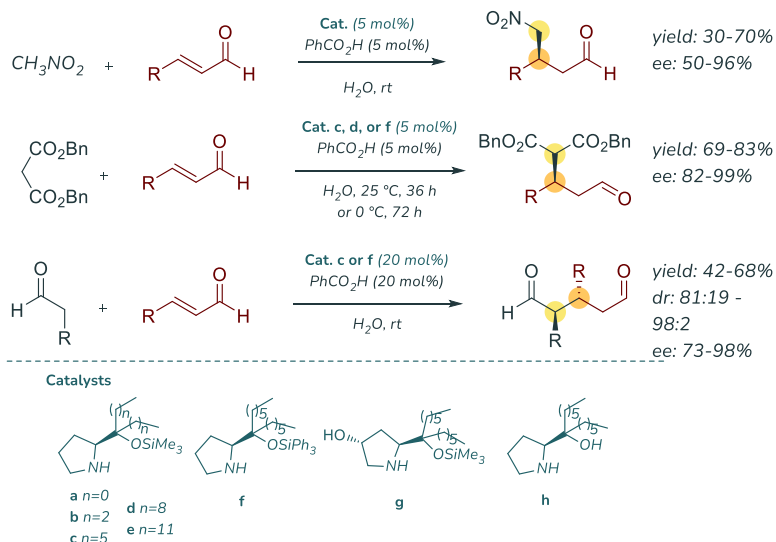
function, able to shield the enamine or iminium ion face, consisting of long alkyl chains (Figure 3. 1). The library of new catalysts has been used in various asymmetric transformations to perform C-C bond formation by activating carbonyl compounds with excellent performance (Scheme 3. 1). The corresponding reactive iminium ion derived from the enals/aldehyde α,β -unsaturated generated the conjugate addition

¹ B. S. Vachan, M. Karuppasamy, P. Vinoth, S. V. Kumar, S. Perumal, V. Sridharan, J. C. Menéndez, *Adv. Synth. Catal.* **2020**, 362, 87.

² D. G. Blackmond, A. Armstrong, V. Coombe, A. Wells *Angew. Chem. Int. Ed.* **2007**, 46, 3798.

³ C. Palomo, A. Landa, A. Mielgo, M. Oiarbide, A. Puente, S. Vera *Angew. Chem.* **2007**, 119, 8583.

product with nucleophiles such as benzyl malonate⁴ and nitromethane,³ and was also able to give Michael addition through a dual enamine/iminium ion mechanism by reaction with a saturated aldehyde.⁵



Scheme 3. 1 Examples of reactions performed with long-chain prolinols

From the experimental data obtained in this work, it was possible to note that the catalysts exhibit good catalytic efficiency in aqueous media at relatively low loading (5 mol% in the first two cases and 20 mol% in the double activation) and that they are able to induce enantio- and diastereo-selection with excellent results just like diaryl prolinol ethers.

⁴ S. Brandau, A. Landa, J. Franzén, M. Marigo, K. A. Jørgensen, *Angew. Chem. Int. Ed.* **2006**, *45*, 4305.

⁵ a) Y. Chi, S. H. Gellman, *Org. Lett.* **2005**, *7*, 4253. b) T. J. Peelen, Y. Chi, S. H. Gellman, *J. Am. Chem. Soc.* **2005**, *127*, 11598. c) P. Melchiorre, K. A. Jørgensen, *J. Org. Chem.* **2003**, *68*, 4151.

The structural analogy between such catalysts is perfectly reflected in the reaction mechanism, since the alkyl chains, despite their flexibility, still generate the steric bulk necessary to shield the stereogenic face.

Also in this case, it has been observed that if the hydroxyl group is not functionalised with a protecting group, a hydrogen bond will be established with the second reactant leading to the formation of the product with opposite enantioselection.

3.2 DoE: a rational approach to improve the experimental responses

Design of Experiments (DoE) is a powerful chemometric method that is frequently used to optimise a specific chemical problem affected by numerous variables, which may be both experimental and instrumental. The rationalisation of the variables associated with the problem to be solved can be multiple, which is why mathematical, computational, and statistical methods come into play to try to solve the problem.⁶ In the following text, we will explain why Experimental Design offers the synthetic chemist an advantage in its use both for reasons of gaining time

⁶ For review and articles about DoE and a deeper discussion on mathematical and statistical aspects, please see: a) Box, G. E. P.; Draper, N. R. In *Empirical Model-Building and Response Surfaces*, Wiley, New York, **1986**; b) Lundstedt, T.; Seifert, E.; Abramo, L.; Thelin, B.; Nyström, Å., Pettersen, J.; Bergman, R. *Chemometrics and Intelligent Laboratory Systems*, **1998**, *42*, 1–2, 3; c) Carlson, R. *Chemometrics and Intelligent Laboratory Systems*, **2004**, *73*, 1, 151; d) Tye, H. *Drug Discovery Today*, **2004**, *9*, 485; (e) Ardini, F.; Soggia, F.; Rugi, F.; Udisti, R.; Grotti, M. *Analytica Chimica Acta* **2010**, *678*, 18; (f) Dejaegher, B.; Vander Heyden, Y. *J. Pharm. Biomed. Anal.* **2011**, *56*, 141; (g) Murray, P. M.; S. N. G. Tyler; Moseley, J. D. *Org. Process Res. Dev.* **2013**, *17*, 40; (h) Di Carro, M.; Ardini, F.; Magi F. *Microchemical Journal*, **2015**, *121*, 172; (i) Westad, F.; Marini, F. *Analytica Chimica Acta*, **2015**, *893*, 14; (j) Brereton, R.G.; Jansen, J.; Lopes, J.; Marini, F.; Pomerantsev, A.; Rodionova, O.; Roger, J. M.; Walczak, B.; Tauler, R. *Anal Bioanal Chem*, **2017**, *409*, 589; (k) Brereton, R.G.; Jansen, J.; Lopes, J.; Marini, F.; Pomerantsev, A.; Rodionova, O.; Roger, J. M.; Walczak, B.; Tauler, R. *Anal Bioanal Chem*, **2018**, *410*, 6691; (l) Debevec, V.; Srčić, S.; Horvat, M. *Drug Development and Industrial Pharmacy*, **2018**, *44*, 3, 566; (m) Weese, M.L.; Ramsey, P.J.; Montgomery, D.C. *Appl Stochastic Models Bus Ind.* **2018**, *34*, 244; (n) Mishra, P.; Biancolillo, A.; Roger, J.M.; Marini, F.; Rutledge, D.N. *Trends in Analytical Chemistry*, **2020**, *132*, 116045.

and resources by focusing our attention on the process aspect of optimising a synthetic process.

3.2.1 Chemometrics

Chemometrics is a branch of chemistry that offers the possibility of studying complex systems of variables systematically and rationally by using mathematical and statistical methods. This is achieved through the extrapolation of the maximum relevant chemical information by analysing a multitude of chemical data derived from properly selected or designed experimental procedures. More specifically, the use of the DoE method stems from the need to rationalise the issues with n -variables, more or less interconnected by each other, by carrying out simultaneous (multivariate) variations between them.

3.2.2 Mathematical information: from chemist to chemometrician

When a synthetic organic chemist is required to synthesise a specific target molecule, firstly it is required to find the most suitable experimental procedure reported in literature by varying the experimental conditions that may influence the success of a chemical reaction. In-depth knowledge of the problem to be solved is fundamental to improve the reactivity or limit the formation of by-products. These experimental variables can be several and, in most cases, interrelated. For example, a given asymmetric catalyst induces greater enantioselection when the reaction temperature is reduced but, at the same time, reducing it may lead to the reaction following different reactive paths, or to solubility problems for example, which may limit the formation of the desired product.⁷ At this point, it is necessary find the experimental parameter has the greatest influence on the yield of the reaction, or the minimisation of the formation of a by-product, the enantiomeric excess or, more in general, on the optimisation of an entire synthetic process. As

⁷ Leardi, R., Marini, F. In *Chemometrics in Food Chemistry*, Vol. 28, Ed.; Elsevier: Amsterdam, 2013, 9.

we know, the experimental parameters that can influence a chemical reaction can be multiple, and at a non-prone-mathematics eye, it is often very difficult to associate them with mathematical variables ($n \times n$ matrices) but, if by hypothesis, two variables insist on a considered system, an "intuitive" strategy can be employed for the optimisation of a chemical reaction. The best condition, or local optimum condition, may be found by serendipity, considering the variation of One Variable At a Time (OVAT) (see Figure 3. 2).⁸

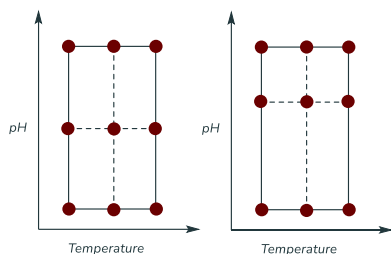


Figure 3. 2 Exploration of chemical space using an OVAT approach

However, in presence of a huge number of variables, it is surely preferable to proceed using a rational approach rather than relying on fate, because there could be a risk of exploring a whole range of conditions that have little or no influence on the outcome (response). In addition, it must be considered that not all experimental variables are independent of each other, there is often a correlation between the variables themselves (dependent variables). From a planning point of view, the DoE represents therefore a methodological approach particularly useful to visualise n -variable systems.⁹ After having thoroughly rationalised the problem both from the theoretical and practical point of view, are establish the variables (the **factors**) that could most influence the result to be optimised (the **multidimensional response surface**). A preliminary screening of n -variables is carried out in order to evaluate, in an approximate way, the variation of the parameter to be optimised (the response). The variables to be considered can be, for example, the solvent, the concentration of a given reagent or catalyst, time, and temperature. At this point, the upper and lower limits (**levels**)

⁸ a) Carlson, R.; Carlson, J. E. In *Data Handling in Science and Technology*, Vol 24; Rutan, S.; Walczak, B., Ed.; Elsevier: Amsterdam, 2005, 1; b) Leardi, R. *Anal. Chim. Acta* 2009, 652, 161;

⁹ Benedetti, B; Caponigro V.; Ardini F. *Critical Reviews in Analytical Chemistry*, 2020, 1.

of the n -dimensional variable surface to be explored (the **experimental domain**) are defined. With the aid of software, a limited number of experiments can be planned to explore the chemical multi-dimensional space exhaustively and rationally and understand the effect of factors and/or model the relationship between dependent and independent variables (See Figure 3. 3).

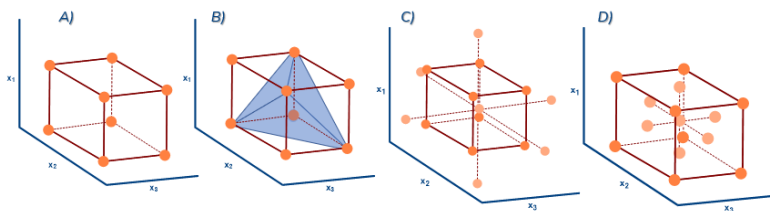


Figure 3. 3 Selected example of graphical representation of a full (A) and fractional (B) factorial design and a circumscribed (C) and a face-centred composite design (D).

More in general by treating the chemical problem as a mathematical function is obtained:

$$(Equation 1) \quad y_i = b_0 + b_1x_1 + b_2x_2 + b_3x_3 + \dots + b_nx_n + b_{12} x_1x_2 + b_{13} x_1x_3 + b_{23} x_2x_3 + \dots + b_{123} x_1x_2x_3 + b_1x_1^2 + b_2x_2^2 + b_3x_3^2$$

where the response to be optimised (dependent variable, y_i) will be given in a first approximation, by the sum of the linear contributions of the factors (independent or uncorrelated variables, $x_1, x_2, x_3, \dots, x_n$) multiplied by the statistical weight they provide to the system (coefficients $b_1, b_2, b_3, \dots, b_n$) plus a constant term (b_0), the interaction factors ($b_{12} x_1x_2, \dots$) and the quadratic factors ($b_1x_1^2, \dots$). The degree to which factors are considered determines the accuracy and level of approximation of the problem to be solved.

This methodology, erroneously poorly exploited by the synthetic/organic community, allows a significant reduction in experimental costs and time compared to the "trial and error" method. In fact, if the mathematical model found at the end (the n -variable surface function) is consistent with the experimental data obtained with the DoE, a multiplicity of information can be obtained, both on the correlation of the variables, but also on the prediction of these variables at each unexplored point of the experimental domain with known precision. In fact, while an OVAT approach provides

information only at the points in the experimental domain where the experiments were performed, a multi-variate approach provides more accurate knowledge of the entire domain. In this way is possible to predict the optimum condition which will be found on a point of an absolute maximum of the response surface (which may not have been investigated in the previous DoE).

3.2.3 The selection of the correct DoE: how to proceed

The selection of the correct DoE is aimed at finding a correct mathematical model that can approximate the experimentally obtained data as closely as possible. In this way, the experimental domain is well represented from an accurate data set.

There are several types of experimental designs that can be applied to optimise a response depending on the nature of the considered experimental variables. The degree of approximation of the problem resolution defines the different DoE models.¹⁰

After performing the experiments generated by the software, and obtaining the desired response, the matrix defining the response surface can be completed. At this point, it is possible to calculate the coefficient of each investigated variable to evaluate and estimate the contribution, positive or negative, that each variable makes to the response and is, therefore, able to identify the experimental direction in which to perform subsequent designs through a careful analysis of the response surfaces (Figure 3. 4).

¹⁰ R. Carlson, *Chemom. Intell. Lab. Syst.*, **2004**, 73, 151.

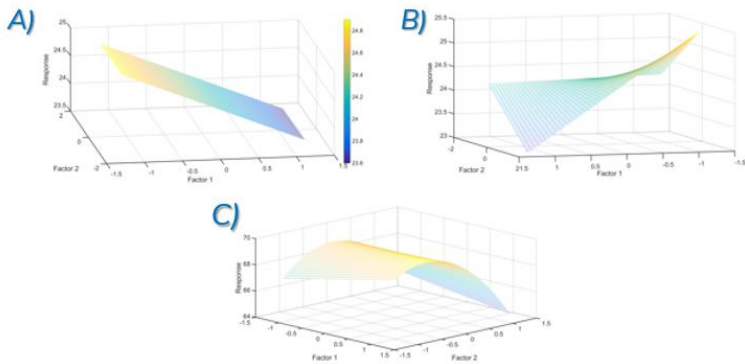


Figure 3. 4 Representation of response surfaces for linear (A), interaction (B) and quadratic (C) models.

Linear model - Screening Design

By considering just only the linear term of the Equation 1, the experimental domain is represented by the n -dimensional function, where n is the number of experimental variables under consideration.

Each variable will be investigated only at two experimental limit values, to which the values -1 and $+1$ will be attributed respectively to the lowest and the highest level.

The linear model will rarely provide a precise description of the analysed system, but will only provide information on which experimental variables make the most significant contribution to solving the problem, without considering possible correlations between them. In this way, it will be possible to carry out a second, more refined experimental design that considers only the significant experimental variables and excludes the less significant ones.

Interaction model - Improvement design

After evaluating which linear variables have the greatest impact on the system, it is appropriate to carry out designs in which it is possible to evaluate the possible interaction effects between the factors themselves to approximate the n -dimensional function more rigorously. It is therefore

necessary to consider also the non-linear terms of the function that describes the response, namely the interaction factors, also called crossed terms ($b_{12} x_1x_2$, $b_{13} x_1x_3$, $b_{23} x_2x_3$... $b_{123} x_1x_2x_3$). By including these terms in the model it will be possible to investigate the effect that two or more variables have simultaneously on the response.

Modeling the response function more accurately, it is possible to calculate prediction models, with a good approximation, for the response located at a point belonging to the experimental domain not yet explored. As with the linear models, only the extremes of the levels for each variable (-1 and +1) are considered in this model.

Quadratic models – optimisation design

If the DoE aims to obtain the maximisation of a response, the quadratic terms of the different factors must also be considered. This implies studying the function describing the response surface at a point of maximum, where there will be a point of discontinuity. In this case, the quadratic terms must also be included to describe the linear and non-linear dependencies between the responses and the variables. This means that 3 levels for each variable have to be studied.

D-Optimal – from screening to optimisation design

Determinant-Optimal Design, or D-Optimal Design, is a more recent and flexible algorithm that can be used for both screening and optimisation stages.¹¹ In this design, all possible linear combinations of the analysed variables (i.e. all matrices) are taken into account to minimise the covariance of the parameter estimates for an analysed model. Subsequently, matrices with the highest determinant are selected to find the more promising experiments.

3.2.4 Example of DoE in organic synthesis

In the following section was reported two different strategies to perform the optimisation of the reaction conditions in organic synthesis. The aim

¹¹ (a) Atkinson, A. C.; Tobias, R. D. J. *Chromatogr. A* 2008, 1177, 1 (b) Leardi, R. In *Encyclopedia of Analytical Chemistry*; Wiley, Ltd: Chichester, UK, 2018, 1.

of this is to highlight how the DoE is a valid approach not strictly related to analytical problems resolution.¹²

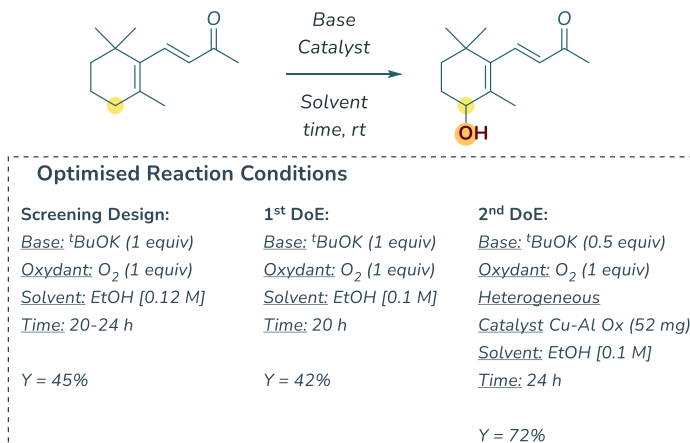
DoE to increase the yield of versatile building block

In this paper, the authors reported the optimisation of the synthesis of an important synthon precursor of 8-hydroxylated terpenes, the γ - or ε -hydroxylated compound obtained via oxidation of α,β - and $\alpha,\beta,\gamma,\delta$ -enones and using oxygen (from the air) in presence of Copper-Aluminium mixed oxide (Cu-Al Ox).¹³

*During a preliminary screening study of the system variables, the authors decided to set some parameters: protic solvent (EtOH), a strong base (*t*BuOK), and the reaction time of 24 h to avoid the possibility to reduce the yield of the desired compound, probably due to overoxidation of the product. Additionally, the atmospheric O₂ was chosen as oxidising reagent, because it was sufficiently adequate for this reaction.*

¹² For selected examples on the application of DoE in academia, see: (a) Jamieson, C.; Congreve, M. S.; Emiabata-Smith, D. F.; Ley, S. V. *Synlett*, **2000**, 1603; (b) Jamieson, C.; Congreve, M. S.; Emiabata-Smith, D. F.; Ley, S. V.; Scicinski, J. *J. Org. Process Res. Dev.*, **2002**, 6, 823; (c) Evans, M. D.; Ring, J. Schoen, A.; Bell, A.; Edwards, P.; Berthelot, D.; Nicewonger, R.; Baldino, C. M. *Tetrahedron Lett.* **2003**, 44, 9337; (d) Veum, L.; Pereira, S. R. M.; Van der Waal, J. C.; Hanefeld, U. *Eur. J. Org. Chem.* **2006**, 1664; (e) Glasnow, T. N.; Tye, H.; Kappe, C. O. *Tetrahedron*, **2008**, 64, 2035; (f) Hajzer, V.; Alexy, P.; Latika, A.; Durmis, J.; Šebesta, R. *Monatsh. Chem.* **2015**, 146, 1541; (g) Ekebergh, A.; Lingblom, C.; Sandin, P.; Wennerås, C.; Mårtensson, J. *Org. Biomol. Chem.* **2015**, 13, 3382.

¹³ M. Miyashita, T. Suzuki, A. Yoshikoshi, *J. Org. Chem.* **1985**, 50, 3377.



Scheme 3. 2 Selected experimental variables and results

To optimise the reaction condition, a 3 levels-Full-Factorial Design was performed by selecting the reported variables in Scheme 3. 2.

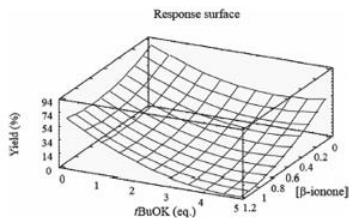


Figure 3. 5 Calculated response surface for the oxidation of β -ionone (figure reported in the article¹³)

Additionally, there were no interactions observed between the variables, and the analysis of the response surface plot reveals that increasing the substrate concentration and the number of base equivalents decreases the yield (Figure 3. 5).

Before proceeding to the new optimisation with a second DoE, further tests were carried out varying the amount of base. For values lower than 1 equivalent the yield worsened but increasing it slightly to 1.2 equivalents, the yield increases from 50% to 55%.

Despite the improvement in yield, the authors decided to optimise the reaction yield by using a heterogeneous catalyst Cu-Al ox, which they had previously synthesised and which showed marked catalytic behavior, especially when it was pre-activated (10 minutes before the use in EtOH with stirring).

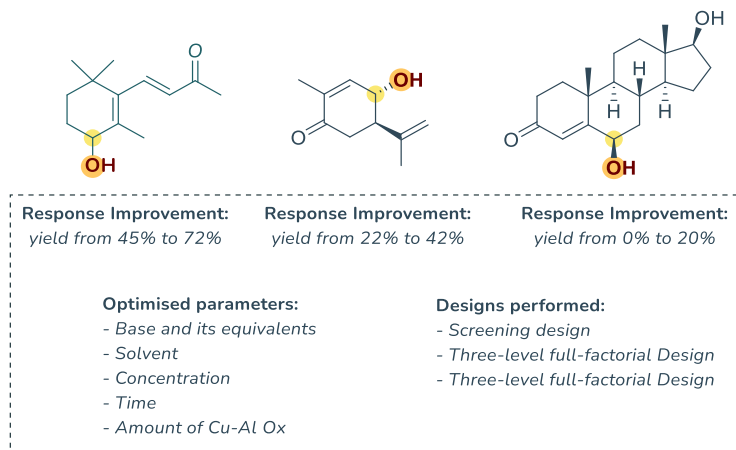


Figure 3. 6 Improved response for some substrate

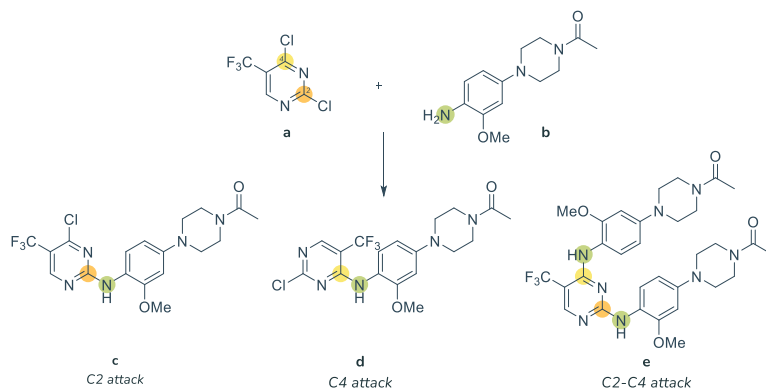
Moreover, this DoE was performed on carvone as starting material, a substrate that is unlikely to be hydroxylated at the allylic position. After that, the second three-levels-Full-Factorial design was employed by changing the concentration of base and carvone as starting material, and also the amount of heterogeneous catalyst. The best condition found in presence of heterogeneous catalyst had increased, for the carvone as starting material the yield from 22% of the preliminary screening to 42% in the second DoE, for the β -inone, from 55% to 72%, and for testosterone, which did not promote the formation of the oxidised compound in the absence of Cu-Al Ox, the authors recorded a 20% conversion (Figure 3. 6).

DoE to solve Regioselective problem

The synthesis reaction was developed and optimised by following a quality by design (QbD) approach, with which a control strategy was developed to improve the level of quality assurance.

In this study, the DoE was applied to determine the correlation between variables involved to optimize the regioselectivity in a crucial synthetic

step concerning the synthesis of an API, the Rocetiletinib.¹⁴ The precursor is derived from the nucleophilic attack of the primary amino compound **b** on the C2 of the pyrimidine ring **a**.



Optimised Reaction Conditions		
Preliminary Screening:	1st DoE: Custom Design	Further optimisation:
Base: NaOAc (1.1 equiv)	Concentration: ^t BuOK (1 equiv)	Order of addition
Solvent: MTBE/ ^t BuOH 1:1	MTBE/ ^t BuOH ratio: 1:1	
Temperature: 25 °C	Equiv of Base: 1.05 equiv	
		Predicted Response:
		(by using response surface analysis)
Conversion 94%	Conversion 96%	Total conversion >80%
Isomer ratio c/d/e:	Isomer ratio c/d/e:	Compound c: Y>50%
76 : 9 : 0.6	76 : 8 : 1.9	Compound d: Y<12%
		Compound e: Y> 1%

Scheme 3. 3 Selected experimental variables and results

As it is well known, using for example 2,4-dichloropyrimidine as an electrophile, without any modification, one obtains a mixture of three compounds in different ratios (**c**, **d**, and **e**) derived from equiprobable nucleophilic attack at positions C-2 and C-4 by amines and alcohols. To try to direct the nucleophilic attack and increase the regioselectivity on C-2, it would be necessary to include a voluminous electron-withdrawing

¹⁴ S. Kapić, I. Nekola, F. Jović, M. Mihovilović, Chem. Biochem. Eng. Q., **2018**, 32, 2, 167

group on C-5 capable of stabilising the positive charge and simultaneously shielding the C-4 position.¹⁵

Additionally by using a Lewis acid, such as ZnCl₂ in the proper amount, is it possible to further shield the C-4 position by the complexation on N-3.

For the preliminary screening solvents, the authors report that more than 120 solvents, and combinations of these, were selected by the PCA method based on chemical and physical properties (solubility in water, boiling point, density, etc.). Of all the solvents, those that did not have polar and lipophilic characteristics were selected. The best condition was found by using CPME/^tBuOH but MTBE/^tBuOH was chosen as mixture solvent because MTBE had a lower boiling point and also is cheaper than CPME. As concerning the screening bases, despite the use of K₂CO₃ as a base, it is the best choice for the regioselectivity (**c**/**d** = 14:1), its use renders difficult the purification of the resulting compound due to the formation of an insoluble salt, the ZnCO₃; instead the ^tBuOK increases the formation of side products **d** and **e**. For this reason, NaOAc, which does not form an insoluble Zinc salt in water, was selected (conversion 95% in 20 h at 25 °C). In this condition, the authors also reported that the increase of the temperature promotes the formation of the compound **e**.

Three final parameters are considered in Custom Design to optimise the process. The screened variables were the solution concentrations, the ratio between the mixture of solvent, and the equivalents of the base. From the experimental data, the author has verified that the excess of the base does not lead to significant changes in the reaction profile but its increase leads to the formation of more hydrolytic impurities (Scheme 3. 3).

The optimum point in the experimental domain previously predicted with response surface analysis was in accordance with experimental data. The order of the additions was another parameter observed by the authors. They found that the addition of the pre-formed anion (by reaction

¹⁵ a) D.T. Richter, J. C. Kath, M. J. Luzzio, N. Keene, M. A. Berliner, M. D. Wessel, *Tetrahedron Lett.* **2013**, 54, 4610. b) J. A. MacPhee, A. Panaye, J. E. Dubois, *Tetrahedron*, **1978**, 34, 3553. c) M. Charton, *J. Am. Chem. Soc.* **1975**, 97, 1552.

between **b** and base) to a solution containing Nucleophile and Lewis acid, provides a low isomer ratio and conversion, instead of adding the base after 1 hour. If, the nucleophile is introduced 1 hour after the addition of the base to the complex (**a**+ZnCl₂), the product substituted **d** is obtained in a yield of less than 2% and the disubstituted **e** is minor than 5%.

Abstract: *The development of an enantioselective enamine-catalysed addition of masked acetaldehyde to nitroalkenes via a rational approach helped to move away from the use of chloroform. The presented research allows the use of water as a reaction medium, therefore improving the industrial relevance of a protocol to access very important pharmaceutical intermediates. Critical to the success is the use of chemometrics-assisted 'Design of Experiments' (DoE) optimisation during the development of the presented new synthetic approach, which allows to investigate the chemical space in a rational way.*

3.3 Target of the project

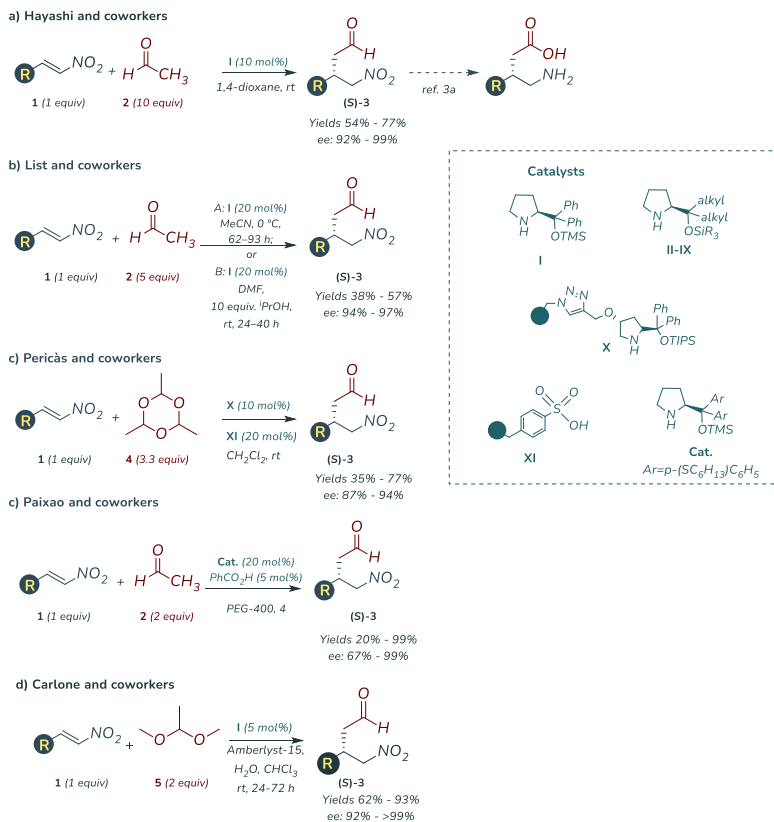
Acetaldehyde is an extremely versatile building block in organic synthesis as it allows two carbon atoms, one of which is a carbonyl function, to be introduced into the final product. As a pure reagent, it requires a whole series of risk assessments that limit its utilisation; it exhibits high reactivity (oligomerisation *in situ*), volatility, and flammability (bp 21° C), without considering its high toxicity through inhalation or skin contact (may cause damage at the cellular and genomic level).¹⁶ The right compromise to use it as a starting material was found by using it as a masked reagent and then deprotecting it *in situ*. Its high reactivity, however, has led many research groups to use it to large excess.¹⁷ Another eco-friendly strategy found in literature was reported by Paixão and coworkers, concerning the use of polyethylene glycol (PEG) as solvent and free acetaldehyde in solution.¹⁸ Although the authors achieved a good yield and enantioselectivity, they mentioned in the

¹⁶ R. Rajendram, R. Rajendram, V. R. Preedy, Chapter 51 - Acetaldehyde: A Reactive Metabolite, Editor(s): Victor R. Preedy, *Neuropathology of Drug Addictions and Substance Misuse*, Academic Press, 2016.

¹⁷ a) Y. Hayashi, T. Itoh, S. Aratake, H. Ishikawa *Angew. Chem. Int. Ed.* **2008**, 47, 2082–2084; b) Y. Hayashi, T. Itoh, M. Ohkubo, H. Ishikawa *Angew. Chem. Int. Ed.* **2008**, 47, 4722–4724. c) P. García-García, A. Ladépêche, R. Halder, B. List *Angew. Chem. Int. Ed.* **2008**, 47, 4719–4721. d) X. Fan, C. Rodríguez-Esrich, S. Sayalero, M.A. Pericàs *Chem. Eur. J.* **2013**, 19, 10814–10817.

¹⁸ K. S. Feu, A. F. de la Torre, S. Silva, M. A. F. de Moraes J. A. G. Corrêa, M. W. Paixão *Green Chem.* **2014**, 16, 3169.

manuscript the difficulty of handling the free reagent and the presence of undesirable side products.



Scheme 3. 4 Enantioselective organocatalysed Michael addition of masked acetaldehyde to nitroalkenes in water versus previous reports

In a previous study carried out in our laboratory,¹⁹ a new methodology was developed which allowed the use of acetaldehyde, masked as acetal, in reduced stoichiometric amounts and without having to carry out any particular expedients in the reaction set-up. The optimisation of the

¹⁹ G. Giorgianni, V. Nori, A. Baschieri, L. Palombi, A. Carlone *Catalysts*, 2020, 10, 1296.

reaction conditions allowed the reagent to be used in modest excess (2 equivalents), using an inorganic resin as an acid to deprotect *in situ* the carbonyl function (which can be easily removed by filtration and reactivated for future use) and simultaneously decrease the catalyst loading (5 mol%).

The critical issue that has been further overcome in the work presented in this thesis concerns the reaction solvent. In the previous work, chloroform was used as the reaction medium, a class II halogenated organic solvent that is not well tolerated by the pharmaceutical industry. This is because it has a negative impact both on the purification of the final product, it may remain in traces as a contaminant, and on problems related to its disposal.

It was therefore decided to use water as the reaction solvent and to examine a wide range of experimental parameters that could increase the performance of the optimisation. The qualitative parameters selected had involved the choice of organocatalysts (most suitable for the aqueous solvent), the acidic co-catalyst, the ionic strength of the solvent medium, and any organic co-solvents. The quantitative parameters were taken into account, the masked acetaldehyde equivalents, the catalyst loading of the organocatalysts and the acid co-catalyst, the reaction concentration, and the reaction time. The large number of parameters considered led us to use the chemometric method of Experimental Design (DoE) in order to efficiently rationalise which experimental variables had the greatest impact on optimising the synthetic process under consideration. DoE is a powerful tool, supported by statistics and mathematics, which is widely used in industries and allows rational exploration of the “chemical space” by performing fewer experiments.²⁰ This has also led to an increase in the

²⁰ For selected examples on the application of DoE in industry, see: (a) Owen, M.; Godbert, S. *Org. Process Res. Dev.*, **2001**, *5*, 324; (b) Laird, T. *Org. Process Res. Dev.* **2002**, *6*, 337; (c) Tye, H.; Whittaker, M. *Org. Biomol. Chem.* **2004**, *2*, 813; (d) Guercio, G.; Perboni, A.; Tinazzi, F.; Rovatti, L.; Provera, S. *Org. Process Res. Dev.*, **2010**, *14*, 840; (e) Murray, P. M.; Tyler, S. N. G.; Moseley, J. D. *Org. Process Res. Dev.*, **2013**, *17*, 40; (f) Stone, S.; Wang, T.; Liang, J.; Cochran, J.; Green, J.; Gu, W. *Org. Biomol. Chem.* **2015**, *13*, 10471; (g) Weissman, S. A.; Anderson, N. G. *Org. Process Res. Dev.*, **2015**, *19*, 1605.

sustainability of the entire optimisation process, as well as gains in terms of time and money.

3.4 Results and discussion

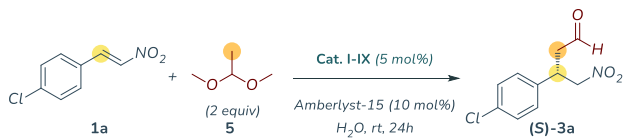
To optimise the reaction conditions leading to the formation of γ -amino acids using water as a solvent, it was initially decided to consider *p*-chloro nitrostyrene as the starting material because:

- it is the precursor of the Baclofen API.
- The enantiomeric excess can be analysed more rapidly by HPLC on a chiral stationary phase (after reduction with sodium boron hydride), contrary to the Pregabalin precursor which, in addition to reduction, requires an additional tosylation step in order to be properly separated.
- It can be easily synthesised on a gram scale, it is solid and is therefore easier to handle (in the case of (*E*)-4-methyl-1-nitropent-1-ene, the electrophilic reagent of pregabalin, it is a highly volatile liquid and is irritant to eyes).

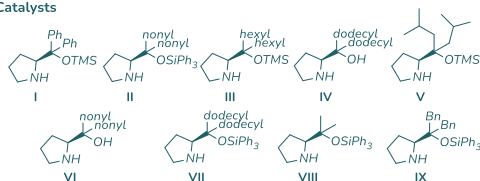
A single batch was synthesised and used throughout the optimisation so that no additional experimental variables were encountered due to the purity of the compound.

In preliminary screening, all the **I-IX** organocatalysts were tested under the same experimental conditions as optimised in the previous work but using distilled water as the solvent.¹⁹ As shown in **Table 3. 1**, only a few catalysts ensured acceptable conversion of the reactants into products even though the reaction was sluggish, although the ee was moderately good. The most promising catalyst has also tested the effect of solution concentration but produced no appreciable change in conversion and enantiomeric excess (entries 7, 10, and 11).

Table 3. 1 Preliminary screening conditions ^a



Catalysts



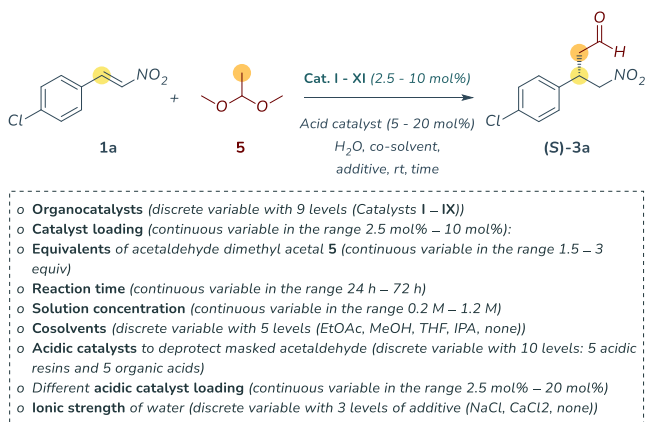
Entry	Catalyst	M (mol/L)	Conv. [%] ^[b]	ee [%] ^[c]
1	I	1.6	27	62
2	II	1.6	<5	n.d.
3	III	1.6	6	79
4	IV	1.6	<5	n.d.
5	V	1.6	<5	n.d.
6	VI	1.6	<5	n.d.
7	VII	1.6	20	79
8	VIII	1.6	12	72
9	IX	1.6	17	61
10	VII	0.8	19	80
11	VII	0.4	18	79

[a] Reactions performed on 0.4 mmol scale; catalyst (0.02 mmol, 5 mol%), 4-chloro- β -nitrostyrene **1a** (60 mg, 0.4 mmol, 1 equiv), acetaldehyde dimethyl acetal **5** (85 μ L, 0.8 mmol, 2 equiv), Amberlyst-15 (14 mg, 10 mol%) and water as solvent at room temperature. [b] Measured by ¹H NMR spectroscopy. [c] Determined by chiral HPLC analysis after conversion of the aldehyde into the corresponding alcohol by reduction with NaBH₄.

This high variability was not at all expected. The problem was extensively re-evaluated by also considering the effect of the solvent and all other experimental variables that might have had the greatest influence on the response of the system considered.

The numerous qualitative and quantitative variables identified (listed below) suggested to prefer a multivariate method to undertake the optimisation process, as by imposing the variables at the chosen levels, number of experiments performed using the OVAT method would have been too high (43200 experiments).

The screened variables were: type of organocatalysts (I-IX) and catalyst loading, equivalents of acetaldehydes dimethylacetal **5**, acidic catalysts to deprotect **5** (organic, inorganic, and immobilised acids were tested) and its loading, reaction time, reaction concentration, presence of co-solvents, ionic strength of water (Scheme 3. 5). By applying a D-Optimal Design the number of experiments was drastically reduced to 34, due to its high modularity in the inclusion of variables in the mathematical algorithm, where the responses to be optimised were conversion and enantiomeric excess.



Scheme 3. 5 Experimental conditions for the first D-Optimal

Despite a considerable number of experiments with yields below 5%, it was still possible to identify from the model generated via principal component analysis (PCA) which experimental variables significantly and positively influenced the system (Figure 3. 8). These variables are the reaction concentration, the catalyst loading, and the choice of organocatalyst.

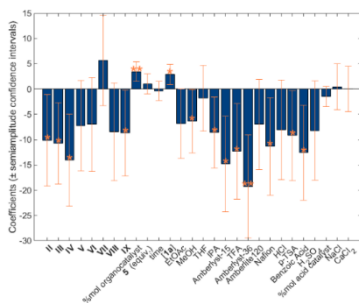


Figure 3. 7 Plot of the coefficients of the mathematical model of the response Y_{NMR} for the first preliminary screening via D-Optimal Design. The significance of the coefficients is labelled with the same convention for asterisks in all the figures: *p-value<0.05, **p-value<0.01, ***p-value<0.001.

Of all the organocatalysts tested, only catalysts **I** and **VII** were found to have the best performance. In the following DoE, however, it was decided to also evaluate the effect of organocatalyst **II** because of its structural similarity to catalyst **VII**. Moreover, the lower level in the following DoE was set at 5% because the loading limit of 2.5% was never able to lead to the formation of the desired product.

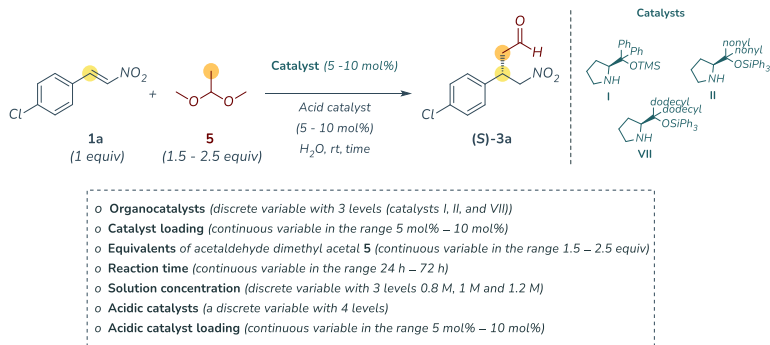
According to the chemometric model, the following parameters were found statistically not significant: the presence of organic

co-solvents and inorganic salts, the number of equivalents of **5**, the reaction time, the type and amount of acid catalyst to deprotect the acetaldehyde dimethyl acetal.

Because of the importance of some of the above-mentioned variables, from a purely synthetic point of view, the last four parameters were reconsidered in the second DoE. This is because chemometric irrelevance has been attributed to a very large number of experiments with a yield lower than 5%.

For this reason, although Amberlite 2900 gave the best results, the Amberlyst-15, Amberlite 1200, and HCl were also included in the next screening. The second D-Optimal design was performed investigating the organocatalysts (**I**, **II**, and **VII**), catalyst loading, equivalents of **5**, reaction time, reaction concentration, acidic catalysts, acidic catalyst loading.

In the second D-Optimal design 42 experiments, including 6 replicates, were performed (Scheme 3. 6).



Scheme 3. 6 Experimental conditions for the second D-Optimal

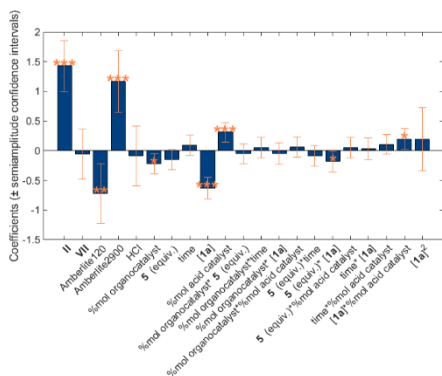


Figure 3. 8 The plot of the coefficients of the mathematical model of the response scores on PC2 (to be minimised in order to maximise Y_{NMR} and ee) for the second screening via D-Optimal Design.

meaning that it positively helps to increase the final response (10 mol% appeared to be the best half measure). On the other hand, the coefficient for reaction time is positive but not significant; as a result, its variation do not affect the final responses to be enhanced. This variable does not significantly correlate with the other variables, so its level can be chosen independently from the conditions used for the other variables. For practical reasons 24 hours was chosen as optimal time reaction. From the analysis of variance acid catalyst loading and equivalents of **5** had shown not influence the response, however, it was necessary to continue

The second model was constructed on PC2 scores and confirmed that the highest results were achieved with organocatalysts **I** and **VII** (Figure 3. 8).

Furthermore, the best acid catalyst in terms of conversion and enantiomeric excess was Amberlite120. As far as the organocatalyst loading is concerned, its coefficient is significant and negative,

investigating their contribution since they proved to correlate each other and with reaction mixture concentration. In detail, the response is maximised when at the same time the equivalents of **5** are at the maximum level (2.5 equivalents), the concentration of the limiting

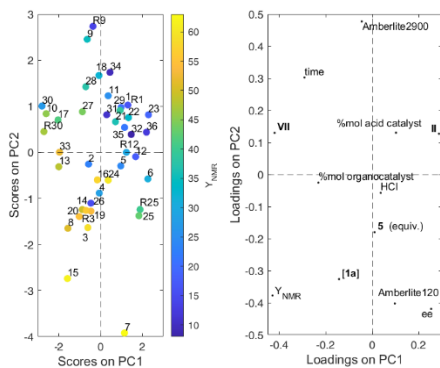
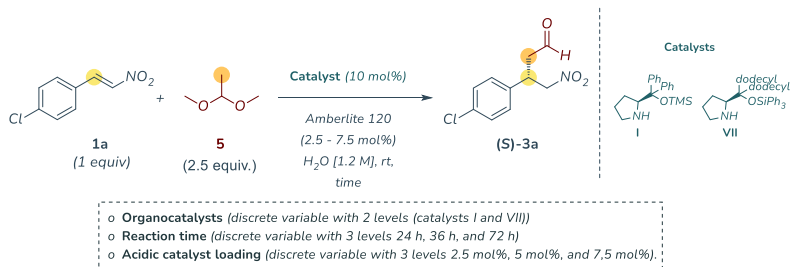


Figure 3. 9 Scores (left) and loadings (right) plots of the Principal Component Analysis (PCA) on the experimental data matrix. The colorbar shows the improving of the yield with the decreasing of the PC2-scores.

reagent in the aqueous medium is at the maximum level (1.2 M), and the acid resin loading is at the minimum level (5 mol%). The catalyst loading and the concentration of the reaction mixture were both significant parameters and favourably contributed to the rise in response. Replicates (inclusion of repeated experiments) were used to evaluate the experimental variability and reproducibility.

The outcome data analysis revealed a good agreement between replicates because they are close in principal component space PC-1 and PC-2; the pattern exhibited by the samples supports the choice of scores on PC2 as the response (to be minimised to maximize Y_{NMR} and ee) (Figure 3. 9). In order to further optimize the reaction conditions for all the responses studied, a third DoE (full factorial design with two variables and two levels) was conducted by using both organocatalysts (**I** and **VII**). The variables studied were (1) reaction time and (2) acid catalyst loading (Scheme 3. 7).



Scheme 3. 7 Experimental conditions for the third Full-factorial design.

The generated model employing organocatalyst VII resulted significant only for the yield and not for ee, as no significant improvements were observed for the latter in the studied experimental domain. Conversely, the yield can be optimised by examining the value of the coefficients. As shown in Figure 3. 10, the coefficient related to the reaction time is

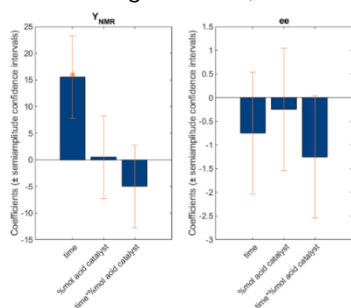


Figure 3. 10 The plot of the coefficients of the mathematical model of the response Y_{NMR} and the ee for the third screening via Full Factorial Design using VII as a catalyst.

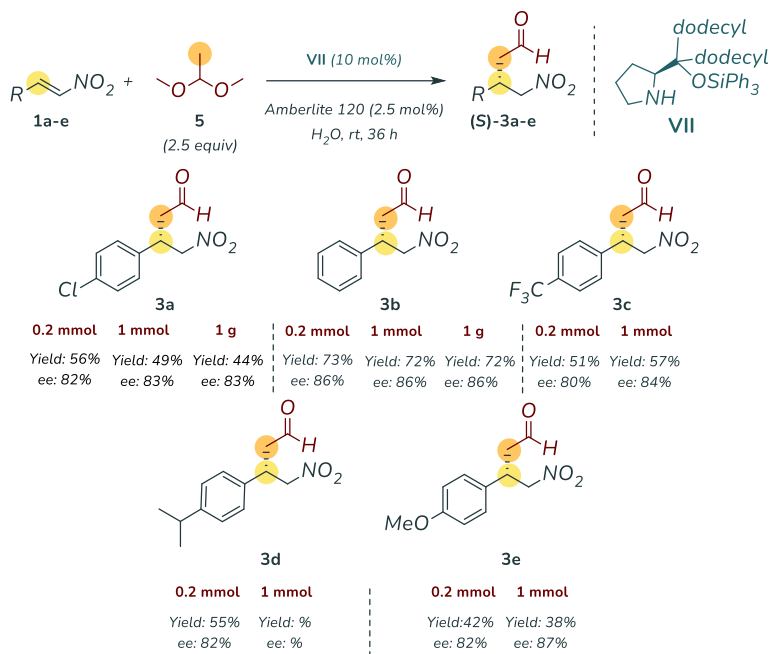
positive; the response is maximised when the time is at its maximum level (36 h). The coefficient for the rate of the acid catalyst is not significant; consequently, the lowest loading (2.5 mol%) is the best choice. These two variables are not correlated with each other; in fact, the resulting chemometric model is linear. The mathematical model (Equation 1) was validated to demonstrate its ability to predict and optimise the response.

Equation 1: $Y_{NMR} (\%) = 43 + 15.5 \cdot \text{time} + 0.5 \cdot \% \text{mol acid catalyst} - 5 \cdot \text{time} \cdot \% \text{mol acid catalyst}$

As concerning the organocatalyst I, the resulting chemometric model was not significant given that none of the coefficients associated with the investigated variables is significant; for this reason, it was discarded.

To evaluate the generality of the reaction, the best condition reaction found through the last Design of Experiments was chosen by varying the electrophile substrates and the reaction scale. (Table 3. 2).

Table 3. 2 Scope of the organocatalysed Michael addition in water with various aromatic nitroalkenes **1a-e**.^[a]



[a] Reactions performed on 0.2 mmol scale; catalyst (0.02 mmol, 10 mol%), nitroalkenes **1a-e** (0.2 mmol, 1 equiv), acetaldehyde dimethyl acetal **5** (0.5 mmol, 2.5 equiv), Amberlite-120 (2.5 mol%) and water as solvent ($[\mathbf{1a-e}]_0 = 1.2 \text{ M}$) at room temperature. Yields of isolated products. The isolated yields are similar to those measured by an internal standard via ^1H NMR spectroscopy (for further details, see experimental section). The enantiomeric excess determined by chiral HPLC analysis after conversion of the aldehyde into the corresponding alcohol by reduction with NaBH_4 .

All aromatic starting material successfully promoted the formation of the desired Michael adducts in good yields and enantioselectivity. As expected, and in agreement with previous reports, nitrostyrene^{17,18} **1b** was found to be the most reactive of all the other nitroalkenes. However, both EDG and EWG are well tolerated.

Nevertheless, both electron-withdrawing and electron-donating groups are well tolerated and several nitrostyrene derivatives successfully afforded the desired Michael adducts in good yields and

enantioselectivity. As regards the reaction scale, even increasing it, no significant decrease in yields and enantiomeric excesses were recorded.

Limitation of the methodology

One limitation found in the developed protocol was found in the use of aliphatic nitroalkenes reported in Figure 3. 11. Indeed, although in the previously optimised reaction in CHCl_3 , these substrates led to the moderate formation of the desired compound,⁷ in water the formation of many byproducts were observed leading to very low yields (Scheme 3. 8).

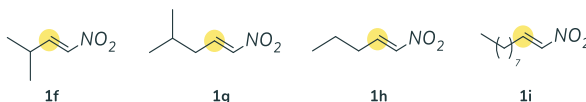
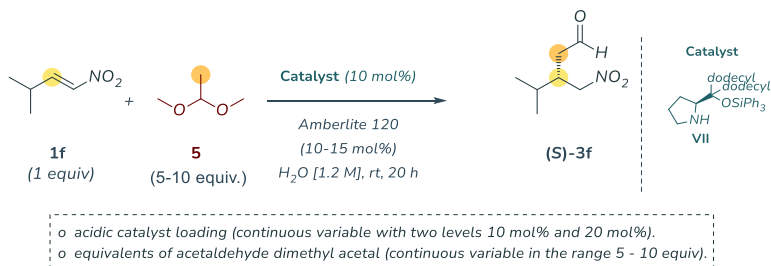


Figure 3. 11 Aliphatic nitroalkenes **1f-i**.

Therefore, it was decided to optimise the reaction conditions for these substrates by employing the nitroalkene **1f**. Two factors (at two different levels), acidic catalyst loading (10 mol% and 20 mol%) and acetaldehyde dimethyl acetal **5** (5 equiv and 10 equiv), were considered for the full-factorial design by performing 7 additional experiments (4 + 3 replicates of the central point) as shown in Scheme 3. 8.



Scheme 3. 8 Experimental conditions for the Full-factorial design on the aliphatic electrophile substrate.

Nevertheless, the coefficients resulted to be non-significant (Figure 3. 12). For this reason is not possible to significantly improve the yield by modifying the selected variables in the local investigated domain and the

general outcome of the analysis indicated the not complete suitability of this strategy for the intended purpose.

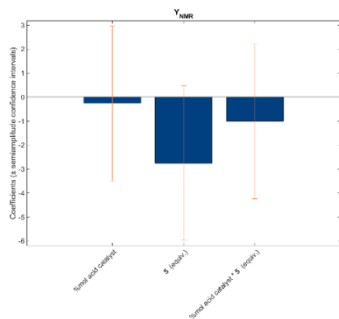


Figure 3.12 Plot of the coefficients of the mathematical model of the response Y_{NMR} for the full factorial design applied on aliphatic substrates.

In order to visualise the real benefit by performing the optimisation through DoE, it may be interesting to compare the development of the optimisation. The first results with **1a** and **5** were obtained with catalyst **I** (conv. 27% and ee 62%). Nine variables were explored running a total of only 90 experiments. This is more striking given the fact that the interaction of the parameters was taken into account and an exploration of

the full chemical space was performed. Response surfaces (Figure 3.13) for **VII** show the effect on yield and ee of selected parameters. The best conditions found enabled to improve both yield and ee (**VII**, yield 63%, ee 82%) in a direct and time-saving manner.

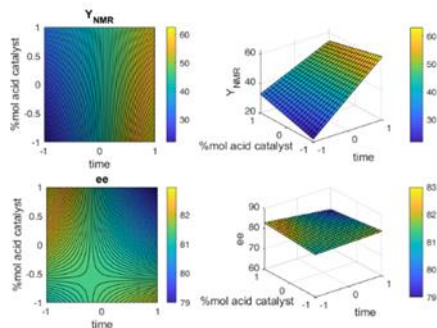


Figure 3.13 Response surfaces for Y_{NMR} and ee for the third Full Factorial Design using organocatalyst **VII**

Conclusion

In conclusion, an industrially appealing protocol for the Michael addition of acetaldehyde to nitroalkenes in water was developed. The investigation was performed with the aim of moving from the use of chloroform to water, and via a rational exploration of the chemical space by using DoE. While a current limitation remains the application to aliphatic nitroalkenes, the corresponding aromatic products were obtained in good yields and high ee.

3.4.1 Experimental section

Acetaldehyde dimethyl acetal **5**, β -nitrostyrene **1b**, **1**, 1,2,4,5-Tetramethylbenzene, *p*-Toluensulfonic acid monohydrate (*p*-TSA), Trifluoroacetic acid (TFA), Hydrochloric acid (HCl), Amberlyst®15 hydrogen form (Amberlyst 15), Amberlite® IRC120 H hydrogen form (Amberlite 120), Amberlyst® 36 (Amberlyst 36), Dowex® Marathon™ MSC hydrogen form (Amberlite 2900), Nafion™ NR50 (Nafion) were purchased by Merck and used as received unless otherwise stated. Silica Gel 60A (35-70 μ), HPLC solvents, and analytical grade solvents were purchased by Merck. Nitroalkenes **1a** and **1c – e** were prepared as previously reported.^{19,21} Catalysts **II – IX** were previously reported.²²

Nuclear magnetic resonance analyses (¹H-, ¹⁹F and ¹³C-NMR spectra) were acquired using a Bruker Advance III 400 MHz spectrophotometer. Chemical shifts (δ) are reported in ppm relative to residual solvent signals for ¹H- and ¹³C-NMR (¹H-NMR: 7.26 ppm for CDCl₃; ¹³C-NMR: 77.0 ppm for CDCl₃). ¹³C-NMR spectra were acquired with ¹H broadband decoupled mode. Coupling constants are given in Hz. Chromatographic purifications of compound **3a – 3e** were performed using automated BÜCHI - Reveleris® X2-UV System. HPLC analyses were acquired using an Agilent 1220 Infinity II liquid chromatographer equipped with a Phenomenex column Lux 3 μ m *i*-Cellulose-5 or Lux 3 μ m Cellulose-1. Racemic samples were prepared using a racemic mixture of (*R,S*)-diphenyltrimethylsiloxymethylpyrrolidine (**I**) as a catalyst at room temperature in chloroform (CHCl₃) overnight. Optical rotations were measured on a ZUZI 412 Digital Polarimeter (tube length: 100 mm).

Assignment of absolute configuration: Absolute configurations of compounds **3a – 3e** were assigned by comparing their absolute optical rotations with the values reported in the literature. The absolute configuration of all other products was assigned by analogy, considering a uniform mechanism of stereinduction.

²¹ V. Adebomi, S. Mahesh, Z. P. Muneeswaran, M. Raj, *Angew. Chem. Int. Ed.* 2020, 59, 7, 2793.

²² C. Palomo, A. Landa, A. Mielgo, M. Oiarbide, Á Puente, S. Vera *Angew. Chem. Int. Ed.* 2007, 46, 8431.

Optimisation of reaction conditions via DoE

DoEs were carried out to determine which variables had the greatest impact on the two responses (yield and enantiomeric excess of the compound **3a**), and in order to maximise them.

General procedure for DoE. The reactions were carried out following the general procedure in accordance with the parameters investigated with Design of Experiment (see the tables below): acetaldehyde dimethyl acetal **5** was added to a suspension of organocatalyst (**I-IX**), nitroalkene **1a** (36.6 mg, 0.2 mmol, 1 equiv), co-solvent (10% v/v), additive (0.11 M in water), and acid catalyst in water. The reaction mixture was left under stirring at 25 °C for the required time. The reaction was quenched with 2 mL of HCl_{aq} 1M, and the aqueous phase was extracted three times with diethyl ether. The combined organic layers were dried over MgSO₄ and concentrated in vacuo after filtration. The crude was purified by using automated BÜCHI - Reveleris® X2-UV System (silica gel, mixture of petroleum ether/ethyl acetate 9:1 v/v) to afford the desired compound. NMR spectra of previously reported compounds were in agreement with those of the authentic samples and/or available literature data. NMR yield was measured by analysing the reaction mixture using 1,2,4,5-Tetramethylbenzene (durene) as an internal standard. The spectrum was recorded using a higher than usual pulse delay (D1=10). The enantiomeric excess (ee) was determined by chiral-enantiopure-stationary-phase HPLC analysis after conversion of the aldehyde into the corresponding alcohol by reduction with NaBH₄ in MeOH by comparison with the authentic racemic material.

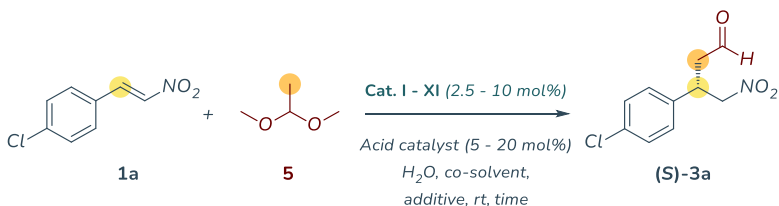
First Design of Experiment – Preliminary screening via D-Optimal Design

In the first DoE the reported variable were investigated:

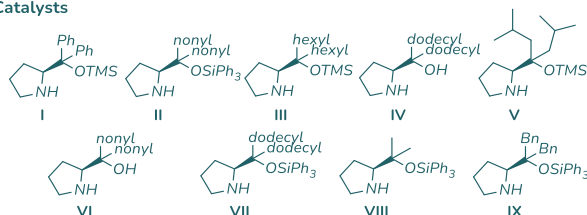
- Organocatalysts (discrete variable with 9 levels (Catalysts **I - IX**)).
- Catalyst loading (continuous variable in the range 2.5 mol% – 10 mol%).
- Equivalentents of acetaldehyde dimethyl acetal **5** (continuous variable in the range 1.5 – 3 equiv).

- Reaction time (continuous variable in the range 24 h – 72 h).
- Solution concentration (continuous variable in the range 0.2 M – 1.2 M).
- Cosolvents (discrete variable with 5 levels (EtOAc, MeOH, THF, IPA, none)).
- Acidic catalysts to deprotect masked acetaldehyde (discrete variable with 10 levels: 5 acidic resins and 5 organic acids).
- Different acidic catalyst loading (continuous variable in the range 2.5 mol% – 20 mol%).
- Ionic strength of water (discrete variable with 3 levels of additive (NaCl, CaCl₂, none)).

Table 3. 3 Experimental conditions for the first D-Optimal.



Catalysts



Entry	Cat. (mol%)	5 (equiv)	Time (h)	[1a]	Co-solv.	Acidic cat. (mol%)	Additive	NMR _{yield}	ee
1	I (10%)	1.5	24	1.2 M	EtOAc	Benzoic acid (20%)	CaCl ₂	12%	85%
2	IV (2.5%)	3	24	0.2 M	-	Amb. 120 (20%)	NaCl	0%	n.d.
3	VIII (10%)	3	24	0.2 M	THF	H ₂ SO ₄ (5%)	-	12%	74%
4	II (2.5%)	1.5	24	0.2 M	IPA	Amb. 2900 (20%)	CaCl ₂	0%	n.d.
5	V (2.5%)	1.5	24	1.2 M	-	Ambertlyst 36 (5%)	CaCl ₂	1%	n.d.
6	V (2.5%)	3	72	1.2 M	MeOH	Benzoic acid (20%)	NaCl	0%	n.d.

Entry	Cat. (mol%)	5 (equiv)	Time (h)	[1a]	Co- solv.	Acidic cat. (mol%)	Additive	NMR _{yield}	ee
7	VII (10%)	1.5	72	1.2 M	-	Nafion (20%)	-	25%	82%
8	II (2.5%)	1.5	72	1.2 M	THF	Amb. 15 (5%)	-	0%	n.d.
9	VI (10%)	3	72	1.2 M	MeOH	Amb. 36 (20%)	-	0%	n.d.
10	VII (10%)	3	24	0.2 M	MeOH	Amb. 15 (5%)	CaCl ₂	15%	82%
11	III (10%)	1.5	24	1.2 M	THF	Nafion (20%)	NaCl	8%	72%
12	IX (2.5%)	3	24	0.2 M	EtOAc	HCl (5%)	-	0%	n.d.
13	II (10%)	3	72	0.2 M	EtOAc	p-TSA (5%)	NaCl	8%	82%
14	IX (10%)	3	72	0.2 M	THF	TFA (20%)	CaCl ₂	4%	n.d.
15	VII (2.5%)	1.5	72	0.2 M	THF	Amb. 36 (20%)	NaCl	3%	n.d.
16	VIII (10%)	1.5	72	0.2 M	-	Amb. 15 (20%)	NaCl	2%	n.d.
17	IV (10%)	1.5	72	1.2 M	IPA	HCl (20%)	CaCl ₂	0%	n.d.
18	I (2.5%)	3	72	0.2 M	IPA	Nafion (5%)	CaCl ₂	3%	n.d.
19	III (10%)	1.5	72	0.2 M	-	Benzoic acid (5%)	-	9%	65.5%
20	III (2.5%)	3	72	1.2 M	EtOAc	H ₂ SO ₄ (20%)	CaCl ₂	0%	n.d.
21	IV (2.5%)	1.5	72	0.2 M	EtOAc	Amb. 2900 (5%)	-	0%	n.d.
22	II (10%)	3	72	0.2 M	EtOAc	p-TSA (5%)	NaCl	0%	n.d.
23	VI (2.5%)	1.5	72	0.2 M	THF	p-TSA (20%)	CaCl ₂	0%	n.d.
24	III (10%)	1.5	72	0.2 M	-	Benzoic acid (5%)	-	0%	n.d.
25	III (2.5%)	3	72	1.2 M	EtOAc	H ₂ SO ₄ (20%)	CaCl ₂	0%	n.d.
26	IX (10%)	1.5	72	0.2 M	MeOH	H ₂ SO ₄ (5%)	NaCl	5%	84%
27	I (10%)	3	72	1.2 M	-	Amb. 2900 (5%)	NaCl	36%	88%
28	V (10%)	1.5	72	0.2 M	IPA	Amb. 120 (20%)	-	2.00%	n.d.
29	IV (10%)	1.5	72	1.2 M	IPA	HCl (20%)	CaCl ₂	0%	n.d.
30	VIII (2.5%)	1.5	72	1.2 M	MeOH	Amb. 120 (5%)	CaCl ₂	5%	83%
31	VI (2.5%)	1.5	24	1.2 M	IPA	TFA (5%)	NaCl	0%	n.d.
32	IV (2.5%)	3	24	0.2 M	-	Amberlite 120 20%	NaCl	0%	n.d.
33	IX (2.5%)	3	24	1.2 M	IPA	p-TSA (20%)	-	0%	n.d.
34	I (2.5%)	1.5	24	0.2 M	MeOH	TFA (20%)	-	0%	n.d.

Based on previous knowledge and preliminary experiments results, nine factors (four qualitative and the remaining ones quantitative) were believed to affect the conversion (Y_{NMR}) and the enantiomeric excess (ee) of product **3a**. The assumed mathematical model, containing only one constant and 28 linear terms, is the following:

$$Y \text{ (both } Y_{NMR} \text{ and ee)} = b_0 + b_{1II} X_{1II} + b_{1III} X_{1III} + b_{1IV} X_{1IV} + b_{1V} X_{1V} + b_{1VI} X_{1VI} + b_{1VII} X_{1VII} + b_{1VIII} X_{1VIII} + b_{1IX} X_{1IX} + b_2 X_2 + b_3 X_3 + b_4 X_4 + b_5 X_5 + b_{6EtOAc} X_{6EtOAc} + b_{6MeOH} X_{6MeOH} + b_{6IPA} X_{6IPA} + b_{6THF} X_{6THF} + b_{7Amberlyst-15} X_{7Amberlyst-15} + b_{7TFA} X_{7TFA} + b_{7Amberlyst-36} X_{7Amberlyst-36} + b_{7Amberlite120} X_{7Amberlite120} + b_{7Nafion} X_{7Nafion} + b_{7HCl} X_{7HCl} + b_{7p-TSA} X_{7p-TSA} + b_{7BenzoicAcid} X_{7BenzoicAcid} + b_{7H2SO4} X_{7H2SO4} + b_8 X_8 + b_{9NaCl} X_{9NaCl} + b_{9CaCl2} X_{9CaCl2}$$

Where terms X_i are the reaction variables:

X_1 : type of organocatalysts

X_2 : catalyst loading

X_3 : equivalents of **5**

X_4 : reaction time

X_5 : reaction concentration

X_6 : cosolvents

X_7 : acidic catalysts to deprotect

X_8 : acidic catalyst loading

X_9 : ionic strength of water

The quantitative variables were investigated using two levels, respectively coded as -1 and +1; whereas the implicit level was used to evaluate the qualitative ones (I for X_1 , absence of cosolvent for X_6 , Amberlite2900 for X_7 , absence of salt for X_9), i.e. each coefficient is to be considered with respect to the implicit level performances. Different combinations of implicit levels were tested without changes in the results. The levels were chosen on the basis of organic expertise:

X_1 : I, II, III, IV, V, VI, VII, VIII, IX

X_2 : 2.5, 10 mol%

X₃: 1.5, 3 equivalents

X₄: 24, 72 h

X₅: 0.2, 1.2 M

X₆: absence of cosolvent, EtOAc, MeOH, IPA, THF

X₇: Amberlyst-15, Amberlyst-36, Amberlite 120, Amberlite 2900, Nafion, HCl, p-TSA, Benzoic Acid, H₂SO₄, TFA

X₈: 5, 20 mol%

X₉: absence of salt, NaCl, CaCl₂

A D-optimal design was performed to identify, among all the possible experiments, the subset leading to the best possible compromise between experimental effort and quality of information by maximising the normalised determinant of the information matrix. The solution with 31 experiments was selected and 3 replicates were added, according to the experimental matrix in Table 2.

The coefficients of the mathematical model in equation (1) were computed by Multiple Linear Regression only for the response Y_{NMR}, since, without its improvement, the exploration of the ee response would be meaningless. The mathematical model for Y_{NMR} (to be maximised) is:

$$(1) Y_{NMR} = 27.1 (***) - 10.1X_{II} (*) - 10.7X_{III} (*) - 14.1X_{IV} (*) - 7.3X_{IV} - 7.0X_{VI} + 5.7X_{VII} - 8.4X_{VIII} - 8.7X_{IX} (*) + 3.4X_2 (***) + 1.0X_3 - 0.4X_4 + 3.0X_5 (*) - 6.8X_{6EtOAc} - 6.3X_{6MeOH} (*) - 1.8X_{6IPA} (*) - 8.6X_{6THF} - 14.8X_{7Amberlyst-15} (*) - 12.3X_{7TFA} (*) - 19.3X_{7Amberlyst-36} (***) - 7.0X_{7Amberlite120} - 11.3X_{7Nafion} (*) - 8.1X_{7HCl} - 9.2X_{7p-TSA} (*) - 12.6X_{7BenzoicAcid} (*) - 8.2X_{7H2SO4} - 1.5X_8 + 0.4X_{9NaCl} + 0.04X_{9CaCl2}$$

Concerning the variable X₁, b_{1i} are always negative, except for the coefficient of organocatalyst VII that is positive, even though slightly not significant. Therefore, organocatalysts I and VII seem to be the ones cause an improvement of the Y_{NMR}. Organocatalyst II is retained for its structural similarity with VII, despite of its negative b_{1II}. Moreover, we were also interested to investigate the effects related to the possible hydrophobic interaction by considering the different alkyl side chains. As expected, the increase of the catalyst causes an increase of Y_{NMR},

nevertheless exceed the 10%mol is not convenient so it is maintained as upper limit for X_2 . Similar considerations can be done for X_5 , because its increase leads to an improvement of the response, but [1a] higher than 1.2 M is not experimentally feasible. Against expectation, instead, b_3 and b_4 are not significant. This outcome could be biased by the bad results obtained; therefore, we decide to further investigate the equivalents of 5 and the reaction time in the next designs. The coefficients of all the cosolvents are negative since their introduction in the reaction environment decreases Y_{NMR} . On the contrary, the presence of salts does not contribute in any way to the response since all the coefficients are not significant. Therefore, it is reasonable to exclude variables X_6 and X_9 in the further investigation (no additive and salts will be used in the reaction). Respect to the variable X_7 the performances of all the acidic catalysts are worse (negative coefficients) than those of the implicit level. Nevertheless, Amberlyst-15, Amberlyst-36 and HCl are further investigated in addition to Amberlite2900 because of their performances previously investigated.¹ The loading of the acidic catalyst has a negative coefficient, even though slightly not-significant, so we decided to keep the variable X_8 changing the levels.

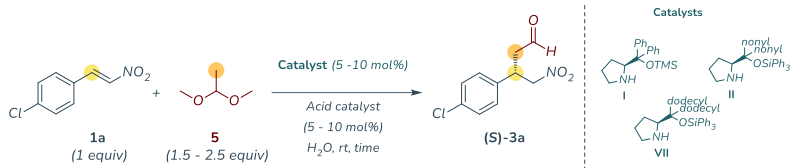
This first DoE was used as exploratory screening to decide the further approaches, for this reason no model validation was performed.

Second Design of Experiment - screening via D-Optimal Design

In the second DoE the reported variable were investigated:

- Organocatalysts (discrete variable with 3 levels (catalysts I, II, and VII)).
- Catalyst loading (continuous variable in the range 5 mol% – 10 mol%).
- Equivalents of acetaldehyde dimethyl acetal (continuous variable in the range 1.5 – 2.5 equiv).
- Reaction time (continuous variable in the range 24 h – 72 h).
- Solution concentration (discrete variable with 3 levels 0.8 M, 1 M and 1.2 M).
- Acidic catalysts (a discrete variable with 4 levels).
- Acidic catalyst loading (continuous variable in the range 5 mol% – 10 mol%).

Table 3. 4 Experimental conditions for the second D-Optimal.



Entry	Catalyst (mol%)	Acidic Catalyst (mol%)	5 (equiv)	Time (h)	[1a]	NMR _{yield}	ee
1	II 10%	Amberlyst 15 5%	2.5	24	0,8	13%	80%
2	VII 5%	Amberlyst 15 5%	2.5	24	1	15%	77%
3	I 10%	Amberlyst 15 5%	1.5	72	1,2	41%	83%
4	VII 10%	Amberlite 120 5%	1.5	24	0,8	16%	81%
5	I 5%	Amberlite 120 5%	2.5	72	0,8	15%	82%
6	II 5%	Amberlite 120 5%	2.5	24	1,2	17%	81%
7	I 10%	Amberlite 120 5%	2.5	24	1,2	63%	86%
8	VII 5%	Amberlite 120 5%	1.5	72	1,2	32%	76%
9	II 5%	Amberlite 2900 5%	1.5	72	0,8	19%	77%
10	VII 10%	Amberlite 2900 5%	2.5	72	0,8	24%	76%
11	II 10%	Amberlite 2900 5%	1.5	24	1,2	15%	80%
12	I 5%	HCl 5%	1.5	24	0,8	13%	87%
13	VII 10%	HCl 5%	1.5	72	0,8	26%	78%
14	VII 5%	HCl 5%	1.5	24	1,2	27%	78%
15	VII 5%	HCl 5%	2.5	72	1,2	57%	81%
16	II 10%	HCl 5%	2.5	72	1,2	37%	78%
17	VII 5%	Amberlyst 15 10%	1.5	72	0,8	22%	75%
18	II 10%	Amberlyst 15 10%	2.5	72	0,8	18%	76%
19	VII 10%	Amberlyst 15 10%	1.5	24	1	35%	83%
20	VII 10%	Amberlyst 15 10%	2.5	24	1,2	34%	78%
21	II 5%	Amberlyst 15 10%	2.5	72	1,2	19%	80%

Entry	Catalyst (mol%)	Acidic Catalyst (mol%)	5 (equiv)	Time (h)	[1a]	NMR _{yield}	ee
22	II 10%	Amberlite 120 10%	1.5	24	0,8	18%	78%
23	II 5%	Amberlite 120 10%	2.5	24	0,8	13%	80%
24	II 10%	Amberlite 120 10%	2.5	72	1	41%	78%
25	I 5%	Amberlite 120 10%	1.5	24	1,2	22%	85%
26	VII 10%	Amberlite 120 10%	2.5	72	1,2	12%	81%
27	VII 5%	Amberlite 2900 10%	1.5	24	0,8	22%	82%
28	I 10%	Amberlite 2900 10%	1.5	72	0,8	19%	83%
29	I 5%	Amberlite 2900 10%	2.5	24	1	13%	84%
30	VII 10%	Amberlite 2900 10%	1.5	72	1,2	15%	75%
31	I 5%	Amberlite 2900 10%	2.5	72	1,2	11%	85%
32	I 10%	HCl 10%	2.5	24	0,8	8%	84%
33	VII 5%	HCl 10%	2.5	72	0,8	33%	74%
34	II 5%	HCl 10%	1.5	72	1	8%	78%
35	II 10%	HCl 10%	1.5	24	1,2	14%	80%
36	II 5%	HCl 10%	2.5	24	1,2	11%	83%
R1	II 10%	Amberlyst 15 5%	2.5	24	0,8	19%	78%
R3	I 10%	Amberlyst 15 5%	1.5	72	1,2	33%	83%
R9	II %	Amberlite 2900 5%	1.5	72	0,8	11%	78%
R12	I 5%	HCl 5%	1.5	24	0,8	16%	84%
R25	I 5%	Amberlite 120 10%	1.5	24	1,2	19%	85%
R30	VII 10%	Amberlite 2900 10%	1.5	72	1,2	24%	77%

By taking into account the results of the first DoE, we retained 7 factors (two qualitative and five quantitative) reducing and/or changing the correspondent levels. At this step, a mathematical model contained one constant, 10 linear terms, 10 interaction terms and one quadratic term was considered:

$$(1) Y \text{ (both } Y_{NMR} \text{ and ee)} = b_0 + b_{1II} X_{1II} + b_{1VI} X_{1VI} + b_{1VII} X_{1VII} + b_{2Amberlite120} X_{2Amberlite120} + b_{2Amberlite2900} X_{2Amberlite2900} + b_{2HCl} X_{2HCl} + b_3 X_3 + b_4 X_4 + b_5 X_5 + b_6 X_6 + b_7 X_7 + b_{34} X_3 X_4 + b_{35} X_3 X_5 + b_{36} X_3 X_6 + b_{37} X_3 X_7 + b_{45} X_4 X_5 + b_4 X_4 X_6 + b_{47} X_4 X_7 + b_{56} X_5 X_6 + b_{57} X_5 X_7 + b_{67} X_6 X_7 + b_{66} X_6^2$$

Where terms X_i are the reaction variables:

X_1 : type of organocatalysts

X_2 : acidic catalyts to deprotect

X_3 : organocatalyst loading

X_4 : equivalents of **5**

X_5 : reaction time

X_6 : reaction concentration

X_7 : acidic catalyst loading

As for the first DoE, the quantitative variables were investigated using two or three levels, coded as -1 (low-level), 0 (mid-level) and +1 (high-level); whereas the implicit level was used to evaluate the qualitative ones (**I** for X_1 and Amberlyst-15 for X_2). The levels are the following:

X_1 : **I, II, VII**

X_2 : Amberlyst-15, Amberlite120, Amberlite2900, HCl

X_3 : 5, 10 mol%

X_4 : 1.5, 2.5 equivalents

X_5 : 24, 72 h

X_6 : 0.8, 1, 1.2 M

X_7 : 5, 10 mol%

A second D-optimal design was performed and the solution with 36 experiments came out. Six replicates were further selected from the latter sub-set exploiting again a D-optimal design. The experimental matrix is

showed in Table 4. Principal Component Analysis (PCA) was then performed on the experimental matrix. PCA is an exploratory analysis method which lays on the bilinear decomposition of the data matrix into a set of scores (called principal components) and a set of loadings (which “weight” the relationship between original and latent variables). From the geometrical point of view, it can be seen as the projection of the observations onto the directions of maximum variance (i.e., the PCs). This, among the others, provides a number of benefits; in particular, the realization of graphical representations (as the scores and loadings plots discussed below) suitable for the interpretation of the system under study.

The scores and loadings plot of the PCA performed on the experimental matrix, the Y_{NMR} and the ee values were used to take a decision about how to deal with the two-responses problem. As it can be seen from Figure 3 of the manuscript, a trend of the experiment points (colored according to the increasing of the responses) can be highlighted in the scores plot: the highest is Y_{NMR} , the lowest is the scores on PC2, as for ee. Both the responses, indeed, have high and negative loadings on PC2. Driven by these considerations, the Scores on PC2 was selected as compromise-response.

The coefficients of the mathematical model in equation (3) were again computed by Multiple Linear Regression for the response Scores on PC2 (to be minimised):

$$(2) \text{ Scores on PC2} = -0.7 (*) + 1.4X_{1\text{III}} (***) - 0.06X_{1\text{VII}} - 0.7X_{2\text{Amberlite120}} (***) + 1.2X_{2\text{Amberlite2900}} (***) - 0.09X_{2\text{HCl}} - 0.2X_3 (*) - 0.1X_4 + 0.09X_5 - 0.6X_6 (***) + 0.3X_7 (***) - 0.05X_3X_4 + 0.05X_3X_5 - 0.05X_3X_6 + 0.06X_3X_7 - 0.09X_4X_5 - 0.2X_4X_6 (*) + 0.05X_4X_7 + 0.03X_5X_6 + 0.1X_5X_7 + 0.2X_6X_7 (*) + 0.2X_6^2$$

In the scenario of Scores on PC2 minimization (maximization of Y_{NMR} and ee), the considerations of the first-DoE about the organocatalysts are confirmed. Indeed, the positive coefficient of organocatalyst I suggests, as expected, a decrease of the original responses when it is employed. At the same time, the performances of II and VII can be considered good and comparable. Taken Amberlyst-15 as implicit level, Amberlite120 (negative and significative coefficient) results to be the best acidic catalyst, instead of Amberlite 2900 ($b_{2\text{Amberlite2900}}$ is positive and

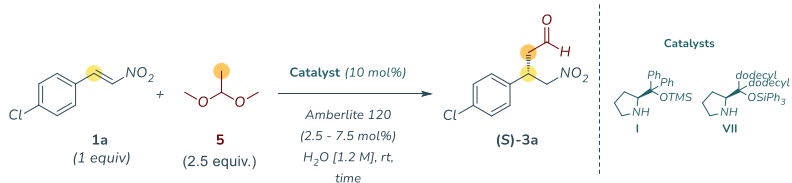
significant) suggested by the previously design, in the improvement of Y_{NMR} and ee. The coefficient of the organocatalyst loading is negative and significant and no interaction terms are, so its increase would lead to an increase of the responses (decrease of Scores on PC2). Nevertheless, exceed the actual loading is not experimentally convenient. Conversely, time's linear coefficient is positive even though slightly not-significant, so it would be convenient to decrease the level of this variable on the basis of a time-saving criterion. The variable X_4 shows a not significant linear term (negative) and a significant interaction term (negative) X_4X_6 . The reaction concentration's coefficients are negative and significant for both the linear and the interaction term (X_4X_6). The variable X_7 shows positive and significant coefficients for linear and interaction term with variable X_6 . Therefore, these variables should be considered simultaneously. Y_{NMR} and ee would improve when, at the same time, X_4 (equivalents of **5**) and X_6 (reaction concentration) are at the highest-level and X_7 (acidic catalyst loading) is at its lowest-level. The experimental conditions suggested as optimal for the improving of the conversion and the enantiomeric excess of the product **3a** result to be the ones already investigated in the point 7 of the design. This second DoE was not validated for the same reason as the first-one.

Third Design of Experiment - Full Factorial Design

To further optimise the reaction conditions for all the responses under study, the third Design of Experiments was performed. The variable investigated were:

- Organocatalysts (discrete variable with 2 levels (catalysts I and VII))
- Reaction time (discrete variable with 3 levels 24 h, 36 h, and 72 h)
- Acidic catalyst loading (discrete variable with 3 levels 2.5 mol%, 5 mol%, and 7,5 mol%).

Table 3. 5 Experimental conditions for the third DoE – Full Factorial.



Entry	Catalyst	Amberlite 120 (mol%)	Time (h)	NMR _{yield}	ee%
1	I	2,5%	16	35%	85%
2	I	2,5%	36	31%	86%
3	I	7,5%	16	19%	90%
4	I	7,5%	36	38%	85%
5	I	5%	24	46%	87%
6	I	5%	24	55%	84%
7	I	5%	24	51%	87%
8	VII	2,5%	16	22%	81%
9	VII	2,5%	36	63%	82%
10	VII	7,5%	16	33%	83%
11	VII	7,5%	36	54%	79%
12	VII	5%	24	43%	80%
13	VII	5%	24	41%	81%
14	VII	5%	24	36%	80%

The last D-optimal Design suggested aims at exploring the surrounding domain of the experimental point 7; for this reason, the latter was taken as central point of two Full Factorial Designs with two variables (the only ones on which we can further act) and two levels, one for each of the organocatalysts (I and VII) resulting the most suitable. The mathematical models were assumed to be:

- (1) $Y_{\text{organocatalyst I}} \text{ (both } Y_{\text{NMR}} \text{ and ee)} = b_{10} + b_{11} X_1 + b_{12} X_2 + b_{112} X_{12}$
- (2) $Y_{\text{organocatalyst VII}} \text{ (both } Y_{\text{NMR}} \text{ and ee)} = b_{v10} + b_{v11} X_1 + b_{v12} X_2 + b_{v112} X_{12}$

Where terms X_i and respective levels are:

X_1 : reaction time, levels 16, 36 h

X_2 : acidic catalyst loading, levels 2.5, 7.5 %mol

and all the other factors are maintained as in the point 7 (see Table 6) because is not convenient to change them.

The two experimental matrices in Table 6 showed the experiments (entries 1-4) used to compute the models and the ones (entries 5-7) for the validation of the DoE using the VII organocatalyst.

The coefficients, showed in Figure 1, of the mathematical model in equation (5) were computed by Multiple Linear Regression both for Y_{NMR} and ee:

$$(7a) Y_{NMR-I} = 30.8 (***) + 3.8X_1 - 2.3X_2 + 5.8X_{12}$$

$$(7b) Y_{ee-I} = 86.5 (***) - 1.0X_1 + 1.0X_2 - 1.5X_{12}$$

All the coefficients in both the models result not significant, i.e. it is not possible to improve Y_{NMR} and ee changing the selected variables in the investigated domain. For this reason, organocatalyst I was rejected; however, as it stands, it allows to obtain product **3a** with 31% of conversion and 87% of enantiomeric excess.

The coefficients of the mathematical model in equation (6), showed in the Figure 4 of the manuscript, were as usual computed by Multiple Linear Regression both for Y_{NMR} and ee:

$$(8a) Y_{NMR-VII} = 43.0 (***) + 15.5X_1 (*) - 0.5X_2 - 5.0X_{12}$$

$$(8b) Y_{ee-VII} = 81.3 (***) - 0.75X_1 - 0.25X_2 - 1.3X_{12}$$

Concerning the conversion modeling in equation (8a), it can be highlighted that only an increase of reaction time would lead to an increase of the yield and, therefore, it would be advisable to use the acidic catalyst at its lowest loading in a perspective of reaction-economy. This is also suggested looking at the response surface (Figure 2) calculated on the model. It can be represented by a plane with a maximum in the point (36h, 2.5%mol of acidic catalyst). In the equation (8b) only the constant term is significant, so further improving of the enantiomeric excess is not possible in the explored domain. This is confirmed by the very low slope of the plane representing the ee response surface in Figure 2. Looking more deeply at the shape of ee-surface we can note a slightly distortion of the plane due to which ee can be improved both with experimental conditions (36h, 2.5%mol of acidic catalyst) and (24h, 7.5%mol of acidic catalyst), and mostly in this last point. Nevertheless, with the aim of find the best compromise between the two responses, we selected as optimal

the solution (36h, 2.5%mol of acidic catalyst), highlighted in yellow in both the planes.

It is also interesting to note, comparing equation (7b) and (8b), that the enantiomeric excess is higher with the organocatalyst I, but it is worth losing around 6% of ee to gain around 12% and more of conversion with the organocatalyst VII.

The final models (8a-b) were validated using 3 replicates of the central point as test set (entries 5-7) and the Student's T-distribution at 5% as level of significance. Concerning the yield, the predicted value with its semiamplitude of confidence interval is $(43.0 \pm 7.7)\%$ and the experimental one is $(45.3 \pm 7.5)\%$; whereas, the predicted value of ee is $(81.3 \pm 1.3)\%$ and the experimental is $(80.3 \pm 1.4)\%$.

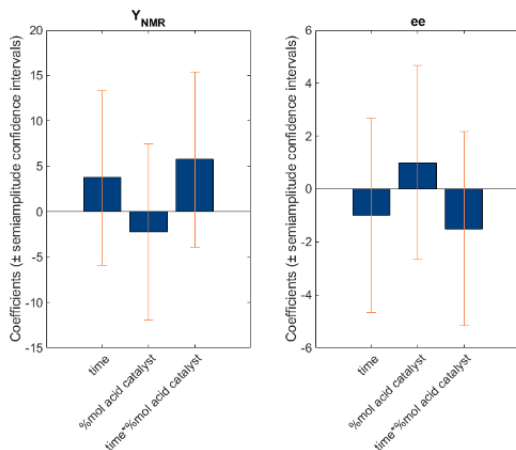


Figure 3. 14 Plot of the coefficients of the mathematical models of the responses Y_{NMR} and ee (both to be maximised) in the third Full Factorial Design using the organocatalyst **1**.

Fourth DoE on aliphatic substrates - Full Factorial Design

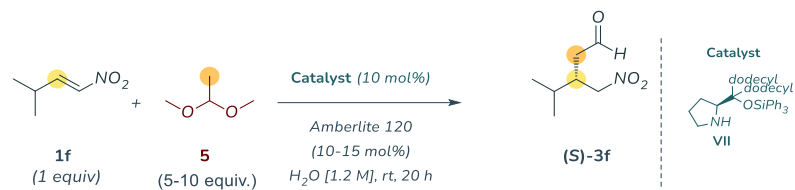
In this case we decided to evaluate the following variables using (E)-3-methyl-1-nitrobut-1-ene **1f**:

- acidic catalyst loading (continuous variable with two levels 10 mol% and 20 mol%).
- equivalents of acetaldehyde dimethyl acetal (continuous variable in the range 5 - 10 equiv).

We chose to investigate only these variables as we considered that a more similar approach to the conditions found in the literature²³ would probably have led to the best results from an organic perspective. We therefore increased the loading of acid catalyst and the equivalents of masked reagent in order to raise the local concentration of free acetaldehyde and have a higher probability of forming the Michael addition product.

²³ a) Hayashi, Y.; Itoh, T.; Aratake, S.; Ishikawa, H. *Angew. Chem. Int. Ed.* **2008**, *47*, 2082; b) Hayashi, Y.; Itoh, T.; Ohkubo, M.; Ishikawa, H. *Angew. Chem. Int. Ed.* **2008**, *47*, 4722; c) García-García, P.; Ladépêche, A.; Halder, R.; List, B. *Angew. Chem. Int. Ed.* **2008**, *47*, 4719; d) Fan, X.; Rodríguez-Escrich, C.; Sayalero, S.; Pericàs, M.A. *Chem. Eur. J.* **2013**, *19*, 10814.

Table 3. 6 Experimental conditions for the aliphatic starting materials.



Entry	5 (equiv)	Amberlite 120 (mol%)	NMR _{yield}
1	10	20	14
2	5	10	20
3	5	20	22
4	10	10	17
5	7.5	15	27
6	7.5	15	25
7	7.5	15	24

The last design of experiment aims at exploring the generality of the reaction and the applicability of the previously optimised conditions on some selected aliphatic substrates. A full factorial design with two factors (acidic catalyst loading and equivalents of acetaldehyde dimethyl acetal) and two levels was conceived and computed, resulting in seven experiments, (4 + 3 replicates at the central point). The assumed mathematical model is:

$$(9) \quad Y_{NMR} = b_0 + b_1 X_1 + b_2 X_2 + b_{12} X_{12}$$

Where terms X_i and respective levels are:

X_1 : acidic catalyst loading, levels: 10 mol%, 20 mol%

X_2 : acetaldehyde dimethyl acetal, levels: 5 equiv, 10 equiv

Table 8 showed the experiments used to compute the model.

The coefficients of the mathematical model in equation (9) were computed by Multiple Linear Regression:

$$(10) \quad Y_{NMR} = 18.5(***) - 0.25X_1 - 2.75X_2 - 1.00 X_{12}$$

All the coefficients (except for b_0) result not significant, i.e. it is not possible to significantly improve Y_{NMR} modifying the selected variables in

the investigated domain. For this reason, the application of the investigated conditions on aliphatic substrates could not represent the most suitable solution.

Table 3. 7 Experimental conditions for the aliphatic starting materials

Entry	Amberlite 120 (mol%)	5 (equiv)	Y _{NMR}
1	1	1	14
2	-1	-1	20
3	1	-1	22
4	-1	1	17
5	0	0	27
6	0	0	25
7	0	0	24

Synthesis of γ -nitroaldehydes **3a-e**.

General procedure c for the asymmetric Michael addition of acetaldehyde dimethyl acetal to nitroalkenes. Acetaldehyde dimethyl acetal **5** (53 μ L, 0.5 mmol, 2.5 equiv) was added to a suspension of catalyst **VII** (10 mol%), nitroalkene **1a - e** (1 equiv), and Amberlite® IR-120 (2.35 mg, 2.5 mol%) in water (167 μ L, 1.2 M) at 25 °C. The reaction was quenched after 36 h with 2 mL of HCl_{aq} 1M, and the aqueous phase was extracted three times with diethyl ether. The combined organic layers were dried over MgSO₄ and concentrated in vacuo after filtration. The crude was purified by using automated BÜCHI - Reveleris® X2-UV System (silica gel, mixture of petroleum ether/ethyl acetate 9:1 v/v) to afford the desired compound. NMR spectra of previously reported compounds were in agreement with those of the authentic samples and/or available literature data.

3.4.2 Characterisations

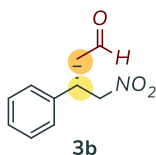
(S)-3-(4-chlorophenyl)-4-nitrobutanal (**3a**)¹ – (25.6 mg, 0.11 mmol, 56% isolated yield, 63% ¹H NMR yield).



Prepared following general procedure using (*E*)-1-chloro-4-(2-nitrovinyl)benzene **1a** (1 equiv, 0.2 mmol, 36.6 mg). ¹H NMR (400 MHz, CDCl₃) δ 9.70 (s, 1H), 7.32 (d, *J* = 8.3 Hz, 2H), 7.18 (d, *J* = 8.3 Hz, 2H), 4.67 (dd, *J* = 12.6, 6.9 Hz, 1H), 4.59 (dd, *J* =

12.6, 7.8 Hz, 1H), 4.06 (m, 1H), 2.94 (d, $J = 7.1$ Hz, 2H). ^{13}C NMR (101 MHz, CDCl_3) δ 198.3 (CO), 136.7 (C_{ar}), 134.0 (C_{ar}), 129.4 ($2\times\text{CH}_{ar}$), 128.8 ($2\times\text{CH}_{ar}$), 79.1 (CH_2), 46.3 (CH_2), 37.3 (CH). $[\alpha]_{\text{D}}^{25} = -0.55$ ($c = 0.22$ in CHCl_3). HPLC (Lux 3 μm *i*-Cellulose-5, Hexane/*i*-Propanol 90:10, flow: 0.5 mL/min., $\lambda=210$ nm) τ_{maj} : 17.2 min; τ_{min} : 15.6 min.

(*S*)-4-nitro-3-phenylbutanal (**3b**)¹ – (28.2 mg, 0.14 mmol, 73% isolated yield, 77% ^1H NMR yield)



Prepared following general procedure using β -nitrostyrene **1b** (1 equiv, 0.2 mmol, 29.8 mg).

^1H NMR (400 MHz, CDCl_3) δ 9.71 (s, 1H), 7.38 – 7.28 (m, 3H), 7.23 (d, $J = 7.6$ Hz, 2H), 4.68 (dd, $J = 12.5, 7.2$ Hz, 1H), 4.62 (dd, $J = 12.5, 7.5$ Hz, 1H), 4.08 (m, 1H), 2.95 (d, $J = 7.0$ Hz, 2H). ^{13}C NMR (101 MHz, CDCl_3) δ 198.7 (CO), 138.1 (C_{ar}), 129.2 ($2\times\text{CH}_{ar}$), 128.2 (CH_{ar}), 127.4 ($2\times\text{CH}_{ar}$), 79.4 (CH_2), 46.4 (CH_2), 38.0 (CH). $[\alpha]_{\text{D}}^{25} = -0.58$ ($c = 0.24$ in CHCl_3); HPLC (Lux 3 μm Cellulose-1, Hexane/*i*-Propanol 90:10, flow: 0.5 mL/min., $\lambda=210$ nm) τ_{maj} : 24.8 min; τ_{min} : 19.6 min.

(*S*)-4-nitro-3-(4-(trifluoromethyl)phenyl)butanal (**3c**)²⁴ – (26.5 mg, 0.10 mmol, 51% isolated yield, 53% ^1H NMR yield)



Prepared following general procedure using (*E*)-1-(2-nitrovinyl)-4-(trifluoromethyl)benzene **1c** (1 equiv, 0.2 mmol, 43.4 mg). ^1H NMR (400 MHz, CDCl_3) δ 9.72 (s, 1H), 7.61 (d, $J = 8.1$ Hz, 2H), 7.38 (d, $J = 8.1$ Hz, 2H), 4.72 (dd, $J = 12.8, 6.8$ Hz, 1H), 4.64 (dd, $J = 12.8, 7.9$ Hz, 1H), 4.16 (m, 1H), 2.99 (d, $J = 6.9$ Hz, 2H). ^{13}C NMR (101 MHz, CDCl_3) δ 198.0 (CO), 142.3 (C_{ar}), 130.4 (q, $^2J_{\text{C-F}} = 32.7$ Hz; C_{ar}), 127.9 ($2\times\text{CH}_{ar}$), 126.2 (q, $^3J_{\text{C-F}} = 3.7$ Hz, $2\times\text{CH}_{ar}$), 123.8 (q, $^1J_{\text{C-F}} = 272.2$ Hz), 78.7 (CH_2), 46.2 (CH_2), 37.5 (CH). ^{19}F NMR (376 MHz, CDCl_3) δ -62.7. $[\alpha]_{\text{D}}^{25} = -0.94$ ($c = 0.23$ in CHCl_3). HPLC

²⁴ W. Chen, H. Fang, K. Xie, M. Oestreich, Chem. Eur. J. 2020, 26, 15126 – 15129

(Lux 3 μm *i*-Cellulose-5, Hexane/*i*-Propanol 95:5, flow: 0.5 mL/min., $\lambda=210$ nm) τ_{maj} : 22.8 min; τ_{min} : 21.6 min.

(*S*)-3-(4-isopropylphenyl)-4-nitrobutanal (**3d**)¹ – (25.8 mg, 0.11 mmol, 55% isolated yield, 77% ¹H NMR yield).



Prepared following general procedure using (*E*)-1-isopropyl-4-(2-nitrovinyl)benzene **1d** (1 equiv, 0.2 mmol, 38.2 mg). ¹H NMR (400 MHz, CDCl₃) δ 9.70 (s, 1H), 7.20 (d, $J = 8.1$ Hz, 2H), 7.14 (d, $J = 8.2$ Hz, 2H), 4.66 (dd, $J = 12.5, 7.5$ Hz, 1H), 4.60 (dd, $J = 12.5, 7.4$ Hz, 1H), 4.05 (m, 1H), 2.95 – 2.83 (m, 3H), 1.22 (d, $J = 6.9$ Hz, 6H). ¹³C NMR (101 MHz, CDCl₃)

δ 199.0 (CO), 148.8 (C_{ar}), 135.3 (C_{ar}), 127.3 (2xCH_{ar}), 127.3 (2xCH_{ar}), 79.5 (CH₂), 46.5 (CH₂), 37.7 (CH), 33.7 (CH), 23.8 (2xCH₃). [α]_D²⁵ = – 1.07 (c = 0.22 in CHCl₃). HPLC (Lux 3 μm *i*-Cellulose-5, Hexane/*i*-Propanol 95:5, flow: 0.4 mL/min., $\lambda=210$ nm) τ_{maj} : 47.9 min; τ_{min} : 43.3 min.

(*S*)-3-(4-methoxyphenyl)-4-nitrobutanal (**3e**)¹ – (18.8 mg, 0.08 mmol, 42% isolated yield, 48% ¹H NMR yield)



Prepared following general procedure using (*E*)-1-methoxy-4-(2-nitrovinyl)benzene **1e** (1 equiv, 0.2 mmol 35.8 mg). ¹H NMR (400 MHz, CDCl₃) δ 9.63 (s, 1H), 7.08 (d, $J = 8.6$ Hz, 2H), 6.80 (d, $J = 8.6$ Hz, 2H), 4.58 (dd, $J = 12.4, 7.2$ Hz, 1H), 4.50 (dd, $J = 12.3, 7.6$ Hz, 1H), 3.96 (m, 1H), 3.72 (s,

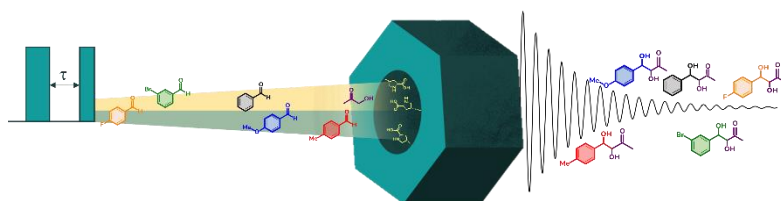
3H), 2.84 (d, $J = 7.1$ Hz, 2H). ¹³C NMR (101 MHz, CDCl₃) δ 198.9 (CO), 159.3 (C_{ar}), 129.9 (C_{ar}), 128.5 (2xCH_{ar}), 114.6 (2xCH_{ar}), 79.7 (CH₂), 55.3 (CH₃), 46.5 (CH₂), 37.4 (CH). [α]_D²⁵ = – 0.83 (c = 0.16 in CHCl₃). HPLC (Lux 3 μm Cellulose-1, Hexane/*i*-Propanol 90:10, flow: 0.5 mL/min., $\lambda=210$ nm) τ_{maj} : 25.8 min; τ_{min} : 23.3 min.

Chapter 4: Investigation of the effect of reagents in an aldol reaction catalysed by an immobilised organocatalyst

Project in collaboration with Prof. Carmine d'Agostino

(Manchester University – UK)

(Unpublished results, manuscripts under preparation)



The work reported in this section investigates the diffusion effect of reagents within the matrix of a supported catalyst in a heterogeneous phase. In particular, the work highlighted that the substituents of the compound itself could influence the TOF. To this end, I present a brief overview of heterogeneous catalysis and how the support, theoretically inert, must be studied in order to avoid undesired reactions and adsorption phenomena that can hamper catalyst performance.

4.1 Heterogeneous catalysis

In a society that is increasingly looking at enhancing the sustainable aspect of synthesis, one of the strategies often used is catalyst immobilisation. Supporting a catalyst has numerous advantages, which justify the number of studies regarding this approach that have been carried out over the last few decades, even in the industrial context.¹ This is because using homogeneous catalysis to perform reactions is not an easy concept to apply. If we think of large-scale industrial processes, the use of homogeneous catalysts (many of which are also very expensive) renders purification and recycling of the catalyst itself problematic. It could even lead to undesirable contamination (such as the presence of transition metals) if the final reaction product.

In an attempt to preserve the catalyst, heterogeneous catalysis is preferred for economic reasons and subsequent reuse. For this purpose, supported catalysts have been synthesised on different supports that make the catalyst immiscible, or semi-immiscible, in the phase in which the reaction is performed.²

Therefore, the most evident advantage of using them is that they can be functionalised with all types of catalysts, depending on the synthetic requirement, removed from the reaction environment, recovered, and reactivated for future reuse using simple methods, which makes their use very attractive for industries.

Despite all these advantages, there is still a certain criticality associated with using these catalysts. The catalytic efficiency of these supported catalysts is often lower than that of the same catalysts used in a homogeneous phase. The phenomenon which mainly contributes to the

¹ Q. H. Fan, Y. M. Li, A. S. C. Chan, *Chem. Rev.* **2002**, 102, 3385.

² a) T. Fulgheri, F. Della Penna, A. Baschieri, A. Carlone, *Curr. Opin. Green Sustain. Chem.* **2020**, 25, 100387; b) F. Cozzi, *Chem. Rev.* **2006**, 348, 1367; c) M. Benaglia, *New J. Chem.* **2006**, 30, 1525; d) M. Gruttadauria, F. Giacolone, R. Noto, *Chem. Soc. Rev.* **2008**, 37, 1666; e) T. E. Kristensen, T. Hansen, *Eur. J. Org. Chem.* **2010**, 3179; f) A. Puglisi, M. Benaglia, V. Chirolì, *Green Chem.* **2013**, 15, 1790.

decrease in catalytic activity can be attributed to the additionally diffusion contributes of the reagents in the reactive system which decreases the kinetics of the reaction.³

When a reagent moves into a solvent in which a supported catalyst is present, in order to be effectively activated by the catalytic site, it must initially diffuse into the solvent medium. It must then penetrate the surface of the supported catalyst and finally bind with the binding site. However, there may be undesirable adsorption phenomena between the reagent and the support itself, which should be theoretically inert. In the case of homogeneous catalysis, on the other hand, the encounter between substrates and catalyst is more immediate because the reagent only interacts with the catalytic site present on the catalyst.

Over the years, supported catalysts have been extensively researched to overcome all the sources that affect reactivity and selectivity to be as efficient as a homogenous phase catalyst.

We will briefly look at the characteristics that differentiate the various types of supported catalysts and then focus on the study aimed at understanding the matrix effect of a catalyst based on the core of a proline functionalised on mesoporous silica (SBA-15).

4.1.1 Supported catalyst

Several types of supported catalysts differ in the choice of structural elements. The wide structural variability of supported catalysts is reflected in the different catalytic activities resulting from them. The four main structural elements must be chosen appropriately to guarantee effective enantioselective heterogeneous catalysis (Figure 4. 1).⁴

³ A. F. Trindade, P. M. P. Gois, C. A. M. Afonso, *Chem. Rev.* **2009**, 109, 418

⁴ B. Altava, M. I. Burguete, E. García-Verdugo, S. V. Luis, *Chem. Soc. Rev.* **2018**, 47, 2722.



Figure 4. 1 Schematic representation of a supported catalyst

To best rationalise the type of requirements that need to be solved, several factors must be taken into account:

- the chemical-physical nature of the inert substrate
- the type of chemical bond that binds the polymer to the catalytic function
- the nature of the spacer (which influences the exposure of the sites themselves to the solvent medium)
- the number of catalytic sites which are actually used as catalysts

The support (or **matrix**) is a material that, as a fundamental property, must be inert and not participate in any manner in the catalytic cycle. Its function must therefore only be to support, and therefore immobilise, the chiral catalyst and attempt to insoluble it in the reaction medium in which the reaction is to be conducted. Very often, however, it can still affect the heterogeneous catalytic system. Generally, the polymeric support is commercially available and is therefore purchased. Depending on the nature of the matrix, the anchor points that allow the catalytic site to remain bound to the matrix are known as **linkers**.

These can establish different types of interaction between the different functionalities, which can be of an ionic or covalent nature. Naturally, a strong chemical bond is preferred, i.e., covalent, which can establish a stronger and more stable interaction to avoid the release of the catalytic (soluble) function in solution. On the other hand, the **spacer** is another element that often comes between the support and the catalytic functionality, essentially for two reasons. The first concerns the distancing of the catalytic functionality from the matrix for possible negative interactions that would compromise catalysis or lead to unexpected reactions (see the first example in 4.1.3 paragraph); the second is to give the catalytic site a lower structural rigidity to allow the

substrates to interact better with the active site.⁵ The choice of spacer must also be made appropriately in this case, as a long chain could lead to low selectivity since a confined chiral environment would not be created. In addition, the spacer may also contain other catalytic functions that can help the reactivity and selectivity of the reaction, as if it were a true bifunctional catalyst (see the third example in 4.1.3 paragraph).⁶

The **active catalytic site** could be functionalised with a large number of organic catalyst, but also with metal ligand, photocatalyst or photosensitizer for example, to perform the desired reaction in order to better recycle the catalyst.³ Depending on the type of material used, the catalytic functionalities may be adsorbed on the surface or be located within pores or within the material itself. As far as surface adsorption is concerned, the catalytic site will certainly be more exposed to the solvent medium but will have fewer binding sites than porous materials. Indeed, in this case, the surface area within which to bind the catalytic sites increases considerably. The density of the active site, and its accessibility by reagents and products, affects the rate and selectivity of the reaction (see the second example in the 4.1.3 paragraph). This occurs because if there is no adequate mass transfer, the active site can be poisoned by products and reagents that accumulate in the catalytic site and do not allow it to interact with new reagent molecules.⁷ The different characteristics of supported catalysts will be discussed in more detail in the next section.

⁵ F. Calderón, R. Fernández, F. Sánchez, A. Fernández-Mayoralas, *Adv. Synth. Catal.* **2005**, 347, 1395.

⁶ a) D. Font, S. Sayalero, A. Bastero, C. Jimeno, and M. A. Pericàs, *Org. Lett.* **2008**, 10, 2, 337. b) S. Rostamnia, E. Doustkhah, *RSC Adv.*, **2014**, 4, 28238; c) J. Lauwaert, E. G. Moschetta, P. Van Der Voort, J. W. Thybaut, C. W. Jones, G. B. Marin, *J. Catal.* **2015**, 325, 19; d) J. Lauwaert, J. Ouwehand, J. De Clercq, P. Cool, P. Van Der Voort, J. W. Thybaut, *Catal. Commun.* **2017**, 88, 85; e) S. L. Jain, A. Modak, A. Bhaumik, *Green Chem.* **2011**, 13, 586; f) N. A. Brunelli, C. W. Jones, *J. Catal.* **2013**, 308, 60.

⁷ P. Munnik, P. E. de Jongh, K. P. de Jong, *Chem. Rev.* **2015**, 115, 6687.

4.1.2 Matrix: types and structural characteristics

Insoluble organic polymers were the first to be used as supports for performing heterogeneous catalysis. These are polymers of synthetic origin consisting of one or more components that influence their chemical and physical behaviour. Merrifield introduced the use of a polymer as a support for catalytic purposes to optimise the synthesis of peptide sequences, coining the term "solid phase", which won him the Nobel Prize

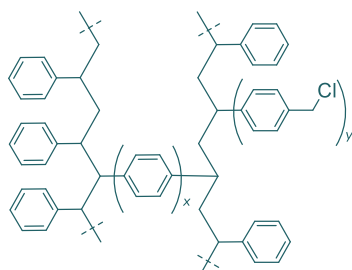


Figure 4. 2 Merrifield resin: copolymer of styrene and divinylbenzene

in Chemistry in 1984.⁸ As the author reported in the cited article, the "growing peptide chain was in the completely insoluble solid phase at all times. It was for this reason that the term solid-phase peptide synthesis was introduced to describe the new method." The mentioned resin was a chloromethylated copolymer of styrene and divinylbenzene, in the

form of 200-400 mesh beads, which has a degree of reticulation determined by the amount of added crosslinker, divinylbenzene (Figure 4. 2).

From a morphological point of view, in his work, he presented the resin as porous and with the right-sized cavities to allow the reagents to penetrate inside, especially in the presence of swelling solvents. Indeed, the degree of cross-linking of a polymer is a crucial parameter. This influences the swelling of the polymer when immersed in a solvent, which consequently affects the accessibility of the reagents to the binding sites by diffusive phenomena therefore the activity (Figure 4. 3).

⁸ R. B. Merrifield, *J. Am. Chem. Soc.* **1963**, 85, 14, 2149.

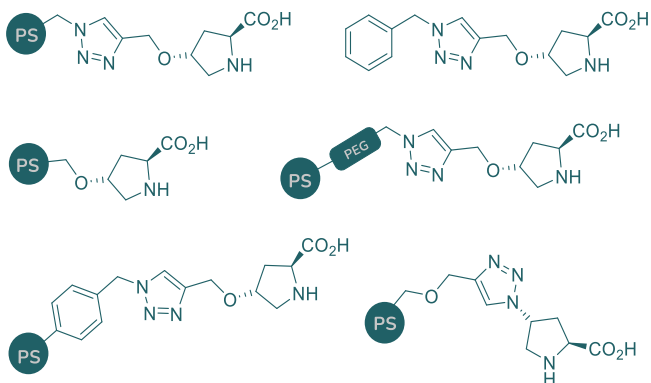


Figure 4. 3 Heterogenised Proline on polystyrene (PS) support

On the other hand, **soluble organic polymers** are used for a dual purpose, the first being as solid support on which to stably anchor the catalyst, while the second is for their ability to be soluble in the solvent medium, thus offering all the advantages of homogeneous catalysis. After carrying out the reaction, simply by varying the polarity of the solvent, it is possible to remove the supported catalyst from the reaction medium by precipitation of the catalyst from the solvent medium. They generally consist of linear or branched polymers. In the case of linear polymers, one of the first catalysts developed contained a high-molecular-weight polyethylene glycol matrix (PEG 5000) functionalised at the end with a quaternary ammonium salt for phase-transfer catalysis (Figure 4. 4).⁹

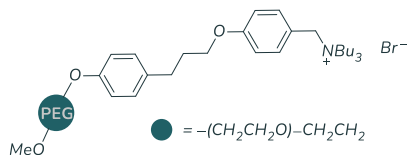


Figure 4. 4 Quaternary ammonium salt supported on PEG

However, using a linear polymer with high molecular weight is not convenient. Functionalisation with the active catalytic site is only carried

⁹ M. Benaglia, A. Puglisi e F. Cozzi, *Chem. Rev.* **2003**, 103, 3401.

out at the end of the polymer chain, which entails a considerable material expenditure compared to the catalytic load. This is why branched polymers are often preferred. This is because branched polymers have several binding sites for attaching catalytic functionalities, which are the nucleus, the branches, and the ends of the branches respectively. This allows a considerable increase in catalytic sites for the same molecular weight of the polymer for greater efficiency, although it is often preferable to bind only at the ends.

For **inorganic** substrates, the most commonly used are based on ordered porous silica matrix. These materials have a high surface area combined with large and uniform porosity, giving the structure a high degree of crystallinity.

According to IUPAC, the different siliceous materials are differentiated according to the size of the pore in macroporous (>50 nm), mesoporous (2-50 nm), and microporous (pore size <2 nm). Therefore, the pore size in catalysis is a fundamental parameter to be controlled. It must allow the free diffusion of solvent and reagent within the cavity to perform the catalytic function better. They also have high mechanical stability and robustness.

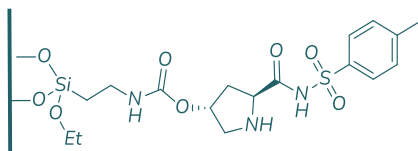


Figure 4. 5 Example of heterogenized Proline on silica support

One disadvantage in their use may be that the material does not appear to be completely inert due to acidic silanol groups near the catalytic site, which could affect the catalytic process itself.

To overcome this problem, the silanol residues are often protected by the insertion of so-called capping to limit their acid activity, or they are functionalised by introducing spacers to move the catalytic site away from the acid groups themselves (Figure 4. 5). In this case, the choice of spacer must be made by finding a good compromise between rigidity and selectivity. On the other hand, the presence of silanol groups makes these

materials easily functionalisable¹⁰ through click or multi-step reactions with organosilanes, and their characterisation generally proceeds through the use of solid-state nuclear magnetic resonance (mainly through experiments with ¹³C and ²⁹Si).¹¹ For the previously mentioned reasons, they are considered fascinating materials for application for catalytic purposes, in heterogeneous phase or in flow (as we will see in the examples below), and as drug delivery systems, gas sensors, or chiral coatings for chromatographic separation.¹²

Another type of support attracting increasing interest is **magnetic nanoparticles (MNP)**. These are spheres of iron oxides (mainly Fe₃O₄) varying in size between 1 and 100 nm that form the core of the support. Due to the magnetic properties of iron, it considerably facilitates catalyst recovery. The supported catalysts on MNP are reused for many catalytic cycles as they are very robust (Figure 4. 6). The main drawback to their use is the low inertness of the support and the fact that they tend to form aggregates, limiting their efficiency.¹³ To avoid this problem, it is preferred to coat the magnetic core with different functionalisation, either polyacrylate or phosphates.

¹⁰ a) S. Rostamnia, E. Doustkhah, *RSC Adv.* **2014**, 4, 28238; b) J. Lauwaert, E. G. Moschetta, P. Van Der Voort, J. W. Thybaut, C. W. Jones, G. B. Marin, *J. Catal.* **2015**, 325, 19; c) J. Lauwaert, J. Ouwehand, J. De Clercq, P. Cool, P. Van Der Voort, J. W. Thybaut, *Catal. Commun.* **2017**, 88, 85; d) S. L. Jain, A. Modak, A. Bhaumik, *Green Chem.* **2011**, 13, 586; e) N. A. Brunelli, C. W. Jones, *J. Catal.* **2013**, 308, 60.

¹¹ a) A. Ciogli, P. Simone, C. Villani, F. Gasparrini, A. Lagana, D. Capitani, N. Marchetti, L. Pasti, A. Massi, A. Cavazzini, *Chem. Eur. J.* **2014**, 20, 8138; b) B. Grunberg, T. Emmler, E. Gedat, I. Shenderovich, G. H. Findenegg, H.-H. Limbach, G. Buntkowsky, *Chem. Eur. J.* **2004**, 10, 5689; c) N. Raveendran Shiju, A. H. Alberts, S. Khalid, D. R. Brown, G. Rothenberg, *Angew. Chem. Int. Ed.* **2011**, 50, 9615.

¹² a) V. Chaudhary, S. Sharma, *J. Porous Mater.* **2017**, 214, 741; b) D. Kotoni, A. Ciogli, C. Molinaro, I. D'Acquarica, J. Kocergin, T. Szczerba, H. Ritchie, C. Villani, F. Gasparrini, *Anal. Chem.* **2012**, 84, 6805.

¹³ O. Gleeson, G.L. Davies, A. Peschiulli, R. Tekoriute, Y. K. Gunko, S. J. Connors, *Biomol. Chem.* **2011**, 9, 7929.

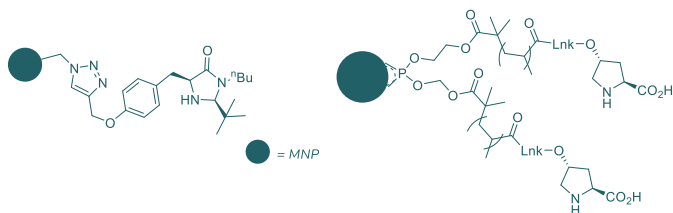


Figure 4. 6 Examples of heterogenised catalysts on Magnetic Nano Particles

Over the years, other supports have been used to optimise catalytic performance by anchoring increasingly versatile organocatalysts to synthetic ends. For example, thermo- or pH-responsive materials (Figure 4. 7 respectively **A** and **B**), which function in a similar way to organic polymers but take advantage of different triggers (in this case, temperature and pH) to be easily separated from the phase they are in.

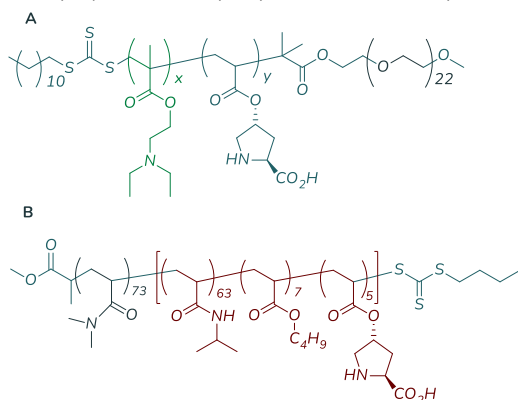


Figure 4. 7 Example of pH-responsive (A) and thermoresponsive (B) catalysts polymer

For example, by combining different polymeric portions, it is possible to obtain a copolymer, i.e., a polymer consisting of different monomeric groups arranged alternately and which, at a chemical and physical level, has the characteristics of each group.¹⁴ It is therefore possible to work

¹⁴ A. del Prado, M. Pintado-Sierra, M. Juan-y-Seva, R. Navarro, H. Reinecke, J. Rodr'iguez-Hernandez, C. Elvira, A. Fernandez-Mayoralas, A. Gallardo, *Polymer Chemistry*, 2017, 55, 7, 1228.

with a support that can change its behaviour, for example by becoming soluble or vice versa when the temperature or polarity of the solvent changes, or by assuming a micellar structure following a change in the pH of the reaction environment. Consequently, this makes it possible to create a favourable environment in solution for both the reactants and the catalyst during catalysis, which can then be modified once it has finished and the catalytically active species recovered. In this case, part of the research effort has been made to improve the catalytic activity of proline in water. Several studies have reported that proline accelerates the reaction rate and has better selectivity in the presence of a small amount of water, but when water is used as a solvent, low yields are obtained with little or no enantio-selection.^{15,16} For this reason, various strategies are employed to achieve the desired hydrophobic environment within the aqueous system.



Figure 4. 8 Organo-textile catalyst

A final remarkable example is the organo-textile catalysts developed by Benjamin List¹⁷ on which authentic pieces of fabric (made of nylon) were anchored (Figure 4. 8). Catalytic activity was not eroded even after over 300 cycles of reuse.

¹⁵ D. Font, S. Sayalero, A. Bastero, C. Jimeno, and M. A. Perica`s, *Org. Lett.* **2008**, 10, 2, 337.

¹⁶ H. A. Zayas, A. Lu, D. Valade, F. Amir, Z. Jia, R. K. O'Reilly and M. J. Monteiro, *ACS Macro Lett.* **2013**, 2, 327.

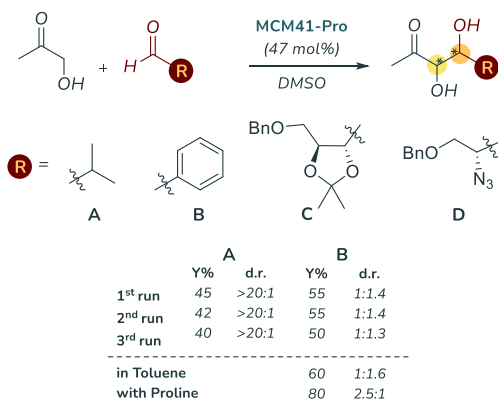
¹⁷ J. Lee, T. Mayer-Gall, K. Opwis, C. Eui Song, J. S. Gutmann, B. List, *Science* **2013**, 341, 6151, 1225.

4.1.3 Selected examples

In this section, we will see the influence of the nature of the support leading to heterogenisation of the catalyst in relation to the catalytic performance of homogeneous amino-catalysed reactions. In particular, we will see how interactions with the acidic groups of a porous inorganic resin leads to a variation in stereoselectivity. Subsequently, we will show how the a priori structural design may prove to be the correct strategy for guaranteeing the spatial proximity of two catalytic units to carry out bifunctional catalysis. Lastly, we will examine the degree of cross-linking of an organic polymer, which manages to generate a chiral microenvironment suitable for promoting enantioselective reactions with a relatively low catalyst loading for heterogeneous catalysis.

Interactions with the acidic groups of a porous inorganic matrix

*In the first example reported, the authors have used a lamellar mesoporous siliceous material to heterogenise the proline derivative. The tested reaction was the aldolic reaction between hydroxyacetone and various aldehydes. Good yields were obtained and, even when reusing the catalyst for three cycles, no reduction in enantioselectivity was observed, but there was a slight decrease in yield, probably due to the loss of catalytic material. However, the interesting thing is that a inversion of diastereoselectivity was observed for some substrates (**B**, **C**, and **D**; Scheme 4. 1) by using the supported catalyst, compared with the use of L-proline as a catalyst.*



Scheme 4. 1 Aldol reaction performed with *L*-Proline heterogenized on silica support (MCM41)

substances, a hydrogen bond could be established between the silanol groups of the support and the aldehydes, which would promote the preferential formation of the anti- product.

They noticed a decrease in the ratio between the two diastereoisomers and the preferential formation of the syn diastereoisomer even in less polar solvents than DMSO, which they did not observe when comparing the reaction performed using *L*-proline in homogeneous solution. The authors themselves hypothesised that for the tested

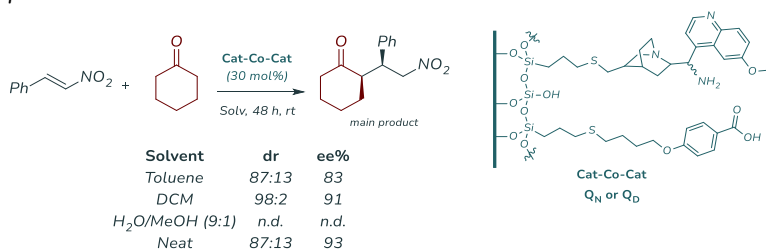
Bifunctional supported catalyst

In the example shown, the catalytic performance in a Michael addition reaction between saturated cyclic ketones and *trans*- β -nitrostyrene of a heterogeneous silica-based catalyst containing a primary amine moiety, consisting of 9-amino-9-deoxy-*epi*-quinine (or quinidine) and its achiral acid cocatalyst (benzoic acid) bonded to the same activated silica support (Scheme 4. 2).¹⁸

The design of the catalyst, in particular the length and flexibility of the spacers, provided to be optimal for carrying out the dual activation of the reactants in the same bifunctional catalyst, as there was a reasonable distance between them for a productive interaction, especially with regard to enantioselectivity and diastereoselection.

¹⁸ A. Ciogli, D. Capitani, N. Di Iorio, S. Crotti, G. Bencivenni, M. P. Donzello, and C. Villani, *Eur. J. Org. Chem.* **2019**, 2020.

After careful characterisation of the supported catalyst, using several techniques, the authors reported that the average distance between anchoring sites of the acidic fragments in **Co-Cat** is approximately 9 Å and the distance between the anchoring sites of quinine or quinidine fragments in **Cat-Co-Cat** is around 16 Å calculated from the starting surface area of the silica matrix and the amount of acid and quinine or quinidine.



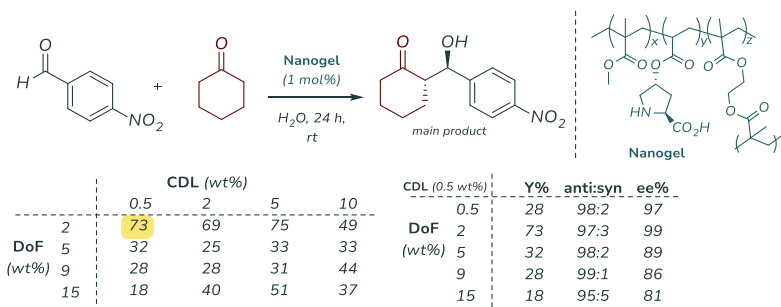
Scheme 4. 2 Michael addition performed with heterogenised bifunctional catalyst

Furthermore, the supported catalyst was tested in continuous-flow conditions producing the chiral drug warfarin, a common anticoagulant, showing how these catalytic systems can be implemented to conduct amino-catalysed reactions with large-scale applications.

Cross-linking and degree of catalyst functionalisation

This last example was reported in order to understand how the perfect balance between the cross-linking density (CDL) and the degree of catalyst functionalisation (DoF) with the active sites can be crucial to the successful performance of the entire catalytic process. In their work, Longbottom and co-workers evaluated the reactivity of a series of nanogel catalysts in a model reaction of aldol addition in water. The catalysts in question were designed to create nanoreactors that would allow the confinement of the reactants close to the catalytic site. The catalysts consist of a catalytic core of L-Proline supported on an organic polymer consisting of poly(methyl methacrylate) (PMMA) at different cross-linking densities (range 5-10 wt%) and different degrees of catalyst functionalisation (range 2-15 wt%).

After characterising the morphology of the various synthesised systems by DLS and TEM measurements, the reactivity was studied as a function of the number of catalytic sites, determining that the enantioselectivity of the reaction increases with a low number of catalytic sites present (**Scheme 4.3**). This was attributed to a decrease in the hydrophobic effect of the system, since a higher number of prolines leads the nanogel to sequester the reagents in a less effective fashion.



Scheme 4.3 Aldol reaction performed by evaluating different DoFs and CDLs

The degree of cross-linking of the polymer was then taken into consideration. For the same catalyst loading (1%), a precise range of CDLs was identified within which the reaction proceeds with good selectivity. This result, as suggested by the authors themselves, can be attributed to the presence of a suitable number of hydrophobic nanoreactors with the appropriate dimensions to host the reagents. Therefore, neither too dense to allow the nanoreactor cavity to accommodate the reagents, nor too large to lose the contribution due to the hydrophobic effect.

4.2 T_1/T_2 parameter as indicator of surface affinity with the molecules

The use of NMR technique is considered a versatile strategy for monitoring the interaction between reagents and the surface of the matrix because it is a non-destructive and rapid technique.¹⁹

In this case, the T_1/T_2 ratio is considered, where T_1 and T_2 are two parameters that depend on the rotational and translational motions of the molecule under investigation. This way, it is possible to determine the affinity of a molecule for the surface of the solid matrix on the basis of how much this molecule is "restrained" by the interaction. More specifically, T_1 is the spin-lattice relaxation and it measures the longitudinal component of the magnetisation vector (by a convention on the z-axis).

$$M_z = M_0(1 - 2e^{-\tau/T_1})$$

(Equation 1)

T_1 determines the NMR signal strength related to an observed nucleus. It is determined by acquiring a suitable number of NMR experiments using the Inversion Recovery sequence (Figure 4. 9).²⁰ The first impulse imparted is a 180° pulse, which bends the magnetization along the z-axis (-z) followed by a time τ in which the spin relaxes. Before it returns to its equilibrium position, a subsequent 90° pulse is given. This last pulse is given to recover the magnetisation information along the z-axis (M_z) as the receiving coil is placed in the xy-plane. Depending on the τ given, the time delay with which the 90° pulse is given, for short τ the magnetization component will be in the negative quadrant (-x;-y;-z component). When the time between the two pulses increases, the M_z component will also increase so that, for long enough τ , the core will relax almost completely

¹⁹ C. D'Agostino, J. Mitchell, M. D. Mantle, L. F. Gladden, *Chem. Eur. J.* **2014**, *20*, 1

²⁰ E. Fukushima, S. W. Roeder, *Experimental pulse NMR*, Addison-Wesley, US, **1981**.

and after giving the second pulse (at 90°) the value recorded on the xy plane will be close to unity.

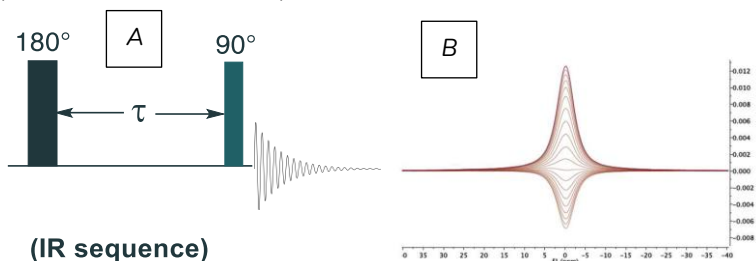


Figure 4.9 a) Representation of inversion recovery (IR) sequence employed to measure the T_1 . b) FIDs (IR) of solvent in the catalyst, after phasing and baseline correction, plotted vs time to obtain the T_1 value.

T_2 , on the other hand, is defined as the spin-spin relaxation or transverse component and can be derived from the Equation 2.

$$M_{xy} = M_0 e^{-t/T_2}$$

(Equation 2)

This parameter is obtained from another sequence, this time echo, the CPMG sequence.²¹ With CPMG sequence is it possible to separate (and therefore eliminate) the contribution due to the inhomogeneities of the magnetic field (Figure 4. 10). In this case a first 90° pulse is applied (which bends the magnetization M_z on the rotating reference $x'y'$ plane), during the delay τ , the magnetization component will start to deflect and rotate. Subsequently, a first 180° impulse will be given which will cause the spin to rotate along the x' axis (again of the rotating reference system). The latter causes the magnetisation to be at least partially rephased and produces a signal called an echo.

²¹ H. Y. Carr, E. M. Purcell, *Physical review*, 1954, 94, 630.

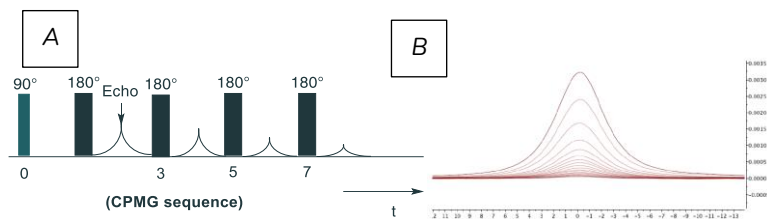


Figure 4.10 a) Representation of CPMG sequence employed to measure the T_2 . b) FIDs (CPMG) of cyclohexane in the catalyst, after phasing and baseline correction, plotted vs time to obtain the T_2 value.

If significant molecular diffusion is present, more delay is needed to refocus the spins, otherwise there is a risk of underestimating the T_2 value.

However, by assessing the T_1/T_2 ratio, it is possible to evaluate the slowing down, and consequent affinity, of the molecule within a solution in which a solid catalyst matrix is present.

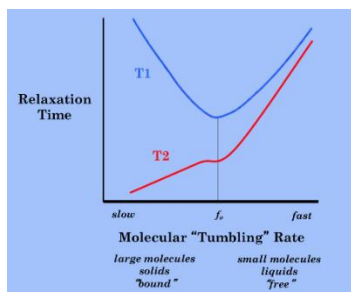


Figure 4.11 Relaxation time in function of tumbling rate

When molecules (of low molecular weight) are free to move in bulk of solvent, the ratio between the two parameters will be close to unity because, as can be seen from Figure 4.11, both will have similar high relaxation rates (fast molecules). If the molecules are heavier or encounter obstacles, as in the case of supported catalysts, they are slowed down as their diffusion in the solvent medium is hindered. While the T_1 component still has high relaxation time values, T_2 decreases, which means that the T_1/T_2 ratio will be $\gg 1$ and directly proportional to the nature of the interaction itself.²²

²² a) G. Di Carmine, D. Ragno, A. Massi, C. D'Agostino, *Org. Lett.* **2020**, 22, 13, 4927; b) J. Ward-Williams, J.-P. Korb, L. Rozing, A. J. Sederman, M. D. Mantle, L. F. Gladden, *J. Phys. Chem. C* **2021**, 125, 16, 8767.

Abstract: *In this article, we report a study investigating the interaction between the surface of a supported catalyst and aromatic aldehydes in an aldol reaction between hydroxyacetone and differently substituted benzaldehydes. The catalyst considered is a heterogeneous L-proline immobilised on nanostructured silica support (SBA-15). The results reveal that the higher the affinity of the aldehydes for the matrix, the lower the reactivity of the system analysed will be. This tendency could be attributed to an increased competition at the catalytic site between the hydroxyacetone and the aldehydes, which inhibits the formation of the desired aldol product.*

4.3 Target of the project

Albeit organocatalysis is considered a sustainable and robust platform²³ delivering various catalytic activations,²⁴ low turnover numbers (TON) are still considered a critical issue to exploit this synthetic strategy in industry. The immobilisation of the catalyst on an inert, mechanically stable, and robust support is an approach that is becoming increasingly widespread in industry, also because of the fact it can be easily recovered, recycled, and implemented in flow systems.²⁵

²³ a) B. List, R. A. Lerner and C. F. Barbas, *J. Am. Chem. Soc.* 2000, **122**, 2395; b) K. A. Ahrendt, C. J. Borths and D. W. C. MacMillan, *J. Am. Chem. Soc.* 2000, **122**, 4243; c) S. Mitsumori, H. Zhang, P. H.-Y. Cheong, K. N. Houk, F. Tanaka and C. F. Barbas, *J. Am. Chem. Soc.* 2006, **128**, 1040; d) A. Dondoni and A. Massi, *Angew. Chem. Int. Ed.* 2008, **47**, 4638.

²⁴ a) P. Melchiorre, M. Marigo, A. Carlone and G. Bartoli, *Angew. Chem. Int. Ed.* 2008, **47**, 6138; b) A. Carlone and L. Bernardi, *Phys. Sci. Rev.* 2019, **4**, 20180097.

²⁵ a) M. B. Plutschack, B. Pieber, K. Gilmore and P. H. Seeberger, *Chem. Rev.* 2017, **117**, 11796; b) D. Cantillo, O. de Frutos, J. A. Rincón, C. Mateos and C. O. Kappe, *Org. Lett.* 2014, **16**, 896; c) T. Tsubogo, T. Ishiwata and S. Kobayashi, *Angew. Chem. Int. Ed.* 2013, **52**, 6590; d) I. Atodiresei, C. Vila and M. Rueping, *ACS Catal.* 2015, **5**, 1972; e) C. De Risi, O. Bortolini, A. Brandolese, G. Di Carmine, D. Ragno and A. Massi, *React. Chem. Eng.* 2020, **5**, 1017-1052; f) D. Ragno, A. Brandolese, D. Urbani, G. Di Carmine, C. De Risi, O. Bortolini, P. P. Giovannini and A. Massi, *React. Chem. Eng.* 2018, **3**, 816; g) A. Brandolese, M. D. Greenhalgh, T. Desrues, X. Liu, S. Qu, C. Bressy and A. D. Smith, *Org. Biomol. Chem.* 2021, **19**, 3620; h) A. Brandolese, D. Ragno, G. Di Carmine, T. Bernardi, O. Bortolini, P. P. Giovannini, O. G. Pandoli, A. Altomare and A. Massi, *Org. Biomol. Chem.* 2018, **16**, 8955; i) D. Ragno, C. Leonardi, G. Di Carmine, O. Bortolini, A. Brandolese, C. De Risi and A. Massi, *ACS Sustain. Chem. Eng.* 2021, **9**, 24, 8295.

Anchoring the organocatalyst on inert support makes it insoluble and prone to heterogeneous catalysis. However, the experimental conditions cannot simply be converted from homogeneous catalysis due to the adsorption phenomena related to the variation of the chemical environment which affects the formation of the transition state (TS) and the stabilisation of reactive intermediates.²⁶

The support very frequently has a crucial role to the modulation of interactions between catalyst, reagents and solvent. To this end, an in-depth study of these interactions is highly desirable in order to critically rationalise the catalytic behaviour and possibly refine the structure of the supported catalyst.

In a recent study,²⁷ our group collaborated to evaluate the effect of different solvents on the heterogeneous proline-organocatalyst functionalised on the mesoporous SBA-15 matrix. In particular, it was evaluated the reactivity and adsorption effects using relaxation measurement via low field NMR by monitoring the T_1/T_2 parameter. The benchmark reaction taken into account was the aldol reaction between hydroxyacetone and benzaldehyde carried out in different solvents in order to study the solvent effects on the matrix and the catalyst performance by comparing the results in homogeneous phase by using L-Proline in the same solvent.

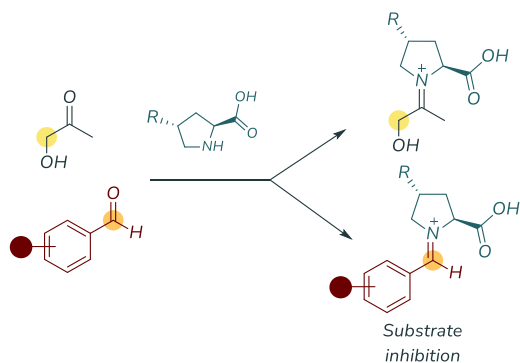
Following from that, my research focused on the effect of adsorption of substituted benzaldehydes on the silica matrix of the support (SBA-15) to provide insights into effects on the catalyst activity. In particular, to demonstrate the competitive adsorption between substrates with different electronic structures to gain a deeper understanding of the

²⁶ a) A. T. Krzyzak and I. Habina, *Microporous Mesoporous Mater.* 2016, **231**, 230; b) D. Weber, J. Mitchell, J. McGregor and L. F. Gladden, *J. Phys. Chem. C*, 2009, **113**, 6610; c) D. W. Aksnes, K. Førland and L. Kimtys, *J. Mol. Struct.* 2004, **708**, 23; d) I. Habina, N. Radzik, T. Topoń and A. T. Krzyżak, *Microporous Mesoporous Mater.* 2017, **252**, 37.

²⁷ G. Di Carmine, L. Forster, S. Wang, C. Parlett, A. Carlone, C. D'Agostino, *React. Chem. Eng.* 2022, **7**, 269.

problems encountered when performing organocatalytic C-C formation reactions on solid surfaces.²⁸

It is known that the aldol reaction between ketones and benzaldehydes also proceeds via a non-productive side reaction, in absence of water as co-solvent, which reduces the yield of the reaction (Scheme 4. 4).²⁹



Scheme 4. 4 Competitive reaction: correct activation of hydroxyacetone (top) and inhibition of the catalyst by benzaldehyde (bottom)

Furthermore, it was observed that a by-product results from the activation by proline of the benzaldehyde via iminium ion, since the latter does not have protons that can be enolised in the α -position.

4.4 Result and discussion

The examined reaction is the aldol reaction between hydroxyacetone (activated via enamine by L-proline derivative) and a series of substituted benzaldehydes with Electron Withdrawing Groups (EWG) and Electron Donating Groups (EDG). Aldehydes with different substituents were

²⁸ K. Kandel, S. M. Althaus, C. Peeraphatdit, T. Kobayashi, B. G. Trewyn, M. Pruski, I. I. Slowing, *Journal of Catalysis* **2012**, 291, 63

²⁹ N. Zotova, A. Franzke, Alan Armstrong, D. G. Blackmond, *J. Am. Chem. Soc.* **2007**, 129, 49, 15100

considered in order to assess their surface adsorption effect as a function of the electronic effect on the reaction reactivity. The selection of the aldehydes, in addition to allowing a study of the evaluation of the electronic effects, was appropriately based on the physical state of the benzaldehydes, which had to be liquid. This made it possible to assess the phenomenon of diffusion of these on the surface of the supported catalyst using NMR techniques.

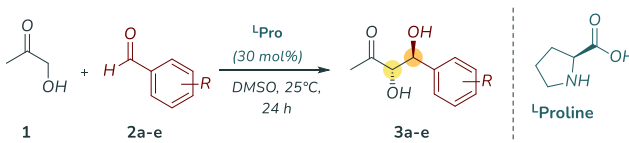
To obtain this information, at the University of L'Aquila, reactions with L-Proline (homogeneous phase) and in the heterogenized Proline on SBA-15 using different aldehydes containing EWG groups (2-F and 3-Br-benzaldehyde), benzaldehyde (taken as a standard reference) and EDG groups (4-MeO- and 4-Me-benzaldehyde) were performed.

SBA-15 functionalised with L-Proline was provided to us by the group of D'Agostino who synthesised and characterised it using the synthetic procedure reported in the previous work.²⁷

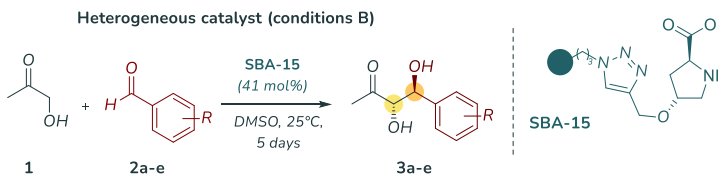
This set of experiments, shown in Table 4. 1, made it possible to determine the stereoselectivity of the aldol reaction using the two catalysts and the turnover frequency (TOF) parameter associated with catalyst activity. As can be seen from the table, and as expected, the reaction performed with proline always gave better results regarding TOF than the catalyst in a homogeneous phase. additionally, a higher TOF value was recorded for halogenated substrates. No significant variations were recorded for diastereoselection. For the enantiomeric excess, a slight decrease in enantioselection using the supported catalyst could be notice, possibly due to the presence of H-bonds formed with the silanol groups in the support.

Table 4. 1 Comparison between experimental results obtained with the homogeneous (A) and heterogeneous (B) phase procedure^a

Homogeneous catalyst (conditions A)



Heterogeneous catalyst (conditions B)



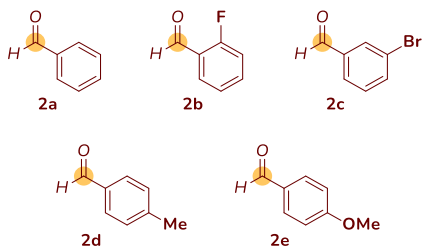
2 R=	Conditions	TOF [h ⁻¹] × 10 ³	dr	ee%
H (2a)	A	60.7	74:26	88 (42)
	B	11.3	79:21	78 (29)
2-F (2b)	A	93.3	77:23	86 (23)
	B	18.9	72:28	80 (28)
3-Br (2c)	A	104.0	76:24	68 (41)
	B	15.9	73:27	73 (54)
4-Me (2d)	A	53.9	73:27	90 (43)
	B	6.2	72:28	80 (32)
4-MeO (2e)	A	60.6	73:27	88 (48)
	B	10.9	71:29	76 (31)

[a] Reaction conditions A: hydroxyacetone **1** (2.4 mmol, 24 equiv.), aldehydes **2a–e** (0.1 mmol, 1 equiv.), L-Proline (30 mol%), DMSO (0.8 mL); Reaction conditions B: hydroxyacetone **1** (2.4 mmol, 24 equiv.), aldehydes **2a–e** (0.1 mmol, 1 equiv.), ^LPro-SBA-15 (42 mol%), DMSO (0.8 mL), 25 °C, 24h. TOF calculated from the averaged rate over the course of reaction (1 day for the homogeneous catalyst and 5 days for the immobilised catalyst) as mmolproduct/(mmolcat × time in seconds). dr determined by ¹H NMR analysis of the crude reaction mixture. ee determined by HPLC on a chiral stationary phase; ee values of minor diastereoisomer are reported in brackets.

In parallel, NMR spectra were recorded from the group in Manchester University with two different sequences to determine the T_1/T_2 parameter. As mentioned in paragraph 4.2, T_1/T_2 is considered a robust parameter to detect the affinity of a liquid diffusing through the surface of a solid. Indeed, as shown in Table 4. 2, it can be appreciated that substrates containing EDG groups are more affinitive to the support than

benzaldehyde, taken as a reference, and other substrates in which EWG groups are present. For all aldehydes, the value $T_1/T_2 > 1$, demonstrates that these substrates present a good affinity for the matrix.

Table 4. 2 NMR data analysis for T_1/T_2 parameter



Reactant	T_1 [ms]	T_2 [ms]	T_1/T_2 [-]
2a	51 ± 1	13.4 ± 0.3	3.81 ± 0.09
2b	36 ± 1	11.0 ± 0.2	3.27 ± 0.08
2c	87 ± 2	24.5 ± 0.5	3.55 ± 0.09
2d	111 ± 2	25.5 ± 0.5	4.35 ± 0.10
2e	85 ± 2	21.3 ± 0.4	3.99 ± 0.10

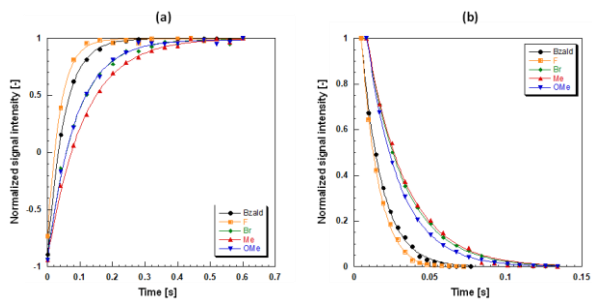


Figure 4. 12 (a) T_1 inversion recovery and (b) T_2 CPMG experimental data for the various benzaldehyde derivatives adsorbed within the $^4\text{Pro-SBA-15}$ -immobilized proline catalyst. Solid lines are fitting to (a) Equation (1) and (b) Equation (2).

The T_1/T_2 parameter is greater for substrates substituted with methyl- and methoxy-groups than for halogen derivatives.

In order to rationalise the data sets obtained (For T_1/T_2 see Figure 4. 12), the two parameters were plotted to visualise the activity as a function of adsorption (TOF vs. T_1/T_2). As can be observed from Figure 4. 13, it emerged that the substituents that best promote the reaction are those loosely bound with the matrix. This apparently counterintuitive effect is due to the phenomenon of substrate inhibition.

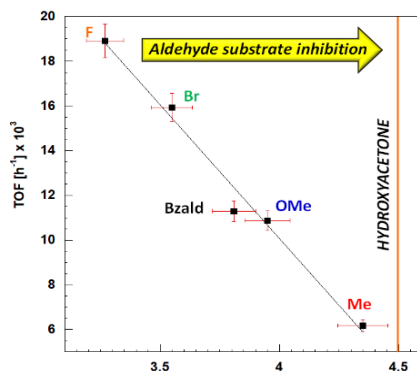


Figure 4. 13 Final plot concerning the adsorption (T_1/T_2) of the aldehydes of the system considered as a function of their reactivity (TON); the orange line shows the affinity value of the hydroxyacetone.

In fact, when looking at the T_1/T_2 parameter for the reagent **1** that effectively has to be activated by the supported proline (the hydroxyacetone **1**; orange line), it has a value much closer to the benzaldehydes substituted with EDG groups.

Therefore, the low TOF for these substrates was attributed to the much more pronounced competition between the two reagents to form the **activated compound of the** reaction under consideration and the side reaction.

Conclusion

In this work, the effect of adsorption on the solid support matrix (T_1/T_2) of the catalyst (*L*-Pro-SBA-15) by substituted aldehydes with different electronic groups as substituents as a function of their reactivity (TOF) was evaluated. This study made it possible to evaluate the behaviour of a series of benzaldehydes in contact with the surface of a heterogenised

catalyst. The affinity of these compounds was much higher for EDG substituent groups than for aldehydes with EWG groups. This allowed us to attribute the decrease in reactivity, as corroborated by the TOF values for the benchmarks reaction, to a plausible substrate inhibition for these compounds that poison the silica support.

Furthermore, the use of NMR proved to be a fundamental tool for obtaining diffusion data in an easy, fast and non-destructive manner.

4.4.1 Experimental section (performed in L'Aquila University)

Hydroxacetone **1**, aldehydes **2a-2e**, and Durene were purchased by Merck and Fluorochem and used as received unless otherwise stated. Analytical grade solvents were purchased by Merck and Carlo Erba. Silica Gel 60A (35-70 μ) and HPLC solvents were purchased by Merck.

Nuclear magnetic resonance analyses (^1H -, ^{19}F and ^{13}C -NMR spectra) were acquired using a Bruker Advance III 400 MHz spectrophotometer. Chemical shifts (δ) are reported in ppm relative to residual solvent signals for ^1H - and ^{13}C -NMR (^1H -NMR: 7.26 ppm for CDCl_3 ; ^{13}C -NMR: 77.0 ppm for CDCl_3). ^{13}C -NMR spectra were acquired with ^1H broadband decoupled mode. Coupling constants are given in Hz. Diastereoisomers ratio (anti/syn) was determined by the integration of NMR signals related to diastereotopic protons of the crude mixture.

Chromatographic purifications of compounds **3b**, **3c**, and **3d** were performed using automated BÜCHI - Reveleris® X2-UV System. Optical rotations were measured on a ZUZI 412 Digital Polarimeter (tube length: 100 mm). HPLC analyses were acquired using an Agilent 1220 Infinity II liquid chromatographer equipped with a Phenomenex column - Lux 3 μm -i-Cellulose 5, Lux 3 μm -i-Cellulose 1 and Lux 3 μm -i-Amylose 1). Racemic samples were prepared using a racemic mixture of D-Proline and L-Proline as a catalyst at 35 °C in dimethyl sulfoxide (DMSO) overnight.

High-resolution mass spectra were recorded in Manchester University.

Optical rotations were measured on a ZUZI 412 Digital Polarimeter (tube length: 100 mm).

Assignment of absolute configuration: Absolute configurations of compounds **3b** – **3d** were assigned by comparing their absolute optical rotations with the values reported in the literature. The absolute configuration of all other products was assigned by analogy, considering a uniform mechanism of stereinduction.

General procedure: To a mixture of ^LProline (3,5mg, 30 mol%) or ^LPro-SBA-15³⁰ (78 mg, 41 mol%), hydroxyacetone **1** (165 μL, 2.4 mmol, 24 eq) and DMSO (800 μL) was added the aldehyde **2a-e** (0.1 mmol, 1 eq). After the reaction mixture was stirred at room temperature for 24 h (with *L*-Proline) or 5 days (with ^LPro-SBA-15 catalyst). The reaction was quenched with 5 mL of NH₄Cl 0.5 M. Then the aqueous mixture was extracted with DCM (4 x 5 mL) and the combined organic layer was washed with brine and dried over MgSO₄ and concentrated in vacuo after filtration.

the mixture was added 1 mL of internal standard in CDCl₃ (we used a stock solution containing 0.5 eq of durenene with respect to the aldehyde).

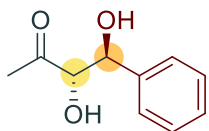
The products have not been purified.

NMR yield was determined by ¹H-NMR of the crude reaction mixture using durenene as internal standard and D1=10 s; the diastereoisomeric ratio was determined by ¹H-NMR of the crude mixture setting D1=10 s; the final products **3b-3d** were isolated as a mixture of diastereoisomers, the NMR data of compounds **3a** and **3e** are in accordance with the literature (see below); Compounds **3b**, **3c** and **3d** were characterised as a mixture of diastereoisomers, reporting the full characterisation of only anti product; the ee value was determined by HPLC on a chiral stationary phase.

³⁰ The catalyst loading of ^LPro-SBA-15 = 0.5254 [0.1*(41/100)*1/0.5254 = 0.078 g = 78 mg]

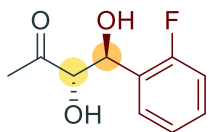
4.4.2 Characterisations

(3S,4S)-3,4-dihydroxy-4-phenylbutan-2-one (3a):³¹



Synthesised in accordance with general procedure using benzaldehyde (10.2 μ L, 0.1 mmol). ¹H NMR (400 MHz, Chloroform-d) δ 7.40–7.30 (m, 5H), 5.00 (d, J = 4.2 Hz, 1H), 4.46 (d, J = 4.2 Hz, 1H), 1.97 (s, 3H). HPLC (Lux 3 μ m-Cellulose 5, Hexane/*i*-Propanol 90:10), flow: 0.7 mL/min, λ =210 nm, Anti diastereoisomers (t_{major} : 8.3 min.; t_{minor} : 7.3 min.) Syn diastereoisomers (t_{major} : 10.8 min.; t_{minor} : 11.3 min.)

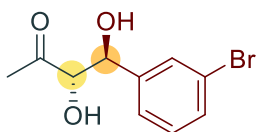
(3S,4S)-4-(2-fluorophenyl)-3,4-dihydroxybutan-2-one (3b)



Synthesized in accordance with general procedure using 2-fluorobenzaldehyde (11 μ L, 0.1 mmol). ¹H NMR (400 MHz, Chloroform-d) δ 7.34 – 7.27 (m, 1H), 7.23 – 7.15 (m, 1H), 7.10 – 7.00 (m, 1H), 5.32 (d, J = 3.6 Hz, 1H), 4.61 (s, 1H), 3.69 (s, 1H), 2.97 (s, 1H), 2.03 (s, 2H). ¹³C NMR (101 MHz, Chloroform-d) δ 207.3 (CO), 159.6 (C, d, $J_{\text{C-F}}$ = 245.4 Hz), 129.8 (CH, d, $J_{\text{CHar-F}}$ = 8.3 Hz), 128.1 (CH, d, $J_{\text{CHar-F}}$ = 4.1 Hz), 126.0 (C, d, $J^{\text{1C-F}}$ = 13.3 Hz), 124.4 (CH, d, $J_{\text{CHar-F}}$ = 3.4 Hz), 115.3 (CH, d, $J_{\text{CHar-F}}$ = 21.8 Hz), 79.8 (CH, d, $J_{\text{CH-F}}$ = 1.8 Hz), 69.3 (CH, d, $J_{\text{CH-F}}$ = 1.5 Hz), 27.4 (CH₃, d, $J_{\text{CH3-F}}$ = 1.6 Hz). HPLC (Lux 3 μ m-cellulose 5, Hexane/*i*-Propanol 95:5), flow: 0.5 mL/min, λ =210 nm, Anti diastereoisomers (t_{major} : 19,1 min.; t_{minor} : 21,5 min); Syn diastereoisomers (t_{major} : 25,4 min.; t_{minor} : 27,5 min.). $[\alpha]_{\text{D}}^{25}$ = +69,3 (c = 0.12 in chloroform, 80% ee); HRMS m/z calc. for [C₁₀H₁₁O₃F + Na⁺] = 221.0584; found: 221.0575.

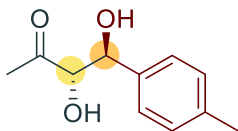
³¹ F. Calderón, R. Fernández, F. Sánchez, A. Fernández-Mayoralas, *Adv. Synth. Catal.*, **2005**, 347, 1395.

(3S,4S)-4-(3-bromophenyl)-3,4-dihydroxybutan-2-one (3c):



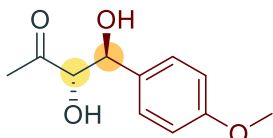
Synthesized in accordance with general procedure using 3-bromobenzaldehyde (12 μL , 0.1 mmol). ^1H NMR (400 MHz, Chloroform- d) δ 7.62 – 7.57 (m, 1H), 7.47 (dt, J = 7.8, 1.4 Hz, 1H), 7.33 (d, J = 7.8 Hz, 1H), 7.30 – 7.22 (m, 1H), 4.95 (s, 1H), 4.43 (t, J = 4.5 Hz, 1H), 3.76 (t, J = 4.4 Hz, 1H), 2.02 (s, 1H). ^{13}C NMR (101 MHz, CDCl_3) δ 207.8 (CO), 141.5(C), 131.3 (CH), 130.1 (CH), 129.4 (CH), 124.9 (CH), 122.8 (C), 80.8 (CH), 74.4 (CH), 27.7 (CH $_3$). HPLC (Lux 3 μm -Amylose 1, Hexane/*i*-Propanol 97:3), flow: 0.5 mL/min, λ =210 nm, Anti diastereoisomers (t_{major} : 46,9 min.; t_{minor} : 49,0 min); Syn diastereoisomers (t_{major} : 57,7 min.; t_{minor} : 80,5 min). $[\alpha]_{\text{D}}^{25}$ = +64.6 (c = 0.34 in chloroform, 73% ee); HRMS m/z calc. for $[\text{C}_{10}\text{H}_{11}\text{O}_3\text{Br} + \text{Na}^+]$ = 280.9773; found: 280.9784.

(3S,4S)-3,4-dihydroxy-4-(*p*-tolyl)butan-2-one (3d)



Synthesized in accordance with general procedure using 4-methylbenzaldehyde (12 μL , 0.1 mmol). ^1H NMR (400 MHz, Chloroform- d) δ 7.31 - 7.27 (m, 2H), 7.20 - 7.17 (m, 2H), 4.96 (s, 1H), 4.45 (t, J = 4.2 Hz, 1H), 3.57 (d, J = 4.6 Hz, 1H), 2.77 (s, 1H), 2.35 (d, J = 1.7 Hz, 2H), 1.99 (s, 1H). ^{13}C NMR (101 MHz, CDCl_3) δ 208.1 (CO), 138.0 (C), 136.0 (C), 129.3 (CH), 126.1 (CH), 81.0 (CH), 74.9 (CH), 27.6 (CH), 21.1 (CH $_3$). HPLC (Lux 3 μm -Amylose 1, Hexane/*i*-Propanol 90:10), flow: 0.4 mL/min, λ =210 nm, Anti diastereoisomers (t_{major} : 15,3 min.; t_{minor} : 16,6 min.) Syn diastereoisomers (t_{major} : 18,1 min.; t_{minor} : 23,4 min). $[\alpha]_{\text{D}}^{25}$ = +82.6 (c = 0.06 in chloroform, 80% ee); HRMS m/z calc. for $[\text{C}_{11}\text{H}_{14}\text{O}_3 + \text{Na}^+]$ = 217.0835; found: 217.0827.

(3S,4S)-3,4-dihydroxy-4-(4-methoxyphenyl)butan-2-one (3e):³²



Synthesized in accordance with general procedure using 4-methoxybenzaldehyde (12.2 μL , 0.1 mmol). ^1H NMR (400 MHz, Chloroform-*d*) δ 7.31 – 7.26 (m, 2H), 6.99 – 2.97 (m, 2H), 4.97 (d, $J = 4.2$ Hz, 1H), 4.45 – 4.44 (s, 1H), 3.81 (s, 3H), 3.70 (bs, 1H), 3.11 (bs, 1H), 1.99 (s, 3H). HPLC (Lux 3 μm -Amylose 1, Hexane/*i*-Propanol 95:5, flow: 0.5 mL/min, $\lambda=210$ nm) Anti diastereoisomers (t_{major} : 42,5 min.; t_{minor} : 49,6 min.) Syn diastereoisomers (t_{major} : 60,7 min.; t_{minor} : 80,8 min)

³² M. Bigovic, V. Maslak, Z. Tokic-Vujosevic, V. Divjakovic, R.N. Saicic, *Org. Lett.* **2011**, 13, 17, 4720.

Chapter 5: Conclusion

During my PhD studies, I tried to overcome some critical issues found in aminocatalysis; I tried to rationalise every aspect we encountered and exploit it to our advantage.

I was able to increase the catalytic efficiency of peptide sequences by exploiting their intrinsic ability to fold and form supramolecular structures under appropriate conditions. The confinement effect of the reactants obtained by the self-assembly process was demonstrated by performing a comparison between sequences not capable of supramolecular aggregation and catalyst in its assembled form. Due to the high variety of individual amino acids found in nature, and consequently the high modulability of the short peptide sequences that can be synthesised, the proof-of-concept demonstrated in this work offers the possibility of investigating the reactivity of a range of peptide sequences that are capable of different types of activation exploiting the supramolecular effect.

I have optimised the reaction conditions of a synthesis leading to the formation of products of pharmaceutical interest formed in an aqueous solvent using water-compatible catalysts, making it potentially interesting for industry. Furthermore, this developed protocol was found using an already widely-used optimization strategy in industry. The DoE is a powerful tool that has allowed us to explore the space of experimental variables rationally and comprehensively by performing a limited number of experiments compared to those often used by varying one variable on time. Performing a limited number of experiments is an essential factor from an environmental point of view. For industry, it is also crucial in terms of both time and economic resources.

I evaluated the degree of affinity of the support of a heterogeneous catalyst by studying the diffusive behaviour of the reagents of the benchmark reaction. A catalyst supported on a siliceous material containing proline as an active site was considered and its activity in an aldol reaction was tested. In particular, the degree of affinity of the support related to the reactivity with one of the substrates was studied to assess the effectiveness of the catalyst itself in relation to possible substrate inhibition.

Acknowledgements

During these three years, I feel I have to thank so many people, things and emotions that have made me realise how strong I can also be.

I would like to thank Professor Armando Carlone for having accompanied me with infinite patience along this journey, and for giving me the opportunity to prove myself with a challenge project.

I would like to thank Dr Fabio Pesciaioli, I thank him for all the times we have engaged in very long "dialogues concerning two chief words (chemistry) systems". His presence reminded me of the passion and search for beauty in my work, every day. Precisely as it had been handed down to me by Professor Marco Bella, whom I thank infinitely for instilling in me an immediate love of what I continue to do every day.

Thank you to my research group, who gave me the determination to move forward and not throw things away. Each of you has allowed me to grow and understand the value of help.

I would like to thank all the professors, colleagues, and students at the University of L'Aquila. Thank you for having welcomed me as if I had always been there. Thank you again for those warm smiles and your "good morning" present every morning. I will miss that corridor.

I would like to thank the City of L'Aquila. I thank it for its rebirth, its beautiful and constantly changing appearance. Special thanks to the mountains that crown it and the snow that has always made me happy.

I would like to thank my parents, sister, family, the family I have chosen, and faraway friends (but equally near). Each one of you helped me not to falter in insecurity by holding my hand when I most needed it.

*“Sorridente e siate felici,
quanto stanchi sarete tornati”
Guido Chiaravalle*